UNIVERISTY OF CALIFORNIA, SAN DIEGO

Characterization of the BST2/Tetherin cytoplasmic tail and understanding BST2-mediated NF-κB activation

A dissertation submitted in partial satisfaction of the requirements for the degree Doctor of Philosophy

in

Biomedical Sciences

by

Maryan Girgis Soliman Rizk

Committee in charge:

Professor John C. Guatelli, Chair
Professor Michael I. David
Professor Daniel Donoghue
Professor Douglas Richman
Professor Bruce Torbett

2017

The Dissertation of Maryan Girgis Soliman Rizk is approved, and it is acceptable in quality and form for publication on microfilm and electronically:

_____

_____

_____

_____

_____
Chair

University of California, San Diego

2017

Table of Contents

List of Figures and Tables

FIGURES

List of Abbreviations

3AT	3-amino-1,2,4-triazole
AD	GAL4-activation domain
AP-1	Adaptor protein complex 1
AP-2	Adaptor protein complex 2
AP-3	Adaptor protein complex 3
Arf1	ADP-ribosylation factor 1
Art-tetherin	Artifical-tetherin
BFA	Brefeldin A
BST2	Bone marrow stromal antigen 2
CD	Cytoplasmic tail domain
CD4	Cluster of differentiation 4
COPI	Coatomer protein I
COPII	Coatomer protein II
CSK	C-src kinase
CT	Cytoplasmic tail
CTLA-4	Cytotoxic T-lymphocyte protein 4
CXCL10	C-X-C motif chemokine 10
DD	Death domain
DMPK	Dystrophia Myotonica Protein Kinase
EBOV	Ebola virus
ER	Endoplasmic reticulum
GAL4	Regulatory protein Gal4
GBF1	Golgi-specific brefeldin A-resistance guanine nucleotide exchange factor 1
GDB	Gal4-DNA binding domain
GP	Glycoprotein
GPI	Glycosylphosphatidylinositol
HA	Hemagglutinin
HCK	Hematopoietic cell kinase
HCV	Hepatitis C virus
HIV-1	Human immundeficiency virus 1
HIV-2	Human immundeficiency virus 2
HSV-1	Herpes simplex virus 1
HSV-2	Herpes simplex virus 2
IAV	Influenza A virus
IFNβ	Interferon beta
IL-6	Interleukin-6
ILT7	Immunoglubulin-like transcript 7
ITAM	Immunosuppressor tyrosine-based activation motif

Iκβ	Inhibitor of kappa beta
KSHV	Kaposi's Sarcoma Herpes Virus
LCK	Lymphocyte cell-specific protine-tyrosine kinase
LSECtin	Liver and lymph node sinusoidal endothelial cell C-type lectin
MLD	Mucin-like domain
MLV	Murine leukemia virus
MyD88	Myeloid differentiation primary response protein MyD88
NAE	NEDD8-activating enzyme
NEDD8	Neural precursor cell expressed developmentally down-regulated protein 8
NF-κB	Nuclear Factor kappa B
RBD	Receptor-binding domain
SCF	Skp, cullin, F-box containing complex
SIV	Simian immunodeficiency virus
SP	Signal peptide
SYK	Spleen tyrosine kinase
TAB1	TAK-1-binding protein 1
TAB2	Tak-2-binding protein 2
TACE	Tumor-necrosis alpha converting enzyme
TAK1	TGF-β-activated kinase 1
TGF-β	Transforming growth factor beta
TGN	*trans*-Golgi network
TGN38	*trans*-Golgi network resident protein 38kD
TIR	Toll/interleukin-1 receptor homology domain
TK	Thymidine kinase
TLR4	Toll-like receptor 4
TM	Transmembrane domain
TRAF2	TNF receptor-associated factor 2
TRAF6	TNF receptor-associated factor 6
uPAR	Urokinase receptor (uPA receptor)
VLP	Virus-like particle
VP40	Viral protein 40
Vpu	Viral protein U
WT	Wild-type
β-TrCP	Beta-transducin repeate-containing protein

Amino Acid Residues

Ala or A	Alanine
Arg or R	Arginine

Asn or N	Asparagine
Asp or D	Aspartic acid
Cys or C	Cysteine
Gln or Q	Glutamine
Glu or E	Glutamic acid
Gly or G	Glycine
His or H	Histidine
Ile or I	Isoleucine
Leu or L	Leucine
Lys or K	Lysine
Met or M	Methionie
Phe or F	Phenylalanine
Pro or P	Proline
Ser or S	Serine
Thr or T	Threonine
Trp or W	Tryptophan
Tyr or Y	Tyrosine
Val or V	Valine

Acknowledgements

I would first like to thank my dissertation advisor, John Guatelli, for the endless amount of patience and support that he offered me as a graduate student in his lab. John has been a true mentor to me through his example as a brilliant thinker and scientist and through his advice and guidance in my research and career pursuits. In every step of the way, whenever I doubted my own abilities, John was there to help me regain my confidence as a researcher and scientist. Even after a six-months leave, John had confidence in me and took me back to continue my doctoral studies in his lab. He showed me that mentorship is a mixture of knowledge, curiosity, guidance, and compassion. Thank you, John!

I thank my mother for her love, self-denial, and prayers all along to help me get to where I am today. She has always been there for me whenever I needed a listening ear and advice about my education and career. I want to also thank my aunt, who has been like a second mother to me. She was always there to help me with practical advice and to encourage me to take things one step at a time. She never ceased to pray for me and to lift up my spirit with her smile. I also want to thank my brother, who always knew how to say just the right things at the right time and carried many burdens off my shoulders whenever I needed time away to work in the lab or write. Even though he has passed, I want to thank my father for instilling in me a love of knowledge and a deep desire to be a lifelong learner. I also want to thank all of my family in Egypt for their continuous prayers and their love and support the past five years as I told them every year that I could not visit them until the year after. I also thank my church family for their love, patience, and prayers.

I want to thank all of members of the Academic Enrichment Programs at UCSD for helping me prepare for graduate school. I would like to thank Dr. Thomas Brown of the McNair program, Dr. Jacqueline Azize-Brewer of the California Alliance for Minority Participation Program, and the director Dr. David Artis for his support and when he told all the summer researchers in 2010 that “You get out of research what you put into it.” I have held on to this advice until today. I also want to thank my undergraduate research and teaching advisors: Dr. Alexander Zambon, Dr. Julian Schroeder, and Dr. Shelley Halpain. I thank Dr. Rosalind Streichler and Dr. Ekihiro Seki for believing in me and supporting me with their advice and encouraging words. I also want to thank the leaders of the Biomedical Sciences Program for their continuous support and help.

I want to thank my minor proposition committee members: Dr. Victor Nizet, Dr. Farah Sheikh, and Dr. John Young. I also thank my dissertation committee: Drs. Michael David, Daniel Donoghue, Douglas Richman, and Bruce Torbett. In our lab, I would like to thank current and former members of the Center for AIDS Research: Marissa Suarez, Jasmine Chau, Aaron Oom, Brianna Scott, Laura Layman, Steven Lada, Stephen Espitia, Amey Mukim, Savitha Deshmukh, Drs. Andrey Tokarev, Mary Lewinski, Shilpi Sharma, Rajendra Singh, Peter Ramirez, Charlotte Stoneham, Thomas Vollbrecht, Davey Smith, Nadejd Beliakova-Bethell, Celsa Spina, and Matthew Strain.

I would also like to thank those who fed my spirit and strengthened my faith in God throughout my PhD: Fathers Antony Paul, Abraam Ayoub, Moses Samaan, Kyrillos Ibrahim, and Domedious Rizk, and Bishop Kyrillos. I also thank Anthony and Maryanne Shenoda. Ultimately, I thank God for all of my friends and the great individuals He has set on my journey so far.

Chapter II, in part, is a reprint of the material as it appears in Jia X, Weber E, Tokarev A, Lewinski M**,** Rizk M**,** Suarez M, Guatelli J, Xiong Y. 2014. Structural basis of HIV-1 Vpu-mediated BST2 antagonism via hijacking of the clathrin adaptor protein complex 1. *eLife* **3:**e02362. The dissertation author was a contributing author of this paper.

Chapter III, in full, is a reprint of the material as it appears in Rizk MG, Basler CF, Guatelli J. 2017. Cooperation of the Ebola proteins VP40 and GP1,2 with BST2 to activate NF-κB independently of virus-like particle trapping. *Journal of Virology* doi:10.1128/JVI.01308-17. The dissertation author was the primary investigator and author of this paper.

Vita

2012 B.S. University of California San Diego

2012-2016 San Diego Fellow, University of California San Diego Graduate Division

2017 Ph.D. University of California San Diego

Fields of Study

Major Field: Biomedical Sciences

Viral-Host Interactions Studies

Professor John C. Guatelli

Publications

Rizk MG, Basler CF, Guatelli J. 2017. Cooperation of the Ebola proteins VP40 and GP1,2 with BST2 to activate NF-κB independently of virus-like particle trapping. *Journal of Virology* doi:10.1128/JVI.01308-17.

Jia X, Weber E, Tokarev A, Lewinski M**, Rizk M,** Suarez M, Guatelli J, Xiong Y. 2014. Structural basis of HIV-1 Vpu-mediated BST2 antagonism via hijacking of the clathrin adaptor protein complex 1. *eLife* **3:**e02362.

ABSTRACT OF THE DISSERATION

Characterization of the BST2/Tetherin cytoplasmic tail and

understanding BST2-mediated NF-κB activation

by

Maryan Girgis Soliman Rizk

Doctor of Philosophy in Biomedical Sciences

University of San Diego, San Diego, 2017

Professor John C. Guatelli, Chair

BST2/Tetherin is an interferon-induced anti-viral host protein that restricts the release of newly assembled virions of enveloped viruses at the plasma membrane (PM) of infected cells. It also signals to activate NF-κB in a manner that is dependent on the tyrosine 6 residue of its cytoplasmic tail domain (CD). The main goal of this dissertation

is to understand the role of BST2 cytoplasmic tail in signaling and trafficking and how BST2 signaling is modulated in response to proteins of Ebola virus.

I first asked whether the cytoplasmic domain (CD) of BST2 directly binds to the host μ1 protein of the AP1 trafficking complex. Vpu of HIV-1 also binds to this complex and traps BST2 within internal membranes leading to enhanced virion release. I showed, using yeast two-hybrid assays, that the BST2 CD interacts with μ1 via a YxYxxV motif within BST2, in which both Ys and the V are required. Next, I asked whether both tyrosine residues are required for the activation of NF-κB by BST2. I found that tyrosine 6, but not tyrosine 8, is required for signaling likely due to its phosphorylation by Syk kinase. These results indicate that the determinants of membrane sorting and signaling by BST2 CD are overlapping but genetically separable.

To understand the relationship between virion-entrapment and activation of NF-κB by BST2, I studied the modulation of BST2-mediated NF-κB activation in response to the expression of the Ebola virus (EBOV) matrix protein (VP40) and glycoprotein ($GP_{1,2}$). I asked whether the relief of virus-like particle (VLP) restriction by EBOV $GP_{1,2}$ would reduce or inhibit BST2 signaling. VP40 was used as a virion model because it forms VLPs that resemble actual virions of EBOV, whose release is restricted by BST2. Under the conditions of this study, I found that $GP_{1,2}$ and VP40 cooperated with BST2 to induce NF-κB activity. Using a mutant of BST2 lacking the C-terminal GPI anchor, which is defective for virion-entrapment and is not expressed at the PM, I found that BST2 signaling does not require trapping VLPs at the PM and that cooperative signaling with EBOV proteins occurs within internal membranes.

Chapter I

Introduction of BST2/Tetherin as a multifunctional transmembrane protein

Overview of BST2 functions

BST2 is an interferon-induced host protein that acts as an anti-viral factor, termed a restriction factor. It restricts the release of newly assembled virions from the plasma membrane to prevent further dissemination of the virus (1, 2). In studies of retroviruses such as the human immunodeficiency virus 1 (HIV-1) and the murine leukemia virus (MLV), BST2 was also shown to induce activation of an important proinflammatory transcription factor called NF-κB (3, 4). Here, I present a brief historical perspective about the discovery of BST2, the study of BST2 as a host anti-viral restriction factor and activator of NF-κB in the context of HIV-1, and a brief background on the relationship between BST2 and proteins of the Ebola virus.

Historical perspective of BST2/Tetherin

BST2 was first described as a 30- to 36kDa type II transmembrane protein protein that is over-expressed in bone marrow stromal cells (5) and terminally differentiated normal and neoplastic B-cells (6). It was also suggested to play a role in pre-B cell growth mediated by cell-to-cell interactions, which implied that BST2 has a cell-surface receptor (5, 7). Later work indeed showed that surface BST2 that was expressed on HIV-1-infected CD4 cells interacted with the ILT7 receptors on plasmacytoid dendritic cells (8, 9). Early work also showed that BST2 existed as a homodimer that was N-glycosylated on the ectodomain and to contain a conserved tyrosine motif in its cytoplasmic tail (5-7). Later work showed that dimerization is important for the entrapment of virions enveloped viruses by BST2, except Lassa and Marburg viruses (10, 11), and that the tyrosine 6 of the cytoplasmic tail was important for the activation of NF-κB (3, 4, 12, 13). Overall, studies of BST2 so far show that there are unique structural features of BST2 that facilitate its antiviral and proinflammatory

activities. However, many open questions about the normal functions of BST2 have not yet been addressed.

BST2 physically traps virions of enveloped viruses

The innate immune system employs cellular factors called restriction factors in order to counteract viral replication within infected cells. BST2 (or tetherin) is a type-I interferon-induced host protein that restricts the release of enveloped viruses from infected cells; virus families studied so far include members of the retroviridae (HIV-1 and MLV), filoviridae (Ebola and Marburg viruses), arenaviridae (Lassa virus), herpesviridae (herpes simplex virus 1 (HSV1) and Kaposi's sarcoma herpes virus (KSHV)), flavivirdae (hepatitis C virus (HCV)), and orthomyxoviridae (influenza A virus IAV)) (1, 2, 14-22). Early work with HIV-1 showed that BST2 physically traps HIV-1 virions lacking the viral protein U (Vpu) at the plasma membranes of infected cells (1, 2, 23). The unique structure of BST2 enables it to physically anchor nascent virions to the cell surface thus preventing the virus from being freely released from the cells and infecting other cells (24, 25). As shown in Figure I.1, BST2 has an N-terminal cytoplasmic tail, a transmembrane domain, a long rigid coiled-coil ectodomain, and a C-terminal GPI-anchor (26). The transmembrane domain of BST2 and the GPI anchor enable the protein to be inserted physically within the hydrophobic regions of the plasma membrane and the viral envelopes (25, 27). Interestingly, the overall configuration of BST2 is more important than the specific amino acid sequence of the protein as was shown by replacing all the domains of BST2 with structurally similar domains from other proteins (the cytoplasmic and transmembrane domains from the transferrin receptor, the coiled-coil from the protein DMPK, and the GPI anchor of

uPAR) (24). This finding provides an explanation for the ability of BST2 to restrict all enveloped viruses studied so far without the need for sequence-dependent interactions between BST2 and proteins of the newly assembled virions.

BST2 activates NF-κB through its cytoplasmic tail

More recently, BST2 has also been described as an activator of the important innate immune transcription factor NF-κB (3, 4). Since the activity of NF-κB is important for the production of anti-inflammatory cytokines, one model suggests that the activation of NF-κB, which leads to the production of IL-6, CXCL10, and IFNβ, serves as an innate sensing mechanism that is dependent on the entrapment of virions at the plasma membrane (4, 12). Another model was proposed by our group suggesting that BST2-mediated activation of NF-κB does not depend on virion-entrapment (3). The common theme of all of the signaling studies of BST2 is that conserved tyrosine residues within the cytoplasmic tail of BST2 were necessary for signaling (Figure I.1). However, these studies ultimately do not describe the exact mechanism of how BST2 is activated to signal the translocation of NF-κB into the nucleus to activate the transcription of its target genes. A full understanding of how viral proteins activate BST2 signaling within the host cell could provide insight into the exact role of BST2 towards proinflammatory signaling and how this activity becomes harnessed or counteracted by viral proteins. In Chapter III of this dissertation we attempted to better understand the BST2-mediated activation of NF-κB in cooperation with the Ebola viral proteins, VP40 and GP1,2.

The human immunodeficiency virus 1 and BST2

HIV-1 is the causative agent for the acquired immunodeficiency syndrome in humans (reviewed in (28)). Like other enveloped viruses, BST2 traps nascent virions of

HIV-1 lacking Vpu at the surface of infected cells (1, 2). The HIV-1 genome encodes for the expression of genes that do not directly participate in the replication or structural arrangements of virions but rather alter the host anti-viral machinary (reviewed in (29)). These genes encode proteins that are termed accessory proteins, and they counteract the host restriction factors of HIV-1 such as BST2, among others (reviewed in (29)). Vpu is an accessory protein of HIV-1 that is expressed late in the replication cycle of HIV-1 and induces the proteosomal degradation of the CD4 receptor from the surface of infected cells (30, 31). It is 16-kDa (81-residue) type I transmembrane protein with a short and flexible cytoplasmic tail (32, 33). Vpu also acts as an antagonist of BST2 by reducing the levels of BST2 expressed at the plasma membrane, which in-turn increases the release of virions (1, 2, 34, 35).

Vpu drives the lysosomal and proteosomal degradation of BST2 in a manner dependent on the beta transducing repeat-containing protein (β-TrCP) (34, 36, 37). This interaction requires Vpu phosphorylation at serines 52 and 56, which allows it to bind to the WD domain of β-TrCP as part of the E3 ubiquitin-ligase SCF (Skp1, Cullin, F-box) complex (34, 36, 38, 39). Also, Vpu misdirects the trafficking of BST2 to the plasma membrane by trapping the recycled and newly synthesized BST2 in endosomal compartments such as the *trans*-Golgi network (40, 41). Additionally, Vpu displaces BST2 from the assembly sites of virions at the plasma membrane (42-45). Overall, Vpu employs multiple mechanisms to degrade, mistraffick, and displace BST2 in order to enhance virion release. Details regarding the mechanism of the mistrafficking process, which also involves a clathrin-dependent pathway, will be presented in this dissertation in Chapter II (33).

In terms of activation of NF-κB and the proinflammatory response, we and others have shown that the expression of HIV-1 without the Vpu protein increases NF-κB activity via BST2 (3, 4). This process was shown to occur through the activation of the canonical NF-κB pathway in a TGF-β-activated kinase 1 (TAK1)-dependent pathway (3, 4). As mentioned above, Vpu sequesters the β-TrCP protein and this has been shown to lead to the inability of the complex to ubiquitinate the IkB protein (46). The ubiquitination of phosphorylated IkB is required for its degradation, which is in turn required for its dissociation from cytoplasmic NF-κB and leads to the translocalization of NF-κB into the nucleus for the activation of its target genes (47, 48). Thus, Vpu inhibits NF-κB activity although a recent study suggested an alternate, yet unclear, inhibition mechanism besides the sequestration of the B-TrCP complex (49). However, the exact mechanism of how viral expression enhances or induces NF-κB activity in the presence of BST2 is not currently clear. One model suggests that the physical tethering of virions by BST2 leads to the phosphorylation of a tyrosine residue in the cytoplasmic tail of BST2 (12). Presumably, this is due to the dimerization of BST2 where two cytoplasmic tails are close in proximity to each other allowing the formation of a hemi-ITAM motif of two phosphorylated tyrosines (12). This pathway was suggested to use Syk kinase, a src-family kinase, which appears to play a role in the phosphorylation of BST2 although the exact mechanism is not currently clear (12). Findings from our lab did not support the part of the signaling model where BST2 signaling is induced upon the tethering of virions at the plasma membrane (3, 50). We showed this by using a BST2 mutant that was defective for virion tethering while retaining its ability to activate NF-κB (3, 50). We

further support this finding by our study of the Ebola virus, introduced next, and the published data presented in Chapter III.

Ebola virus and BST2

Other viral proteins that have been shown to antagonize BST2 by counteracting the entrapment of virions are the envelope protein (Env) of HIV-2, K5 protein of KSHV, Nef protein of SIV, the virion host shutoff protein (Vhs) and glycoprotein M of HSV1 (17, 51), various glycoproteins of HSV2 (52), and the glycoprotein of Ebola virus. The mechanism of BST2 antagonism by the KSHV K5, HIV-2 Env, and SIV Nef requires the removal of BST2 from the plasma membrane or its degradation (Table I.1 and reviewed in (53, 54). However, the Ebola virus $GP_{1,2}$ protein does not remove BST2 from the plasma membrane, while still enhancing the release of virions (55). The exact mechanism of how $GP_{1,2}$ interacts with BST2 is currently unclear although recent studies have shown that the GP2 subunit and the glycan cap and receptor-binding domain of the GP1 subunit are required for the antagonism of BST2 (56-58). This process was shown to involved the dissociation of BST2 from the matrix protein of Ebola virus, VP40 (57).

Ebola virus is a hemorrhagic fever in the filoviral family. It was discovered in the African Democratic Republic of Congo (formerly Zaire) in 1976, when the first cases of human infection were documented (59). Throughout the last thirty plus years, outbreaks of the virus have occurred in various regions in African with the most recent epidemic of *Zaire* Ebola virus in 2014 in Sierra Leone, Guinea, Liberia, and Nigeria (60). Currently there are five species in the genus *Ebolavirus*, namely *Zaire, Sudan, Tai Forest, Bundibugyo,* and *Reston* (reviewed in (61)). Only the *Reston* species was shown not to

be pathogenic in humans, but is pathogenic in cynomologous Asian Monkeys and African-Green Monkeys (62). Ebola virus is a negative single stranded RNA (-ssRNA) virus that encodes seven main gene produces NP, VP35, VP40, pre-GP, VP30, VP25, and L gene (63-65). The VP40 protein can form non-infectious virus-like particles that closely resemble Ebola virions and thus facilitate the study of Ebola virus release under conditions of biosafety level 2 (66). The $GP_{1,2}$ protein consists of two subunits 1 and 2, as named above GP1 and GP2 (Figure I.2). The GP2 subunit contains the transmembrane domain of the protein. The two subunits form trimers of the dimer and these are the spikes that are found on the surface of virions and VLPs of Ebola virus (67). The Ebola virus GP and VP40 proteins within virus-like particles have been previously shown to induce the activity of NF-κB due to extracellular interactions with innate immune cells and the Toll-like receptor (TLR4) receptor (68-70). Chapter III of this dissertation shows that Ebola virus VP40 and GP1,2 cooperate with BST2 in order to induce NF-κB activity independently of the process of virion-entrapment (50).

Figures and Tables

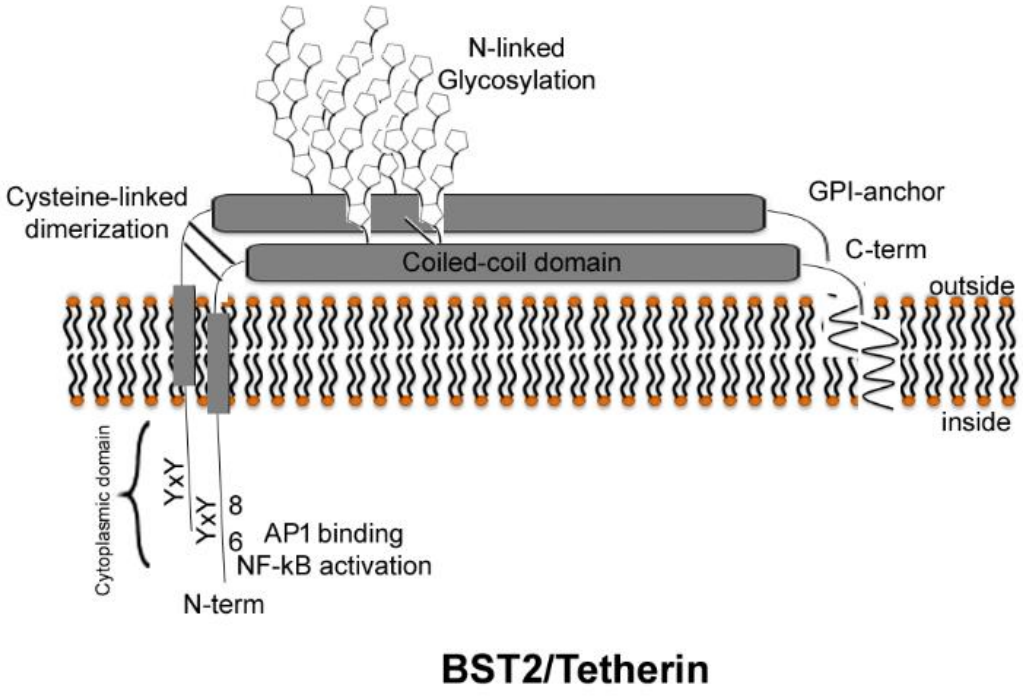

Figure I.1 Structural features of BST2/Tetherin within a phospholipid bilayer. BST2 is a dimer that consists of a cytoplasmic tail domain at the N-terminus followed by a transmembrane domain, a rigid coiled-coil domain, and a GPI-anchor modification. Cysteine-linked dimerization occurs at residues C53, C63, and C91. N-linked glycosylation of asparagines occurs at positions 65 and 92. The GPI-anchor modification occurs at the C-terminus of the protein.

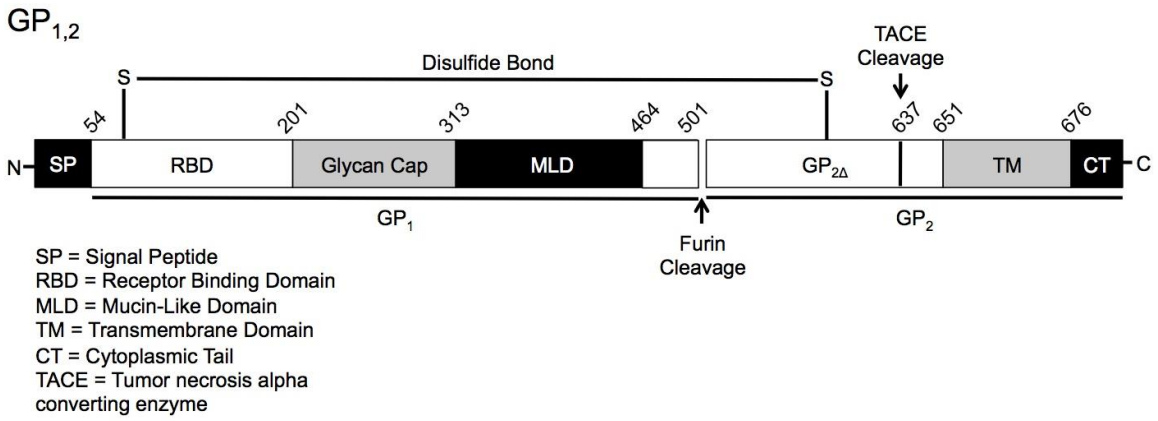

Figure I.2 Schematic of the Ebola virus glycoprotein (GP1,2). Ebola virus glycoprotein surface spike, GP1,2, consists of two subunits: GP1 and GP2. The two subunits are produced as a result of cleavage within the cell by furin proteases. GP1 and GP2 are linked together through a disulfide bond as heterodimers. GP2 contains the transmembrane domain and three units of GP2 form the base of the spike, while three units of GP1 form the chalice – a trimer of dimers. SP stands for the signaling peptide that targets the newly synthized GP towards the endoplasmic reticulum (ER). RBD stands for the receptor-binding domain. The heavily glycosylated regions of the GP1 are termed as the glycan cap and the mucin-like domain. GP1,2 at the cell surface can be cleaved by the tumor necrosis alpha converting enzyme (TACE) to produce a soluble form of GP that contains the full GP1 and a region of the GP2 termed GP2Δ (reviewed in(67)).

Table I.1. Viral antagonists of BST2.

Antagonist	Host	Process Inhibited	Mechanism/s	References
HIV-1 Vpu	Human	Virion Restriction	Endocytosis Degradation Removal from virion-assembly cites	(1, 2, 35, 42, 44, 45, 71-77)
		NF-κB signaling	Unknown	(3, 4)
HIV-2 Env	Human	Virion Restriction	Endocytosis	(78-80)
SIV Nef	Non-human primates	Virion Restriction	Endocytosis	(81-84)
Ebola Glycoprotein (GP1,2)	Human Non-human primates	Virion Restriction	Unknown	(15, 55, 85)
KSHV K5	Human	Virion Restriction	Endocytosis Degradation	(18, 86, 87)

References

1. **Neil SJ, Zang T, Bieniasz PD.** 2008. Tetherin inhibits retrovirus release and is antagonized by HIV-1 Vpu. Nature **451:**425-430.

2. **Van Damme N, Goff D, Katsura C, Jorgenson RL, Mitchell R, Johnson MC, Stephens EB, Guatelli J.** 2008. The interferon-induced protein BST-2 restricts HIV-1 release and is downregulated from the cell surface by the viral Vpu protein. Cell Host Microbe **3:**245-252.

3. **Tokarev A, Suarez M, Kwan W, Fitzpatrick K, Singh R, Guatelli J.** 2013. Stimulation of NF-kappaB activity by the HIV restriction factor BST2. J Virol **87:**2046-2057.

4. **Galao RP, Le Tortorec A, Pickering S, Kueck T, Neil SJ.** 2012. Innate sensing of HIV-1 assembly by Tetherin induces NFkappaB-dependent proinflammatory responses. Cell Host Microbe **12:**633-644.

5. **Ishikawa J, Kaisho T, Tomizawa H, Lee BO, Kobune Y, Inazawa J, Oritani K, Itoh M, Ochi T, Ishihara K, et al.** 1995. Molecular cloning and chromosomal mapping of a bone marrow stromal cell surface gene, BST2, that may be involved in pre-B-cell growth. Genomics **26:**527-534.

6. **Goto T, Kennel SJ, Abe M, Takishita M, Kosaka M, Solomon A, Saito S.** 1994. A novel membrane antigen selectively expressed on terminally differentiated human B cells. Blood **84:**1922-1930.

7. **Ohtomo T, Sugamata Y, Ozaki Y, Ono K, Yoshimura Y, Kawai S, Koishihara Y, Ozaki S, Kosaka M, Hirano T, Tsuchiya M.** 1999. Molecular cloning and characterization of a surface antigen preferentially overexpressed on multiple myeloma cells. Biochem Biophys Res Commun **258:**583-591.

8. **Bego MG, Cote E, Aschman N, Mercier J, Weissenhorn W, Cohen EA.** 2015. Vpu Exploits the Cross-Talk between BST2 and the ILT7 Receptor to Suppress Anti-HIV-1 Responses by Plasmacytoid Dendritic Cells. PLoS Pathog **11:**e1005024.

9. **Cao W, Bover L, Cho M, Wen X, Hanabuchi S, Bao M, Rosen DB, Wang YH, Shaw JL, Du Q, Li C, Arai N, Yao Z, Lanier LL, Liu YJ.** 2009. Regulation of TLR7/9 responses in plasmacytoid dendritic cells by BST2 and ILT7 receptor interaction. J Exp Med **206:**1603-1614.

10. **Andrew AJ, Miyagi E, Kao S, Strebel K.** 2009. The formation of cysteine-linked dimers of BST-2/tetherin is important for inhibition of HIV-1 virus release but not for sensitivity to Vpu. Retrovirology **6:**80.

11. **Sakuma T, Sakurai A, Yasuda J.** 2009. Dimerization of tetherin is not essential for its antiviral activity against Lassa and Marburg viruses. PLoS One **4:**e6934.

12. **Galao RP, Pickering S, Curnock R, Neil SJ.** 2014. Retroviral retention activates a Syk-dependent HemITAM in human tetherin. Cell Host Microbe **16:**291-303.

13. **Cocka LJ, Bates P.** 2012. Identification of alternatively translated Tetherin isoforms with differing antiviral and signaling activities. PLoS Pathog **8:**e1002931.

14. **Jouvenet N, Neil SJ, Zhadina M, Zang T, Kratovac Z, Lee Y, McNatt M, Hatziioannou T, Bieniasz PD.** 2009. Broad-spectrum inhibition of retroviral and filoviral particle release by tetherin. J Virol **83:**1837-1844.

15. **Kaletsky RL, Francica JR, Agrawal-Gamse C, Bates P.** 2009. Tetherin-mediated restriction of filovirus budding is antagonized by the Ebola glycoprotein. Proc Natl Acad Sci U S A **106:**2886-2891.

16. **Sakuma T, Noda T, Urata S, Kawaoka Y, Yasuda J.** 2009. Inhibition of Lassa and Marburg virus production by tetherin. J Virol **83:**2382-2385.

17. **Blondeau C, Pelchen-Matthews A, Mlcochova P, Marsh M, Milne RS, Towers GJ.** 2013. Tetherin restricts herpes simplex virus 1 and is antagonized by glycoprotein M. J Virol **87:**13124-13133.

18. **Pardieu C, Vigan R, Wilson SJ, Calvi A, Zang T, Bieniasz P, Kellam P, Towers GJ, Neil SJ.** 2010. The RING-CH ligase K5 antagonizes restriction of KSHV and HIV-1 particle release by mediating ubiquitin-dependent endosomal degradation of tetherin. PLoS Pathog **6:**e1000843.

19. **Pan XB, Han JC, Cong X, Wei L.** 2012. BST2/tetherin inhibits dengue virus release from human hepatoma cells. PLoS One **7:**e51033.

20. **Pan XB, Qu XW, Jiang D, Zhao XL, Han JC, Wei L.** 2013. BST2/Tetherin inhibits hepatitis C virus production in human hepatoma cells. Antiviral Res **98:**54-60.

21. **Li M, Wang P, Zheng Z, Hu K, Zhang M, Guan X, Fu M, Zhang D, Wang W, Xiao G, Hu Q, Liu Y.** 2017. Japanese encephalitis virus counteracts BST2 restriction via its envelope protein E. Virology **510:**67-75.

22. **Hu S, Yin L, Mei S, Li J, Xu F, Sun H, Liu X, Cen S, Liang C, Li A, Guo F.** 2017. BST-2 restricts IAV release and is countered by the viral M2 protein. Biochem J **474:**715-730.

23. **Fitzpatrick K, Skasko M, Deerinck TJ, Crum J, Ellisman MH, Guatelli J.** 2010. Direct restriction of virus release and incorporation of the interferon-induced protein BST-2 into HIV-1 particles. PLoS Pathog **6:**e1000701.

24. **Perez-Caballero D, Zang T, Ebrahimi A, McNatt MW, Gregory DA, Johnson MC, Bieniasz PD.** 2009. Tetherin inhibits HIV-1 release by directly tethering virions to cells. Cell **139:**499-511.

25. **Venkatesh S, Bieniasz PD.** 2013. Mechanism of HIV-1 virion entrapment by tetherin. PLoS Pathog **9:**e1003483.

26. **Kupzig S, Korolchuk V, Rollason R, Sugden A, Wilde A, Banting G.** 2003. Bst-2/HM1.24 is a raft-associated apical membrane protein with an unusual topology. Traffic **4:**694-709.

27. **Hammonds J, Wang JJ, Yi H, Spearman P.** 2010. Immunoelectron microscopic evidence for Tetherin/BST2 as the physical bridge between HIV-1 virions and the plasma membrane. PLoS Pathog **6:**e1000749.

28. **Becerra JC, Bildstein LS, Gach JS.** 2016. Recent Insights into the HIV/AIDS Pandemic. Microb Cell **3:**451-475.

29. **Strebel K.** 2013. HIV accessory proteins versus host restriction factors. Curr Opin Virol **3:**692-699.

30. **Schubert U, Anton LC, Bacik I, Cox JH, Bour S, Bennink JR, Orlowski M, Strebel K, Yewdell JW.** 1998. CD4 glycoprotein degradation induced by human immunodeficiency virus type 1 Vpu protein requires the function of proteasomes and the ubiquitin-conjugating pathway. J Virol **72:**2280-2288.

31. **Willey RL, Maldarelli F, Martin MA, Strebel K.** 1992. Human immunodeficiency virus type 1 Vpu protein induces rapid degradation of CD4. J Virol **66:**7193-7200.

32. **Zhang H, Lin EC, Das BB, Tian Y, Opella SJ.** 2015. Structural determination of virus protein U from HIV-1 by NMR in membrane environments. Biochim Biophys Acta **1848:**3007-3018.

33. **Jia X, Weber E, Tokarev A, Lewinski M, Rizk M, Suarez M, Guatelli J, Xiong Y.** 2014. Structural basis of HIV-1 Vpu-mediated BST2 antagonism via hijacking of the clathrin adaptor protein complex 1. Elife **3:**e02362.

34. **Mitchell RS, Katsura C, Skasko MA, Fitzpatrick K, Lau D, Ruiz A, Stephens EB, Margottin-Goguet F, Benarous R, Guatelli JC.** 2009. Vpu antagonizes BST-2-mediated restriction of HIV-1 release via beta-TrCP and endo-lysosomal trafficking. PLoS Pathog **5:**e1000450.

35. **Schmidt S, Fritz JV, Bitzegeio J, Fackler OT, Keppler OT.** 2011. HIV-1 Vpu blocks recycling and biosynthetic transport of the intrinsic immunity factor CD317/tetherin to overcome the virion release restriction. MBio **2:**e00036-00011.

36. **Douglas JL, Viswanathan K, McCarroll MN, Gustin JK, Fruh K, Moses AV.** 2009. Vpu directs the degradation of the human immunodeficiency virus restriction factor BST-2/Tetherin via a {beta}TrCP-dependent mechanism. J Virol **83:**7931-7947.

37. **Goffinet C, Allespach I, Homann S, Tervo HM, Habermann A, Rupp D, Oberbremer L, Kern C, Tibroni N, Welsch S, Krijnse-Locker J, Banting G, Krausslich HG, Fackler OT, Keppler OT.** 2009. HIV-1 antagonism of CD317 is species specific and involves Vpu-mediated proteasomal degradation of the restriction factor. Cell Host Microbe **5:**285-297.

38. **Blanchet FP, Mitchell JP, Piguet V.** 2012. beta-TrCP dependency of HIV-1 Vpu-induced downregulation of CD4 and BST-2/tetherin. Curr HIV Res **10:**307-314.

39. **Bai C, Sen P, Hofmann K, Ma L, Goebl M, Harper JW, Elledge SJ.** 1996. SKP1 connects cell cycle regulators to the ubiquitin proteolysis machinery through a novel motif, the F-box. Cell **86:**263-274.

40. **Dube M, Roy BB, Guiot-Guillain P, Mercier J, Binette J, Leung G, Cohen EA.** 2009. Suppression of Tetherin-restricting activity upon human immunodeficiency virus type 1 particle release correlates with localization of Vpu in the trans-Golgi network. J Virol **83:**4574-4590.

41. **Dube M, Roy BB, Guiot-Guillain P, Binette J, Mercier J, Chiasson A, Cohen EA.** 2010. Antagonism of tetherin restriction of HIV-1 release by Vpu involves binding and sequestration of the restriction factor in a perinuclear compartment. PLoS Pathog **6:**e1000856.

42. **McNatt MW, Zang T, Bieniasz PD.** 2013. Vpu binds directly to tetherin and displaces it from nascent virions. PLoS Pathog **9:**e1003299.

43. **Jafari M, Guatelli J, Lewinski MK.** 2014. Activities of transmitted/founder and chronic clade B HIV-1 Vpu and a C-terminal polymorphism specifically affecting virion release. J Virol **88:**5062-5078.

44. **Lewinski MK, Jafari M, Zhang H, Opella SJ, Guatelli J.** 2015. Membrane Anchoring by a C-terminal Tryptophan Enables HIV-1 Vpu to Displace Bone Marrow Stromal Antigen 2 (BST2) from Sites of Viral Assembly. J Biol Chem **290:**10919-10933.

45. **Miyagi E, Andrew AJ, Kao S, Strebel K.** 2009. Vpu enhances HIV-1 virus release in the absence of Bst-2 cell surface down-modulation and intracellular depletion. Proc Natl Acad Sci U S A **106:**2868-2873.

46. **Bour S, Strebel K.** 2000. HIV accessory proteins: multifunctional components of a complex system. Adv Pharmacol **48:**75-120.

47. **DiDonato J, Mercurio F, Rosette C, Wu-Li J, Suyang H, Ghosh S, Karin M.** 1996. Mapping of the inducible IkappaB phosphorylation sites that signal its ubiquitination and degradation. Mol Cell Biol **16:**1295-1304.

48. **Kroll M, Margottin F, Kohl A, Renard P, Durand H, Concordet JP, Bachelerie F, Arenzana-Seisdedos F, Benarous R.** 1999. Inducible degradation of IkappaBalpha by the proteasome requires interaction with the F-box protein h-betaTrCP. J Biol Chem **274:**7941-7945.

49. **Sauter D, Hotter D, Van Driessche B, Sturzel CM, Kluge SF, Wildum S, Yu H, Baumann B, Wirth T, Plantier JC, Leoz M, Hahn BH, Van Lint C, Kirchhoff F.** 2015. Differential regulation of NF-kappaB-mediated proviral and antiviral host gene expression by primate lentiviral Nef and Vpu proteins. Cell Rep **10:**586-599.

50. **Rizk MG, Basler CF, Guatelli J.** 2017. Cooperation of the Ebola proteins VP40 and GP1,2 with BST2 to activate NF-kappabeta independently of virus-like particle trapping. J Virol doi:10.1128/JVI.01308-17.

51. **Zenner HL, Mauricio R, Banting G, Crump CM.** 2013. Herpes simplex virus 1 counteracts tetherin restriction via its virion host shutoff activity. J Virol **87:**13115-13123.

52. **Liu Y, Luo S, He S, Zhang M, Wang P, Li C, Huang W, Hu B, Griffin GE, Shattock RJ, Hu Q.** 2015. Tetherin restricts HSV-2 release and is counteracted by multiple viral glycoproteins. Virology **475:**96-109.

53. **Evans DT, Serra-Moreno R, Singh RK, Guatelli JC.** 2010. BST-2/tetherin: a new component of the innate immune response to enveloped viruses. Trends Microbiol **18:**388-396.

54. **Neil SJ.** 2013. The antiviral activities of tetherin. Curr Top Microbiol Immunol **371:**67-104.

55. **Lopez LA, Yang SJ, Hauser H, Exline CM, Haworth KG, Oldenburg J, Cannon PM.** 2010. Ebola virus glycoprotein counteracts BST-2/Tetherin restriction in a sequence-independent manner that does not require tetherin surface removal. J Virol **84:**7243-7255.

56. **Brinkmann C, Nehlmeier I, Walendy-Gnirss K, Nehls J, Gonzalez Hernandez M, Hoffmann M, Qiu X, Takada A, Schindler M, Pohlmann S.** 2016. The Tetherin Antagonism of the Ebola Virus Glycoprotein Requires an Intact Receptor-Binding Domain and Can Be Blocked by GP1-Specific Antibodies. J Virol **90:**11075-11086.

57. **Gustin JK, Bai Y, Moses AV, Douglas JL.** 2015. Ebola Virus Glycoprotein Promotes Enhanced Viral Egress by Preventing Ebola VP40 From Associating With the Host Restriction Factor BST2/Tetherin. J Infect Dis doi:10.1093/infdis/jiv125.

58. **Vande Burgt NH, Kaletsky RL, Bates P.** 2015. Requirements within the Ebola Viral Glycoprotein for Tetherin Antagonism. Viruses **7:**5587-5602.

59. **Anonymous.** 1978. Ebola haemorrhagic fever in Zaire, 1976. Bull World Health Organ **56:**271-293.

60. **Dixon MG, Schafer IJ, Centers for Disease C, Prevention.** 2014. Ebola viral disease outbreak--West Africa, 2014. MMWR Morb Mortal Wkly Rep **63:**548-551.

61. **Zawilinska B, Kosz-Vnenchak M.** 2014. General introduction into the Ebola virus biology and disease. Folia Med Cracov **54:**57-65.

62. **Fisher-Hoch SP, Brammer TL, Trappier SG, Hutwagner LC, Farrar BB, Ruo SL, Brown BG, Hermann LM, Perez-Oronoz GI, Goldsmith CS, et al.** 1992. Pathogenic potential of filoviruses: role of geographic origin of primate host and virus strain. J Infect Dis **166:**753-763.

63. **Regnery RL, Johnson KM, Kiley MP.** 1980. Virion nucleic acid of Ebola virus. J Virol **36:**465-469.

64. **Elliott LH, Sanchez A, Holloway BP, Kiley MP, McCormick JB.** 1993. Ebola protein analyses for the determination of genetic organization. Arch Virol **133:**423-436.

65. **Sanchez A, Kiley MP, Holloway BP, Auperin DD.** 1993. Sequence analysis of the Ebola virus genome: organization, genetic elements, and comparison with the genome of Marburg virus. Virus Res **29:**215-240.

66. **Noda T, Sagara H, Suzuki E, Takada A, Kida H, Kawaoka Y.** 2002. Ebola virus VP40 drives the formation of virus-like filamentous particles along with GP. J Virol **76:**4855-4865.

67. **Lee JE, Saphire EO.** 2009. Ebolavirus glycoprotein structure and mechanism of entry. Future Virol **4:**621-635.

68. **Lai CY, Strange DP, Wong TAS, Lehrer AT, Verma S.** 2017. Ebola Virus Glycoprotein Induces an Innate Immune Response In vivo via TLR4. Front Microbiol **8:**1571.

69. **Okumura A, Pitha PM, Yoshimura A, Harty RN.** 2010. Interaction between Ebola virus glycoprotein and host toll-like receptor 4 leads to induction of proinflammatory cytokines and SOCS1. J Virol **84:**27-33.

70. **Martinez O, Valmas C, Basler CF.** 2007. Ebola virus-like particle-induced activation of NF-kappaB and Erk signaling in human dendritic cells requires the glycoprotein mucin domain. Virology **364:**342-354.

71. **Andrew A, Strebel K.** 2010. HIV-1 Vpu targets cell surface markers CD4 and BST-2 through distinct mechanisms. Mol Aspects Med **31:**407-417.

72. **Iwabu Y, Fujita H, Kinomoto M, Kaneko K, Ishizaka Y, Tanaka Y, Sata T, Tokunaga K.** 2009. HIV-1 accessory protein Vpu internalizes cell-surface BST-2/tetherin through transmembrane interactions leading to lysosomes. J Biol Chem **284:**35060-35072.

73. **Mangeat B, Gers-Huber G, Lehmann M, Zufferey M, Luban J, Piguet V.** 2009. HIV-1 Vpu neutralizes the antiviral factor Tetherin/BST-2 by binding it and directing its beta-TrCP2-dependent degradation. PLoS Pathog **5:**e1000574.

74. **Schindler M, Rajan D, Banning C, Wimmer P, Koppensteiner H, Iwanski A, Specht A, Sauter D, Dobner T, Kirchhoff F.** 2010. Vpu serine 52 dependent counteraction of tetherin is required for HIV-1 replication in macrophages, but not in ex vivo human lymphoid tissue. Retrovirology **7:**1.

75. **Dube M, Roy BB, Guiot-Guillain P, Mercier J, Binette J, Leung G, Cohen EA.** 2009. Suppression of Tetherin-Restricting Activity upon Human Immunodeficiency Virus Type 1 Particle Release Correlates with Localization of Vpu in the trans-Golgi Network. Journal of Virology **83:**4574-4590.

76. **Skasko M, Tokarev A, Chen CC, Fischer WB, Pillai SK, Guatelli J.** 2011. BST-2 is rapidly down-regulated from the cell surface by the HIV-1 protein Vpu: evidence for a post-ER mechanism of Vpu-action. Virology **411:**65-77.

77. **Skasko M, Wang Y, Tian Y, Tokarev A, Munguia J, Ruiz A, Stephens EB, Opella SJ, Guatelli J.** 2012. HIV-1 Vpu protein antagonizes innate restriction factor BST-2 via lipid-embedded helix-helix interactions. J Biol Chem **287:**58-67.

78. **Hauser H, Lopez LA, Yang SJ, Oldenburg JE, Exline CM, Guatelli JC, Cannon PM.** 2010. HIV-1 Vpu and HIV-2 Env counteract BST-2/tetherin by sequestration in a perinuclear compartment. Retrovirology **7:**51.

79. **Le Tortorec A, Neil SJ.** 2009. Antagonism to and intracellular sequestration of human tetherin by the human immunodeficiency virus type 2 envelope glycoprotein. J Virol **83:**11966-11978.

80. **Lau D, Kwan W, Guatelli J.** 2011. Role of the endocytic pathway in the counteraction of BST-2 by human lentiviral pathogens. J Virol **85:**9834-9846.

81. **Zhang F, Landford WN, Ng M, McNatt MW, Bieniasz PD, Hatziioannou T.** 2011. SIV Nef proteins recruit the AP-2 complex to antagonize Tetherin and facilitate virion release. PLoS Pathog **7:**e1002039.

82. **Zhang F, Wilson SJ, Landford WC, Virgen B, Gregory D, Johnson MC, Munch J, Kirchhoff F, Bieniasz PD, Hatziioannou T.** 2009. Nef proteins from simian immunodeficiency viruses are tetherin antagonists. Cell Host Microbe **6:**54-67.

83. **Jia B, Serra-Moreno R, Neidermyer W, Rahmberg A, Mackey J, Fofana IB, Johnson WE, Westmoreland S, Evans DT.** 2009. Species-specific activity of SIV Nef and HIV-1 Vpu in overcoming restriction by tetherin/BST2. PLoS Pathog **5:**e1000429.

84. **Serra-Moreno R, Jia B, Breed M, Alvarez X, Evans DT.** 2011. Compensatory changes in the cytoplasmic tail of gp41 confer resistance to tetherin/BST-2 in a pathogenic nef-deleted SIV. Cell Host Microbe **9:**46-57.

85. **Kuhl A, Banning C, Marzi A, Votteler J, Steffen I, Bertram S, Glowacka I, Konrad A, Sturzl M, Guo JT, Schubert U, Feldmann H, Behrens G, Schindler M, Pohlmann S.** 2011. The Ebola virus glycoprotein and HIV-1 Vpu employ different strategies to counteract the antiviral factor tetherin. J Infect Dis **204 Suppl 3:**S850-860.

86. **Bartee E, McCormack A, Fruh K.** 2006. Quantitative membrane proteomics reveals new cellular targets of viral immune modulators. PLoS Pathog **2:**e107.

87. **Mansouri M, Viswanathan K, Douglas JL, Hines J, Gustin J, Moses AV, Fruh K.** 2009. Molecular mechanism of BST2/tetherin downregulation by K5/MIR2 of Kaposi's sarcoma-associated herpesvirus. J Virol **83:**9672-9681.

Chapter II

Understanding the role of the cytoplasmic tail of BST2 in trafficking and activation of NF-κB

Abstract

BST2 is an interferon-induced type-II transmembrane protein that traps newly assembled enveloped virions at the plasma membrane. A short cytoplasmic tail domain (CD) is located N-terminal of the transmembrane domain of BST2, followed by a rigid coil-coiled extracellular domain and a glycosylphosphatidylinositol (GPI)-anchor at the C-terminus. Certain viral proteins, such as the Vpu protein of the human immunodeficiency virus 1 (HIV-1), increase viral release by downregulating the levels of BST2 at the plasma membrane by various mechanisms including altering BST2 trafficking. BST2 also activates the NF-κB transcription factor as a potential proinflammatory anti-viral mechanism. Here, we inquired about the role of the cytoplasmic tail of BST2 for the trafficking of BST2 and the activation of NF-κB. In yeast two-hybrid (Y2H) assays, we showed that a conserved dual-tyrosine motif at position 6 and 8 of BST2 facilitates direct binding of the CD with the μ-subunit of the clathrin adaptor protein 1 (AP1), which allows the misdirection of BST2 away from the plasma membrane by Vpu. However, we found that tyrosine 8 was dispensable for the activation of NF-κB, while tyrosine 6 was required, possibly due to its phosphorylation by a src-family kinase, Syk. Syk kinase over-expression enhanced BST2-mediated NF-κB activity and induced a size-shift of a BST2 band in a tyrosine-dependent manner, as seen by Western blot. We also found that the cytoplasmic tail of BST2 alone is not sufficient to activate NF-κB. Overall, our data support the report by Galão et al. 2014 that showed the involvement of Syk kinase in BST2 signaling. In this study, we have enhanced the understanding of the mechanisms underlying BST2 trafficking and signaling and showed that the two processes require overlapping but distinct residues within the BST2 CD.

Introduction

BST2 (also called bone marrow stromal antigen 2, tetherin, CD317, or HM1.24 antigen) is a type-1 interferon induced type-II transmembrane protein. It restricts viral replication by inhibiting viral release from infected cells. BST2 has a cytoplasmic tail domain (CD) on the N-terminus, followed by the transmembrane domain, a long rigid coiled-coil extracellular domain, and a GPI-anchor on its C-terminus (1). This unique structure of BST2 allows it to physically trap newly assembled virions of enveloped viruses at the surface of the cell to prevent viral release (2, 3). The N-terminal domain of BST2 has been shown to play an important role in the natural trafficking and internalization pathways of BST2 (4). More recently, Galão et al. 2012 and Tokarev et al. 2013 showed that BST2 activates NF-κB in a manner dependent on tyrosine residues within the CD of BST2 (5, 6).

The human immunodeficiency virus 1 (HIV-1) has evolved mechanisms to antagonize the BST2-mediated entrapment of virions through its accessory protein called Viral protein U (Vpu). Vpu antagonizes BST2 by downregulating it from the plasma membrane and targeting it for degradation (7-10). One mechanism by which it reduces the levels of BST2 from the plasma membrane is that it misdirects the trafficking of BST2 along the endomembrane system, trapping it within the *trans*-Golgi network (TGN) (11, 12). Vpu has an N-terminal transmembrane domain followed by a flexible cytoplasmic tail (13). Clathrin-mediated trafficking pathways have been shown to faciliate the Vpu-mediated misdirection of BST2 (4, 14, 15). Clathrin adaptor protein (AP) complexes selectively bind to the cytoplasmic tails of cargo proteins based on specific sequences within these proteins. A tyrosine-based sorting motif (YxxΦ) and an acidic dileucine motif ([E/D]xxx[L/I]) in the cargo proteins allow for the binding of AP

complexes in order to mediate the binding of clathrin that leads to vesicle formation (reviewed in (16)). The AP1 complex mediates the clathrin-dependent recycling of proteins from the *trans*-Golgi network to endosomes (17). AP2 mediates clathrin-dependent endocytosis of cargo from the plasma membrane, while AP3 medites the trasport of cargo from endosomes to late endosome and lysosomes (reviewed in (18). The cytoplasmic tail of BST2 has a dual-tyrosine motif that has been previously shown to be involved in the natural trafficking of BST2 (4). Although the dual-tyrosine motif of the BST2CD (YxYxxV) does not conform to the canonical tyrosine-based motif (YxxΦ), we observed direct interactions between the two tyrosines of BST2 with μ1 of AP1 (19). Our group also showed that this motif YxYxxΦ (where Φ is a valine) in the BST2 CD and the ExxxLV motif in the VpuCD participate in the formation of a complex between BST2, HIV-1 Vpu, and AP1 complex (19).

BST2 also activates NF-κB in a TAK-1-depenent pathway that likely involves the formation of a complex with various proteins known to act upstream of the canonical NF-κB pathway (6). BST2 interacts with TRAF2, TRAF6, MyD88, TAB1, TAB2, TAK1, and Syk kinase upstream of NF-κB, as shown by immunoprecipitation (IP) data (6, 20). The interaction of BST2 with TAK1, TAB1, and Syk kinase is dependent on the dual-tyrosine motif of the BST2 cytoplasmic tail (6). A short-form of BST2 that is translated at the thirteenth residue (lacking the first 12 residues which include tyrosines 6 and 8) was defective for activating NF-κB, highlighting the importance of the first 12 residues of the protein towards signaling (21). The same short form of BST2 was non-responsive to the downregulation from the plasma membrane by the HIV-1 Vpu protein, demonstrating the requirement of these first 12 residues of BST2 for the antagonistic function of Vpu

(21). Since the same dual-tyrosine motif is important for both the activation of NF-κB and the downregulation of BST2 from the plasma membrane by Vpu, understanding whether the two functions are mechanistically related can enhance our understanding of the relationship between BST2 sorting and the activation of NF-κB. One study proposed that phosphorylation of one or both tyrosines of BST2 by Syk kinase is required for the activation of NF-κB (20), which suggests that signaling may be a distinct function from sorting of BST2 by the clathrin adaptor proteins.

In order to better understand the mechanism of BST2 CD in trafficking and signaling, we tested for the direct interaction of BST2 CD with the AP-1 μ1 subunit and some of the signaling mediators listed above using yeast 2-hybrid assays. We found that BST2 binds to μ1 in a manner dependent on both tyrosines 6 and 8, while it did not bind to any of the signaling mediators tested. Also, we found that for signaling, only the tyrosine 6 was required but not tyrosine 8, suggesting that two functions use distinct mechanisms while the residues involved overlap. We performed phosphorylation-immunoprecipitation (phopho-IP) experiments in order to determine whether the tyrosine residues of the BST2 cytoplasmic tail are phosphorylated. We found a band by Western Blotting that suggested the phosphorylation of the BST2 tyrosines, in agreement with previously published results (20). We also showed that the over-expression of Syk kinase produced a size-shift of a BST2 band by Western blot of total lysates in a tyrosine 6/8-dependent manner. Thus, our data provide support for the distinct roles of the CD tyrosines towards BST2 sorting and the activation of NF-κB. The data, however, leave open the question of how the phosphorylation of BST2 is induced and whether this phosphorylation could inhibit binding of BST2 to AP1 μ1.

Materials and Methods

Tissue culture, plasmids, and reagents

HEK293T cells (a gift from Nathaniel Landau at New York University) were maintained in Dulbeco's Minimum Essential Media (DMEM) already containing high glucose and L-glutamine (Gibco Thermofisher, Waltham, MA, USA) and supplemented with 10% Fetal Bovine Serum (FBS) (Gimini Bio Products, West Sacramento, CA, USA), 1% Pen/Strep (Gibco), 1X non-essential amino acids (NEAA) (Gibco), and 1X sodium pyruvate (Gibco).

pcDNA3.1-BST2-WT expression plasmid was described previously (6). Point mutations shown in Figure II.3 were created in the BST2 cytoplasmic domain within the pcDNA3.1-BST2 expression plasmid using the Quikchange mutatgensis kit (Agilent, Santa Clara, CA, USA). pcDNA3.1-BST2 -Y6A, -Y8A, -Y6,8A, -V11A, and -V11G were described previously in Jia et al., 2014 (19). Hemagglutinin (HA)-tagged constructs of artificial-BST2 (labeled as Art-Tetherin-HA and dTM Art-Tetherin-HA) were a gift from Paul Bieniasz at Rochefeller University and described previously (22). The N-term WT Art-HA construct, which contains a cytoplasmic tail of the BST2-WT protein, was a gift from George Banting at the University of Bristol and described previously (23). The following plasmids were a gift from Submit Chanda at the Sanford Burnham Prebys Medical Discovery Institute: pXL304-hSyk-V5, pXL304-hLCK-V5, pXL304-hHCK, and pXL304-hCSK. Yeast-expression plasmids pACT2 encoding μ1, μ2, and μ3 and pGBT9 plasmids encoding TGN38 and its tyrosine-to-alanine mutant were obtained from Juan Bonifacino at the National Institutes of Health. pGBT9 plasmids expressing BST2 cytoplasmic domain (BST2 CD) were created by sub-cloning of the first 21 amino acids

of BST2 from the pcDNA3.1-BST2 plasmid using primers for the amplification of the N-terminal end. The BST2 CD WT and mutants were cloned downstream of the yeast GAL4-DNA binding domain (GDB) of the pGBT9 plasmid vector with the *EcoR*I and *Sal*I restriction sites within the multiple cloning site. A flexible linker sequence (GGGSGGGSGGGS) was inserted between the GDB and the BST2CD. pACT2 plasmids expressing human TRAF2, TRAF6, TAK1, and TAB1 were created by subcloning the full-length sequences from pcDNA3.1 expression plasmids in the pACT2 vector. MyD88 and TAB2 were each subcloned into the pACT2 vector as domains (as shown in Figure II.1C). These genes were cloned downstream of the yeast GAL4-activation domain (AD) sequence. pGL4.74 [hRluc/TK] plasmid expressed the reporter *Renilla* luciferase (Promega) under the transcriptional control of a herpes sarcoma virus thymidine kinase promoter. pGL4.32 [luc2P/NF-κB-RE/Hygro] NF-κB firefly luciferase (Promega) plasmid expressed firefly luciferase under the transcriptional control of five copies of an NF-kβ response element.

Polyclonal rabbit anti-BST2 antibody was purchased from the NIH Acquired Immunodeficiency Syndrome Reagent Program (Germantown, MD, USA). Phospho-tyrosine mouse monoclonal antibody against phosphotyrosines (clone P-Tyr-100) and phospho-Syk anibody (clone Tyr323) were purchased from Cell Signaling Technologies (Beverly, MA, USA). Anti-Syk antibody (clone Syk-01) was purchased from BioLegend, Inc. (San Diego, CA, USA). Sodim orthovanadate, lithium acetate dihydrate, and 3-Amino-1,2,4-triazole (3AT) were purchased from Millipore Sigma (St. Louis, MO, USA).

Yeast 2-hybrid assays

AH109 yeast cells (Clontech Laboratories, Inc, Palo Alto, CA, USA) were grown on agar plates made with YPD yeast grown media. Colonies were expanded in YPD liquid media and then used for lithium acetate/herring sperm single-stranded carrier DNA (Clontech Laboratories) with polyethylene glycol (PEG 3350, Millipore Sigma) transformation of target plasmids. Co-transformants expressing GAL4-AD and GAL4-DBD upstream of the target proteins were grown on 2-amino acid dropout (-2DO; -Leu/-Trp) agar plates to assess the success of the transformations. To determine whether an protein-protein interaction occurred, transformants were pooled and then spotted on -3 amino acid dropout plates (-3DO; -Leu/-Trp/-His), as well as -2 for the visual comparison of the spots.

Immunoprecipitation, SDS/PAGE, Western blotting

HEK293T cells were grown in 6-well plates using antibiotic-free DMEM with 10% FBS. The next day, the cells were transfected with pcDNA3.1-BST2 (WT or mutants) using Lipofectamine2000 according to the manufacturer's protocol (Thermo Fisher Scientific, Waltham, MA, USA). At 24-hrs post transfection, the cells were treated with 200μM sodium pervandate to inhibit tyrosine phosphatases for an hour. Cells from two wells of a 6-well plate were pooled together and lysed in the presence of 200μM active sodium orthovandate and protease inhibitors. Anti-mouse or anti-rabbit Dynabeads Magnetic Beads (Thermo Fisher Scientific) were allowed to bind to the primary antibodies overnight and then blocked with 3% bovine serum albumin for about 2-hrs prior to being added to the cleared cellular lysates.

IP samples were eluted off the beads using Laemmli buffer and assayed by SDS/PAGE (sodium dodecyl sulfate polyacrlamide gel electrophoresis) followed by

Western blotting in comparison to the total cells lysates. TrueBlot anti-rabbit and anti-mouse secondary antibodies (Rockland Immunochemicals, Inc., Limerick, PA, USA) were used for the detection of the primary antibodies against target proteins on the Western blots.

Dual-luciferase signaling assay

HEK293T cells were plated on the first day in 12-well plates in antibiotic-free DMEM with 10% FBS. The next day, the cells were transfected as indicated above. At 24-hrs after transfection, the cells were collected and used to perform the dual-glo luciferase assay from Promega (Madison, WI, USA) according to the manufacturer's protocol. Firefly luciferase activity, indicating NF-κB activity, was measured first, quenched, and the *Renilla* luciferase was measured subsequently within the same wells. NF-κB-firefly values were divided by the *Renilla* values to obtain the fold change over background activity. Fold changes were normalized over the negative control sample (pcDNA ctrl) to obtain the values presented in the box and whiskers graphs.

Statistical analysis

The Wilcoxon Rank Sum test was used to determine whether NF-κB activities differed significantly between different groups. *P*-values presented in Table II.2 represent significance within two-group comparisons, where each group contains four technical replicates.

Results

The YxYxxV sequence of the cytoplasmic tail of BST2 facilitates direct binding of BST2 to the μ-subunit of the clathrin adaptor protein 1.

BST2 restricts virions by trapping them at the plasma membrane of infected cells. However, HIV-1 Vpu antagonizes this function of BST2, preventing the entrapment of virions by BST2 at the plasma membrane. One of the routes by which Vpu reduces BST2 levels at the plasma membrane is to trap BST2 within endosomal vesicles or the *trans*-Golgi network (24). In this study, we wanted to understand the structural features governing the interaction of the BST2 cytoplasmic domain (CD) with the AP1 complex in response to Vpu. To do this, our group studied the interactions among VpuCD, BST2CD, and the endosomal trafficking machinery that uses clathrin adaptor protein complexes 1, 2, and 3 (AP1-3). We found that an interaction-complex forms between BST2CD, VpuCD, and subunits of the AP1 complex by determining the crystal structure of a BST2CD-VpuCD fusion protein with μ1 (19). This interaction was dependent on tyrosine 6 and 8 and valine 11 of BST2, while it was dependent on the ExxxLV motif of Vpu (19). Using *in vitro* pull down assays, we found that there was no direct interaction between BST2CD and the μ2 and μ3 subunits of the AP2 and AP3 complexes (19). To confirm these phenotypes in an *in vivo* eukaryotic expression system, we performed yeast 2-hybrid experiments and showed that BST2CD directly bound to the μ1-subunit of AP1 but not to the μ2- and μ3-subunits of AP2 and AP3 (Figure II.1.A). Again, we demonstrated that this interaction was dependent on the dual tyrosine motif at positions 6 and 8 in addition to the hydrophobic valine residue at position 11 (YxxYxxV) in the cytoplasmic tail of BST2 (Figure II.1B and (19)). The crystal structure of the interaction

between BST2CD and AP1 μ1 showed that all three residues of BST2 (Y6, Y8, and V11) participate in the interaction (Figure II.2 and (19)). Overall, our data showed that the direct binding of BST2 to the μ-subunit of the AP1 complex was dependent on a non-canonical dual-tyrosine motif within the cytoplasmic tail of BST2, since the participation of Y6 does not follow the YxxΦ typical cargo recognition motif. Finally, we showed that Vpu hijacks this interaction by also binding to AP1 subunits, γ, σ1, and μ1 (19), in order to keep BST2 trapped within endosomal compartments or the TGN and away from the plasma membrane.

Tyrosine 6 of the BST2CD drives the activation of NF-κB, but the CD alone is not sufficient for activity.

We next sought to understand the role of the BST2CD towards the activation of NF-κB. We, and others, had previously shown that the dual-tyrosine motif (YxY) was important for NF-κB activity (Galao et al., 2012; Tokarev et al., 2013). In this study, we wanted to further inquire about the individual roles of tyrosines 6 and 8 in addition to the valine 11 residues towards signaling. We used a HEK293T transient transfection system to over-express BST2 and tested for its ability to induce NF-κB activity using a luciferase reporter system (see Materials and Methods section). We observed that BST2 signaling required tyrosine 6, and neither tyrosine 8 nor valine 11 (Figure II.3.B, C). Our results here confirmed findings by Galão et al., 2014 (20). Since tyrosine residues of signaling proteins can be phosphorylated through the substitution of their hydroxyl group with the negatively charged phosphoate group, we wanted to test whether mutating the tyrosines to phenylalanines would inhibit signaling. Phenylalanines are similar in structure to tyrosines but lack the hydroxyl group and thus

do not become phosphorylated. We hypothesized that if the hydroxyl group, and thus phoshprylation, were dispensable, then NF-κB activity would not be impaired in the Y6F mutant (Figure II.3.A). We found that both the Y6F and Y8F single mutants were impaired for signaling compared to WT (Figure II.3B and Table II.2), suggesting that phosphorylation is likely required and that tyrosine 8 can play a role in signaling. A mutation of both tyrosines together to phenylalanines also significantly diminished signaling similarly to the alanine double mutation (Figure II.2B and Table II.2). Since phosphate groups are negatively charged, we wanted to test whether having a negative charge at either tyrosine would produce signaling activity. We found that the glutamic acid mutants behaved in a manner similar to the alanine mutants, where Y6E and Y6/8E were significantly impaired for signaling while the Y8E was not (Figure II.3B). Overall, these data suggest that tyrosine 6 is likely phosphorylated and that phosphorylation at this residue is needed for optimal activation of NF-κB by BST2. Finally, since having a bulky hydrophobic residue at tyrosine 8 intermediately impaired signaling, tyrosine 8 appears to have a role in signaling that may not require phosphorylation of the tyrosine.

We observed that tyrosine 8 was required for AP1 μ1 binding, while it was dispensable for the activation of NF-κB, which suggested that BST2's cytoplasmic tail has distinct functions that require different but overlapping residues. To further this distinction, we tested two valine mutants of BST2 for their ability to activate NF-κB. We found that mutating valine to alanine or glycine produced NF-κB activity that was similar to the BST2-WT (Figure II.3C). Thus, we concluded that the valine is dispensable for

signaling, providing further evidence to support the distinction between the trafficking and signaling determinants within the cytoplasmic tail of BST2.

Next, we asked whether the cytoplasmic tail of BST2 alone was sufficient to activate NF-κB. We used an artificial tetherin (Art-tetherin) that contains domains from various proteins fused together to re-create a structurally similar protein that contained the BST2-WT cytoplasmic tail, the transmembrane domain of the transferring receptor the coiled-coil domain of DMPK, and the GPI-anchor signal of uPAR (22). As controls, we used full-length artificial tetherin and a mutant that lacked the transmembrane domain (Figure II.3D). We tested these three artificial tetherins for the ability to induce NF-κB activity and found that none of them were able to signal (Figure II.3D). We confirmed that all of the artificial tetherin proteins were expressed by Western blot (Figure II.3D). Since the Art-tetherin containing the WT CD of BST2 did not signal despite being expressed, we concluded that the cytoplasmic tail of BST2 is not sufficient to induce activity. This finding suggests that additional domains within the BST2 proteins maybe required for the activation of NF-κB.

BST2 is tyrosine-phosphorylated at Y6 and Y8.

Since our mutants of the BST2 cytoplasmic tail showed that phosphorylation is likely important for signaling, we wanted to determine the phosphorylation state of BST2 by phosphotyrosine-immunoprecipitation (phospho-IP) followed by Western blot. In order to inhibit the activity of phosphatases and retain high levels of phosphoproteins in the cells, we treated HEK293T cells that were transfected with BST2 WT or the tyrosine mutants with sodium pervanadate for one hour prior to harvesting the cells (see Materials and Methods for details). We confirmed that the total levels of

phosphotyrosine proteins detected in whole cell lysates were increased in a time-dependent manner post treatment with sodium pervanadate (Figure II.4A). When we performed an IP against BST2 and probed the Western blots for phosphotyrosines, we found smears of pulled-down phosphoproteins that were detected for WT BST2 and the single tyrosine mutants (Y6A and Y8A) but not for the dual tyrosine mutant (Y6/8A) (Figure II.5B). This finding suggested that there may be co-factors of BST2 that are tyrosine-phosphorylated and that these co-factors depended on the presence of either tyrosine 6 or 8, but dissociate from BST2 when both tyrosines were mutated. However, we were not able to observe a band that was clearly BST2 on the blot. We next pulled down total phosphotyrosine proteins and immunoblotted for BST2 (Figure II.4C). We found a band around 23kDa in the BST2-WT lane that was present to a lesser extent in the tyrosine mutant lanes (Figure II.4C) suggesting that BST2 was phosphorylated as a WT protein. This also suggested that both tyrosine 6 and 8 maybe phosphorylated to certain extents despite not being equally required for NF-κB activity. Since we had found that tyrosine 8 might play a role in signaling, tyrosine phosphorylation of this residue may be a compensatory mechanism for phospho-Y6-mediated signaling. Alternatively, phosphorylation of tyrosine 8 could occur as a secondary process that is not directly required for signaling.

The over-expression of Syk kinase increased NF-κB activation by BST2.

One report showed, by siRNA knockdown studies, that Syk kinase is important for the ability of BST2 to activate NF-κB (20). However whether Syk acts upstream or downstream of BST2 is unclear and whether Syk kinase itself phosphorylates BST2 is unknown. We asked whether the over-expression of Syk and additional src-family

kinases, HCK, LCK, and CSK, could enhance BST2-mediated activity. We over-expressed these kinases using various amounts of plasmid to determine their effect on BST2-signaling (Figure II.5). Co-expression of Syk at 300ng and 330ng with BST2 produced NF-κB activity that was statistically more significant than that produced by BST2 alone or Syk alone (Figure II.5A). Statistics were determined using the Kruskull-Wallis test followed by a Dunn's multiple comparisons test (p-values not shown). In contrast, NF-κB activity as a result of the co-expression of LCK, HCK, or CSK with BST2 did not result in statistically significant enhancement (Figure II.5B,C,D). Overall, our data provide further support of the important role of Syk towards BST2-mediated activation of NF-κB. However, whether NF-κB activity increases due to the phosphorylation of BST2 by Syk remained unclear.

We attempted to address the question of how Syk affects BST2 by performing another co-expression experiment and observing BST2 expression by Western blot. We found that the co-expression of Syk with BST2-WT, but not BST2-Y6/8A mutant, produced a shift in one of two prominent bands of BST2 (Figure 6 – lane with the asterisk "*"). We predict that this shifted upper band is the full-length BST2, which contains the first 12 amino acids of BST2 (Figure II.3A), since this is the form of BST2 in which the tyrosines are present. This size-shift of BST2 highly suggests that Syk directly phosphorylates BST2 in a manner dependent on tyrosines 6 and 8, although further studies using the single tyrosine mutants will be required to determine whether both or only one of the tyrosines is responsible for this shift. Also, inhibiting the activity of Syk using either a kinase-dead mutant of Syk or a chemical inhibitor of Syk kinase activity,

such as Bay61, would further clarify whether Syk kinase activity is specifically required for the size-shift of BST2.

BST2 does not directly bind to signaling co-factors upstream of NF-κB in the Y2H assay.

Using the yeast 2-hybrid assay approach, we wanted to determine whether the cytoplasmic tail of BST2 could directly bind to the six signaling mediators that were previously shown to co-immunoprecipitate with BST2: TAK1, TAB1, TAB2, TRAF2, TRAF6, and MyD88 (6). These six proteins are important mediators of the activity of innate immune receptors such as the Toll-like receptor 4 (TLR4) upstream of NF-κB activation (reviewed in (25). One of the caveats of testing direct binding of these proteins to BST2 in this assay is that if phosphorylation were required for signaling, then it could also be required for binding to these co-factors. Thus, without phosphorylation of BST2 in yeast, which might require Syk expression, false negative results would be obtained from the Y2H assay. Nonetheless, we wanted to eliminate the possibility that BST2 CD, without Syk, would still bind to any of these proteins. Indeed, we did not observe binding of any of these co-factors with BST2 except for the death-domain of MyD88 (Figure II.7A and C). This observation about MyD88, however, was not reproducible in a second experiment (data not shown). We split the MyD88 and Tab2 into two domains for the Y2H experiments due to the toxic effects of the full-length proteins on the yeast cells. We confirmed the success of the yeast transformations using a 2-amino acid dropout agar plates (-Leu/-Trp) and by Western blotting of a select set of samples as further confirmation (Figure II.7A and B). In Figure II.7A, we used TGN38 and μ1 as positive controls for the assay to test for direct protein-protein

interactions on 3-amino acid dropout agar plates (-Leu/-Trp/-His). As a negative control, we co-expressed a mutant μ1 with TGN38. These data suggest that direct protein-protein interactions of the BST2CD with the various signaling mediators do not occur in this yeast 2-hybrid system. Adding Syk to the cells as part of a yeast 3-hybrid system may provide further information regarding whether phosphorylation would be required for binding of the BST2 CD to the various signaling proteins tested.

Discussion

In this study, we investigated the role that the cytoplasmic tail domain of BST2 plays in sorting of the protein and the activation of NF-κB. We found that the BST2 cytoplasmic tail tyrosines 6 and 8 and valine 11 are all required for the direct binding of BST2CD with μ1 subunit of the clathrin adaptor protein 1, which also binds to Vpu in order to misdirect the sorting of BST2 away from the plasma membrane (19). We also found that BST2-mediated activation of NF-κB requires a tyrosine at position 6 in order to activate NF-κB and that tyrosine 8 plays a role in signaling that appears to be indirect. We provided further evidence to support a previously published report by Galão et al., 2014 indicating that BST2 tyrosines 6 and 8 are phosphorylated. Our mutagenesis signaling experiments of BST2 suggest that BST2 tyrosine 6 needs to be phosphorylated in order to activate NF-κB, while the phosphorylation of tyrosine 8 appears to be dispensable for signaling, although we suggest that it could play a compensatory role. We show evidence that Syk kinase enhances BST2-mediated signaling likely due to phosphorylation of the tyrosines, although additional experiments will be required to show the specific connection between the kinase activity of Syk and BST2-mediated signaling. Additionally, we found that the cytoplasmic tail domain of

BST2 alone was not sufficient to activate NF-κB, suggesting that other domains within the BST2 protein are needed for signaling. Finally, we found that, in yeast cells, the BST2CD does not bind to a set of signaling co-factors that are known to participate downstream of the TLR4-signaling pathway and that have been previously shown to co-immunoprecipitation with BST2. This lack of binding could be partially explained by the lack of BST2 CD phosphorylation of the tyrosines, which could be required for the binding of these proteins to BST2.

One of the caveats of this study is the use of HEK293T cells that transiently over-express BST2. In this system, one issue that could affect the signaling activity as compared to an endogenous BST2 expression system is the variable ratio of short and long forms within BST2 dimers from experiment to the next. Since the short form is missing the first twelve amino acids, which contain tyrosine 6 and 8, the amount of translated short BST2 can change the levels of NF-κB activity due to the formation of heterodimers of short and long BST2, as has been previously shown (21). In this study by Cocka and Bates, homodimers of the long form of BST2 produced maximal NF-κB activation, while mixtures of long and short forms of BST2 were gradually impaired with increasing amounts of the short form of BST2 (21). As demonstrated by the Western blots in Figure II.6, our system likely expresses both the short and the long forms of BST2, which means that some of the observed effects may vary from one experiment to the next due to the varying ratios of the two forms from experiment to the next. However, the same study showed that HeLa and primary CD4 T-cells, which endogenously express BST2 also produce two bands of BST2 that are designated as long and short form. Thus, having both forms within the system does not take away

from the endogenous-like state of producing both forms of BST2 within the same cells. We also show that the tyrosines 6/8 mutant in Figure II.6 also expresses two bands, suggesting that the impaired NF-κB was not due to an overloaded expression of the short form. In fact, the blot in Figure 11.6 shows that the BST2-Y6/8A mutant long form is better expressed compared to the long form in the BST2-WT. This strengthens our conclusion that the tyrosines play an important role in BST2 signaling activity.

In order to better understand the role of how the tyrosine residues mediate signaling, we performed three sets of mutagenesis experiments to mutate one or both tyrosine residues to alanine, phenylalanine, or glutamic acid. We tested the ability of these mutants to activate NF-κB. Our results here demonstrated that tyrosine 6 is required for the signaling activity, likely due to phosphorylation of this residue. However, since the mutagenesis of tyrosine 8 to phenylalanine impaired signaling significantly, we propose that the residue of position 8 is required for signaling, possibly due to tyrosine phosphorylation although phosphorylation of this residue is likely dispensable due to the unimpaired signaling of the Y8A and Y8E mutants. We suggest that tyrosine 8 may have complementary or compensatory roles towards signaling. Galão et al., 2014 suggested that Syk kinase could be binding to BST2 that has been phosphorylated at tyrosine 6 and that the phosphorylation of tyrosine 8 is secondary as a way of stabilizing the interaction. However, the model of stabilizing the interaction does not fully support the notion proposed by the same group that Syk recognizes BST2 cytoplasmic tail dimers which form a hemITAM motif (20). How tyrosine 8 would stabilize the interaction with Syk, which already recognizes two phosphotyrosine residues, would require further investigation of the structural requirements of this interaction.

Interestingly, we showed that the same tyrosine residues within the cytoplasmic tail of BST2 were required for direct binding of the BST2CD to the μ1 subunit of the AP1 complex. This binding was observed both in vitro pull down assays (19) and yeast 2-hybrid assays, where the BST2CD is not likely phosphorylated. Therefore, it follows that binding of BST2 to μ1 through tyrosine residues 6 and 8 of BST2 does not require their phosphorylation. Since tyrosine 6 of BST2CD appears to play the major role towards signaling, while both tyrosine and valine 11 are required for the binding to μ1, we propose that there are dual mechanistic roles for the BST2 tyrosines. One role mediates sorting while the other mediates signaling. We suggest that if the activation of NF-κB by BST2 requires tyrosine phosphorylation, this process could potentially be inhibitory towards the binding of BST2 with μ1, or vice versa, where the blocking of the tyrosine residues by AP1 in the presence of Vpu prevents the phorphorylation of BST2. A similar model has been previously suggested for the receptor called cytotoxic T-lymphocyte-associated 4 (CTLA-4) where phosphorylation of its cytoplasmic tail tyrosines inhibits the binding of the AP2 complex and endocytosis (26). Further studies will be required in order to understand the distinct roles of the cytoplasmic tail tyrosines of BST2 towards signaling and trafficking. Whether inducing BST2 activation or phosphorylation reduces BST2 binding to AP1 in the context of HIV-1 proviral expression with Vpu expression will be interesting as a potential way of impairing the effect of Vpu on the misdirection of BST2.

Additionally, we observed no direct protein-protein interaction in the yeast cells between BST2 and the signaling mediators that we tested here: Tab1, Tab2, Tak1, TRAF2, TRAF6, and MyD88. There are various potential explanations for the lack of

binding. The first is that if BST2 requires phosphorylation for signaling, it might also require phosphorylation for the binding to any of the proteins above. Since μ1 bound to BST2 in the yeast and we propose that this binding might actually be inhibited by phosphorylation, we suggest that BST2 is unlikely phosphorylated in yeast, which could explain the lack of binding. Another possibility is that these proteins are, in fact, not direct-binding partners of BST2 despite being able to form as a complex in human cells. The complex formation might require additional adaptors that are not yet known. Performing anti-BST2 IP followed by mass spectrometry of the IP sample under various conditions such as viral protein expression, treatment with sodium pervanadate, or over-expression of Syk kinase could potentially identify such adaptors. Also, performing yeast 2-hybrid and BST2/Syk 3-hybrid screens could identify direct-binding partners of BST2, which would expand on our understanding of BST2 signaling and BST2-mediated entrapment of virions as well as open the door towards understanding additional unknown functions of BST2.

We do not currently have a full understanding of the role of the Syk kinase towards BST2 signaling. BST2 was shown to co-immunoprecipitate with Syk kinase in a manner dependent on tyrosines 6 and 8 (20); however, whether Syk binds to phosphorylated BST2 or whether Syk itself phosphorylates BST2 is not fully understood. Our data support the hypothesis that Syk phosphorylates BST2 due to the change in BST2 band size observed by Western blot. In correlation, we observed that Syk kinase overexpression enhanced BST2-mediated signaling suggesting that increases in BST2-phosphorylation also increase activity of NF-κB. Additional studies are needed in order to determine whether the enhanced NF-κB activity and the change

in the size of BST2 band are dependent on the kinase activity of Syk. So far, we showed that this size-shift of BST2 is dependent on tyrosine 6 and 8. A follow-up experiment to determine whether both tyrosine residues or just one is phosphorylated will help decipher the order of events as affected by Syk.

Overall, in this study we observed the differing roles that the BST2 cytoplasmic tail plays in trafficking and NF-κB activity. We demonstrated that the expression of the BST2CD could serve as a potentially useful tool for the identification of BST2-binding partners that do not require the phosphorylation of the cytoplasmic tail tyrosines. A yeast 2-hybrid screen using a library of human cytoplasmic proteins could serve as a tool to enhance the understanding of BST2 function. We also showed that both tyrosines of BST2 play roles in signaling although tyrosine 6 phosphorylation is required while phosphorylation of tyrosine 8 is likely dispensable. Finally, we demonstrate that the over-expression of Syk kinase can be used to understand its role towards BST2-mediated NF-κB activation.

Acknowledgements

The work was supported in part by The James B. Pendleton Charitable Trust, the UCSD CFAR, and the San Diego Fellowship to M.G.R.

We thank Ned Landaw for providing the HEK293T cells. We thank George Banting, Juan Bonaficino, Paul Bieniasz, and the NIH AIDS Reagent Program for providing antibodies and plasmids as indicated in the Materials and Methods section. We thank Sonia Jain and Feng He from the University of California San Diego Center for AIDS Research (UCSD CFAR) Biostatistics Core for their help with statistical

analysis. We thank Andrey Tokarev for training on molecular and cell biology techniques.

Chapter II, in part, is a reprint of the material as it appears in Jia X, Weber E, Tokarev A, Lewinski M**,** Rizk M**,** Suarez M, Guatelli J, Xiong Y. 2014. Structural basis of HIV-1 Vpu-mediated BST2 antagonism via hijacking of the clathrin adaptor protein complex 1. *eLife* **3:**e02362. The dissertation author was a contributing author of this paper.

Figures and Tables

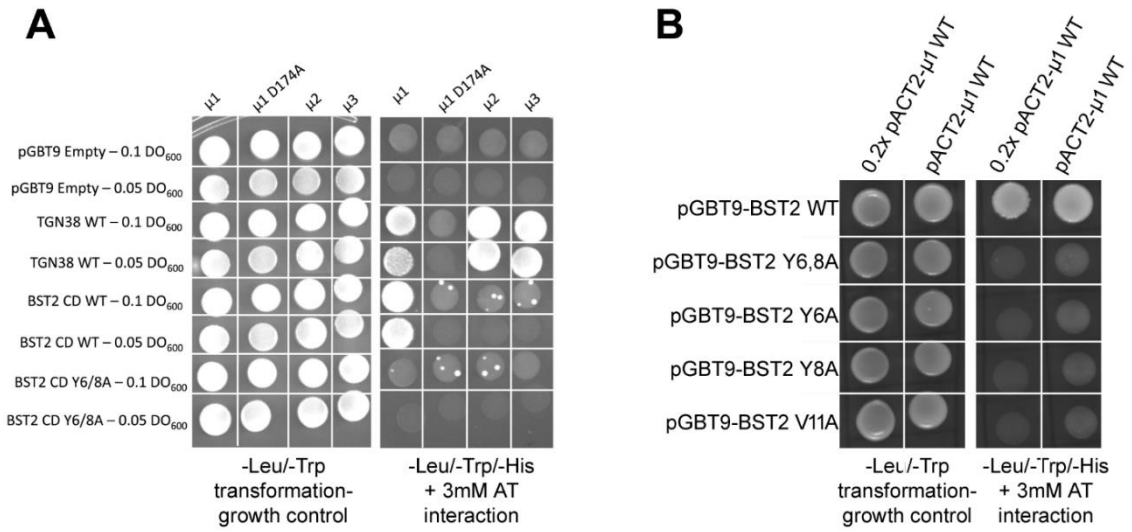

Figure II.1 Yeast 2-hybrid assays showing interaction of the BST2 cytoplasmic domain (BSDT2 CD) and μ-subunits. A) Binding of BST2CD to μ1, but not μ2 or μ3. Growth on -3DO media (-Leu/-Trp/-His) + 3mM 3AT plates indicate the direct interaction between the proteins. Growth on the -2DO (-Leu/-Trp) plates serves as a growth control to ensure that the transformations were successful. '0.5x' indicates plating of one-half the amount of yeast cells relative to other spots. The BST2CD-μ1 interaction is abolished by the tyrosine motif mutation Y6/8A in the BST2CD or the tyrosine-binding pocket mutation D174A in μ1. B) Same assay as shown in A using various mutants of the BST2CD. '0.2x' indicates plating of one-fifth the amount of yeast cells relative to other spots. The BST2-μ1 interaction is abolished by the alanine mutations of the BST2 Y6/8A, Y6A, Y8A, or V11A. [These panels were modified from Jia et al., 2014 and shown here with permissions].

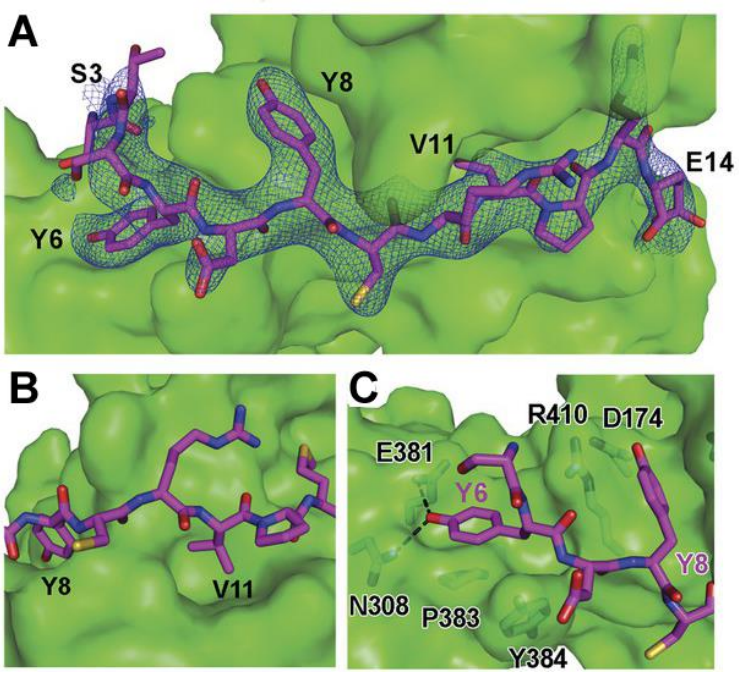

Figure II.2 Structural features of the interaction between BST2 and μ1. A) Difference Fourier map (blue mesh) of BST2CD (magenta sticks) binding to μ1 (green surface). Important residues in BST2CD are labeled. B) V11 partly fills the canonical Φ residue binding-side on μ1. C) Y6 and Y8 residues of BST2 make extensive interactions to μ1. Hydrogen bonds are indicated with dashed lines. [This figure was modified from Jia et al., 2014 and shown here with permissions].

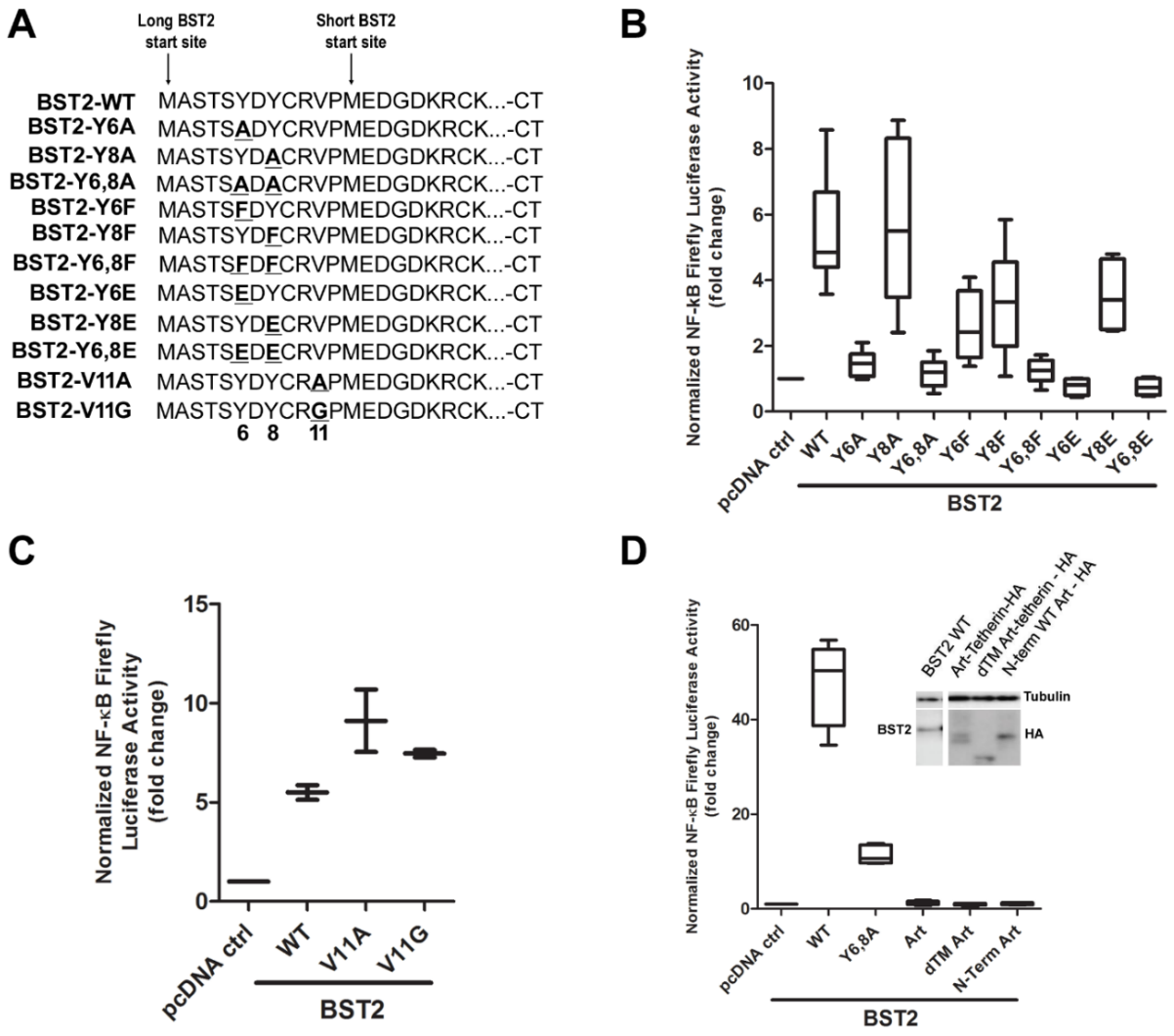

Figure II.3 NF-κB activity requires tyrosine 6 of the BST2 cytoplasmic domain, but the CD alone is not sufficient for signaling. A) Sequences of the cytoplasmic N-terminal domain of BST2 WT and the various mutants used for the signaling experiment. At position 13, an alternate shorter form of BST2 can be coded (labeled as “short BST2 start site”). Full length BST2 start site is labeled as “long BST2 start site”. B) HEK293T cells transiently transfected with BST2 and the luciferase reporter plasmids. NF-κB activity of the various BST2 tyrosine mutants normalized to a negative control (sample transfected with pcDNA3.1 empty plasmid vector alone; pcDNA ctrl). See Materials and Methods section for more details. The box and whiskers represent data from four technical replicates. C) NF-κB activity of the valine 11 mutants of BST2. Normalized fold changes were obtained similarly to those in panel B. The box and whiskers represent data from four technical replicates. D) HEK293T cells transfected with the artificial tetherin genes, which express various domains that are similar to BST2 in structure but not sequence, except for the N-term WT Art that contains the cytoplasmic tail of WT BST2. See Materials and Methods section for more details. The box and whiskers graph represents two technical replicates.

Table II.1 Normalized fold value of NF-κB activity presented in Figure II.3B.

					Percentile	
	Group	**Median**	**Min**	**Max**	**25th**	**75th**
BST2	**WT**	4.843	3.577	8.577	4.391	6.68
	Y6A	1.455	0.9797	2.1	1.073	1.748
	Y8A	5.499	2.408	8.867	3.478	8.32
	Y6,8A	1.202	0.5502	1.849	0.7821	1.501
	Y6F	2.42	1.378	4.089	1.649	3.673
	Y8F	3.333	1.075	5.847	1.991	4.551
	Y6,8F	1.253	0.6513	1.723	0.9369	1.56
	Y6E	0.8112	0.4369	1.006	0.4923	0.9957
	Y8E	3.402	2.463	4.798	2.502	4.644
	Y6,8E	0.7322	0.4643	1.054	0.5005	1.004

Table II.2 Statistical analysis of the NF-κB activity values presented in Figure II.3B.

		Wilcoxon Rank Sum	
Group 1	**Group 2**	**p-value**	**Significant?**
pcDNA ctrl	BST2 WT	0.0002	Yes
		pcDNA ctrl = 1	
BST2 WT	Y6A	0.0002	Yes
	Y8A	0.8785	No
	Y6,8A	0.0002	Yes
	Y6F	0.0011	Yes
	Y8F	0.0281	Yes
	Y6,8F	0.0002	Yes
	Y6E	0.004	Yes
	Y8E	0.0727	No
	Y6,8E	0.004	Yes

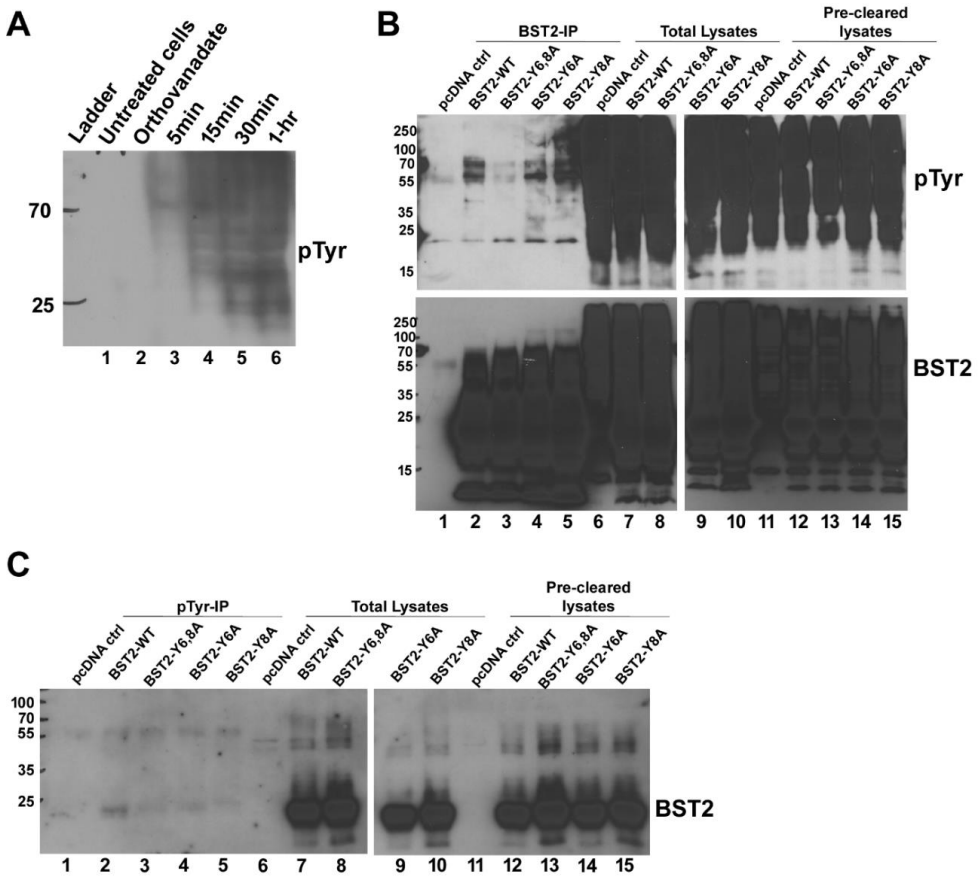

Figure II.4 Immunoprecipitation of transiently transfected BST2 in HEK293T cells. A) HEK293T cells grown in 6-well plates overnight and treated with 200nM sodium pervanadate for 0-, 5-, 15-, 30-, and 60-minutes. Cell lysates were treated with activated sodium orthovandate. “Orthovandate” lane refers to cells that were not treated with sodium pervandate while in culture, while the lysates only were treated with activated sodium orthovanadate. Total levels of tyrosine-phosphorylated proteins are detected. B) Anti-BST2 IP using rabbit polyclonal anti-BST2 antibody on lysates of HEK293T cells transfected with mock (pcDNA ctrl), BST2-WT, BST2-Y6A, BST2-Y8A, or BST2-Y6/8A. Lanes 1-5: IP samples, lanes 6-10: total cellular lysats pre-IP, lanes 11-15: elution of proteins within the total lysates that were bound to beads conjugated with the secondary antibodies (i.e. nonspecific protein binding to beads). Top blots: detection of tyrosine-phosphorylated proteins. Bottom blots: detection of BST2. C) Western blots of IP of total tyrosine phosphorylated proteins, blotting for BST2 using rabbit serum. Lane numbers represent similar sets to those in panel B.

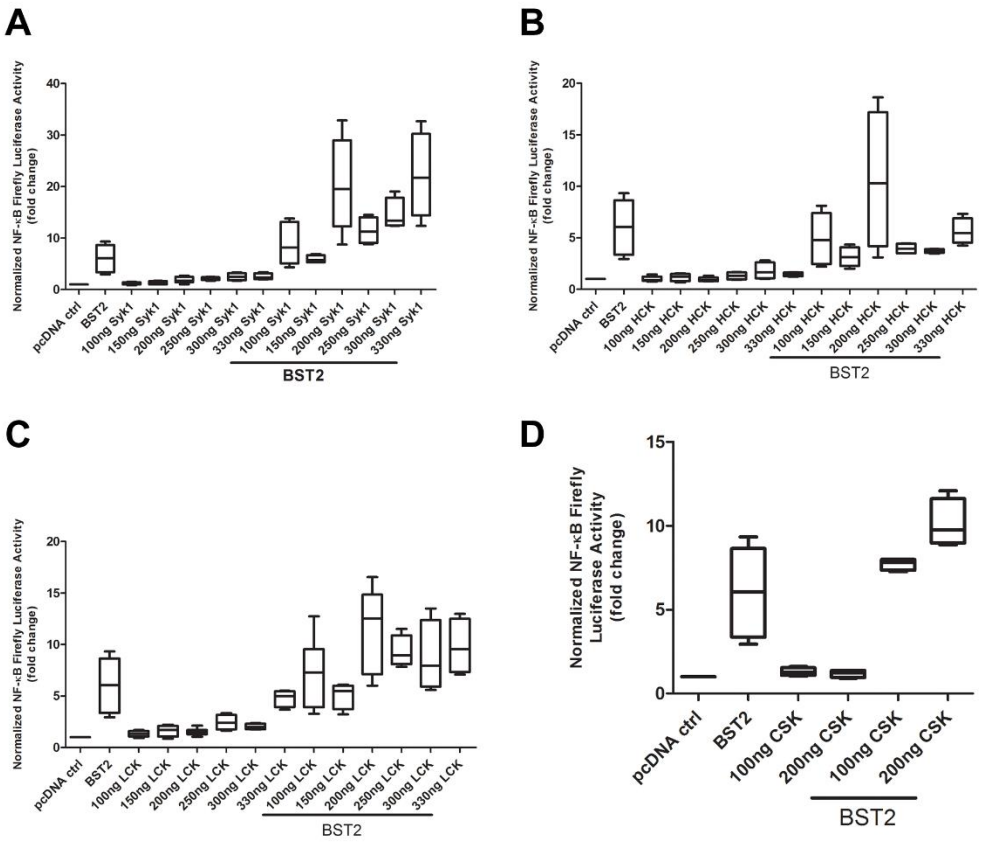

Figure II.5 NF-κB activity of BST2 co-expressed with various src-family tyrosine kinases. A) HEK293T cells plated in 48-well plates and transfected with expression plasmids for BST2 or Syk kinase at the various doses indicated. At 300ng and 330ng Syk co-expression with BST2, the NF-κB activity was more statistically significantly greater than the activity produced by BST2 expression alone. B-D) Same as panel A except for the kinase used: B) HCK, C) LCK, and D) CSK. The data presented here represents two to three independent experiments combined, where each independent experiment contained three to five technical replicates.

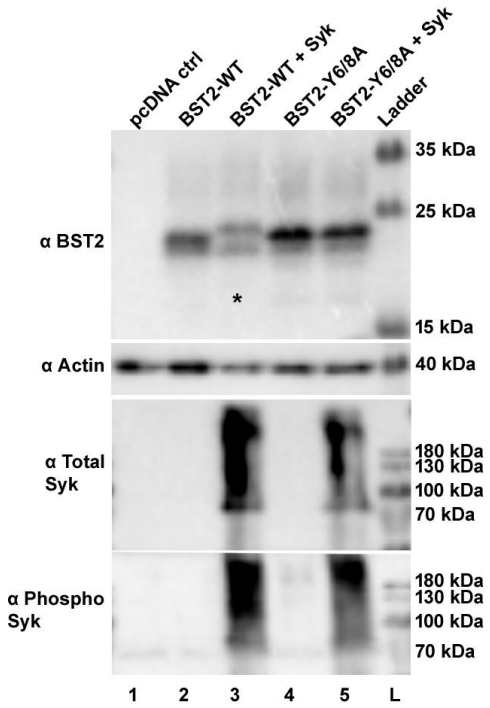

Figure II.6 Syk kinase expression produced a size-shift of the long BST2 band in a manner dependent on tyrosine residues 6 and 8. HEK293T cells were plated in a 6-well plate and transfected the next day with the following plasmids: pcDNA3.1 alone as a negative control; BST2-WT or BST2-Y6/8A alone or with Syk kinase. The next day after transfection, the cells were treated for an hour with 200μM sodium pervanadate and then lysed. The purified cell lysates were loaded on SDS/PAGE gel and protein expression was determined by Western blot. Syk kinase co-expression rendered the upper prominent BST2 band higher in molecular weight. See Materials and Methods for additional details. This blot is representative of two independent experiments.

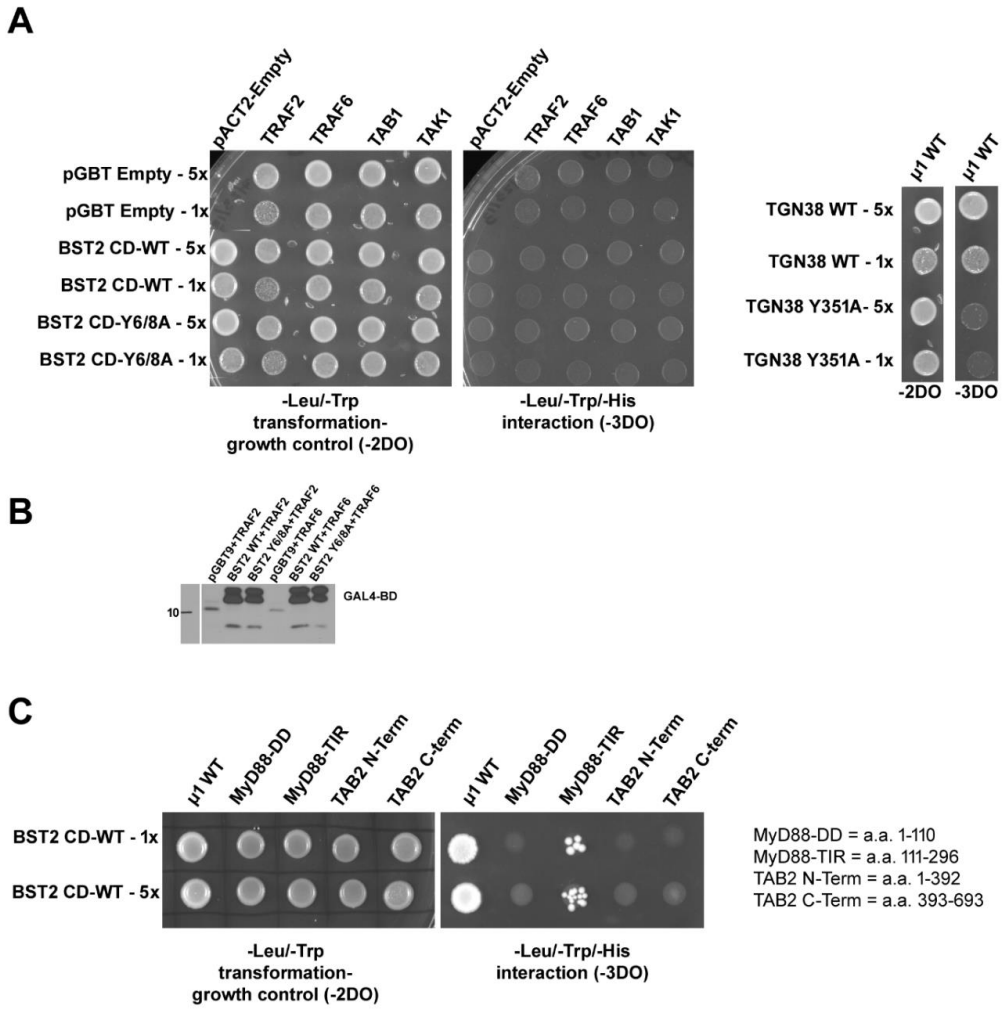

Figure II.7 Yeast 2-hybrid assays to test for the direct interaction of BST2CD with various signaling molecules. A) AH109 yeast cells transformed to express Gal4-DBD-BST2CD on pGBT9 plasmid or any of the signaling molecules listed on pACT2 plasmid as Gal4-AD-[signaling protein]. TGN38 WT and µ1 (on the right) were used as positive controls for the direct interaction between two proteins. The Y2H assay was performed similarly to that presented in Figure II.1A. See Materials and Methods for additional details. The images shown are representative of two independent experiments. B) Western blotting to detect Gal4-DBP (written as BD for binding-domain) to ensure the expression of some of the transformed proteins in yeast cells. The yeast cells were lysed by multiple rounds of freezing and thawing in Laemmli buffer with vortexing. C) Y2H assay similar to that presented in panel A, but using domains of MyD88 and TAB2 proteins rather than the full-length forms, which were toxic to the yeast cells. MyD88-DD: Death domain; MyD88-TIR: Toll-interleukin receptor homology domain; TAB2 N-term: N-terminal domain; TAB2 C-term: C-terminal domain.

References

1. **Kupzig S, Korolchuk V, Rollason R, Sugden A, Wilde A, Banting G.** 2003. Bst-2/HM1.24 is a raft-associated apical membrane protein with an unusual topology. Traffic **4:**694-709.

2. **Hammonds J, Wang JJ, Yi H, Spearman P.** 2010. Immunoelectron microscopic evidence for Tetherin/BST2 as the physical bridge between HIV-1 virions and the plasma membrane. PLoS Pathog **6:**e1000749.

3. **Hinz A, Miguet N, Natrajan G, Usami Y, Yamanaka H, Renesto P, Hartlieb B, McCarthy AA, Simorre JP, Gottlinger H, Weissenhorn W.** 2010. Structural basis of HIV-1 tethering to membranes by the BST-2/tetherin ectodomain. Cell Host Microbe **7:**314-323.

4. **Rollason R, Korolchuk V, Hamilton C, Schu P, Banting G.** 2007. Clathrin-mediated endocytosis of a lipid-raft-associated protein is mediated through a dual tyrosine motif. J Cell Sci **120:**3850-3858.

5. **Galao RP, Le Tortorec A, Pickering S, Kueck T, Neil SJ.** 2012. Innate sensing of HIV-1 assembly by Tetherin induces NFkappaB-dependent proinflammatory responses. Cell Host Microbe **12:**633-644.

6. **Tokarev A, Suarez M, Kwan W, Fitzpatrick K, Singh R, Guatelli J.** 2013. Stimulation of NF-kappaB activity by the HIV restriction factor BST2. J Virol **87:**2046-2057.

7. **Douglas JL, Viswanathan K, McCarroll MN, Gustin JK, Fruh K, Moses AV.** 2009. Vpu directs the degradation of the human immunodeficiency virus restriction factor BST-2/Tetherin via a {beta}TrCP-dependent mechanism. J Virol **83:**7931-7947.

8. **Goffinet C, Allespach I, Homann S, Tervo HM, Habermann A, Rupp D, Oberbremer L, Kern C, Tibroni N, Welsch S, Krijnse-Locker J, Banting G, Krausslich HG, Fackler OT, Keppler OT.** 2009. HIV-1 antagonism of CD317 is species specific and involves Vpu-mediated proteasomal degradation of the restriction factor. Cell Host Microbe **5:**285-297.

9. **Kueck T, Neil SJ.** 2012. A cytoplasmic tail determinant in HIV-1 Vpu mediates targeting of tetherin for endosomal degradation and counteracts interferon-induced restriction. PLoS Pathog **8:**e1002609.

10. **Rollason R, Dunstan K, Billcliff PG, Bishop P, Gleeson P, Wise H, Digard P, Banting G.** 2013. Expression of HIV-1 Vpu leads to loss of the viral restriction factor CD317/Tetherin from lipid rafts and its enhanced lysosomal degradation. PLoS One **8:**e75680.

11. **Dube M, Paquay C, Roy BB, Bego MG, Mercier J, Cohen EA.** 2011. HIV-1 Vpu antagonizes BST-2 by interfering mainly with the trafficking of newly synthesized BST-2 to the cell surface. Traffic **12:**1714-1729.

12. **Dube M, Roy BB, Guiot-Guillain P, Mercier J, Binette J, Leung G, Cohen EA.** 2009. Suppression of Tetherin-Restricting Activity upon Human Immunodeficiency Virus Type 1 Particle Release Correlates with Localization of Vpu in the trans-Golgi Network. Journal of Virology **83:**4574-4590.

13. **Zhang H, Lin EC, Das BB, Tian Y, Opella SJ.** 2015. Structural determination of virus protein U from HIV-1 by NMR in membrane environments. Biochim Biophys Acta **1848:**3007-3018.

14. **Lau D, Kwan W, Guatelli J.** 2011. Role of the endocytic pathway in the counteraction of BST-2 by human lentiviral pathogens. J Virol **85:**9834-9846.

15. **Masuyama N, Kuronita T, Tanaka R, Muto T, Hirota Y, Takigawa A, Fujita H, Aso Y, Amano J, Tanaka Y.** 2009. HM1.24 is internalized from lipid rafts by clathrin-mediated endocytosis through interaction with alpha-adaptin. J Biol Chem **284:**15927-15941.

16. **Pandey KN.** 2009. Functional roles of short sequence motifs in the endocytosis of membrane receptors. Front Biosci (Landmark Ed) **14:**5339-5360.

17. **Valdivia RH, Baggott D, Chuang JS, Schekman RW.** 2002. The yeast clathrin adaptor protein complex 1 is required for the efficient retention of a subset of late Golgi membrane proteins. Dev Cell **2:**283-294.

18. **Park SY, Guo X.** 2014. Adaptor protein complexes and intracellular transport. Biosci Rep **34**.

19. **Jia X, Weber E, Tokarev A, Lewinski M, Rizk M, Suarez M, Guatelli J, Xiong Y.** 2014. Structural basis of HIV-1 Vpu-mediated BST2 antagonism via hijacking of the clathrin adaptor protein complex 1. Elife **3:**e02362.

20. **Galao RP, Pickering S, Curnock R, Neil SJ.** 2014. Retroviral retention activates a Syk-dependent HemITAM in human tetherin. Cell Host Microbe **16:**291-303.

21. **Cocka LJ, Bates P.** 2012. Identification of alternatively translated Tetherin isoforms with differing antiviral and signaling activities. PLoS Pathog **8:**e1002931.

22. **Perez-Caballero D, Zang T, Ebrahimi A, McNatt MW, Gregory DA, Johnson MC, Bieniasz PD.** 2009. Tetherin inhibits HIV-1 release by directly tethering virions to cells. Cell **139:**499-511.

23. **Billcliff PG, Gorleku OA, Chamberlain LH, Banting G.** 2013. The cytosolic N-terminus of CD317/tetherin is a membrane microdomain exclusion motif. Biol Open **2:**1253-1263.

24. **Dube M, Roy BB, Guiot-Guillain P, Mercier J, Binette J, Leung G, Cohen EA.** 2009. Suppression of Tetherin-restricting activity upon human immunodeficiency virus type 1 particle release correlates with localization of Vpu in the trans-Golgi network. J Virol **83:**4574-4590.

25. **Kawai T, Akira S.** 2007. Signaling to NF-kappaB by Toll-like receptors. Trends Mol Med **13:**460-469.

26. **Bradshaw JD, Lu P, Leytze G, Rodgers J, Schieven GL, Bennett KL, Linsley PS, Kurtz SE.** 1997. Interaction of the cytoplasmic tail of CTLA-4 (CD152) with a clathrin-associated protein is negatively regulated by tyrosine phosphorylation. Biochemistry **36:**15975-15982.

Chapter III

Cooperation of the Ebola proteins VP40 and $GP_{1,2}$ with BST2 to activate NF-κB independently of virus-like particle trapping

Abstract

BST2 is a host protein with dual functions in response to viral infections: it traps newly assembled enveloped virions at the plasma membrane of infected cells, and it induces NF-κB activity, especially in the context of retroviral assembly. In this study, we examined whether Ebola virus proteins affect BST2-mediated induction of NF-κB. We found that the Ebola matrix protein, VP40, and envelope glycoprotein, GP, each cooperate with BST2 to induce NF-κB activity, with maximal activity when all three proteins are expressed. Unlike the Human Immunodeficiency Virus type 1 Vpu protein, which antagonizes both virion-entrapment and the activation of NF-κB by BST2, Ebola GP does not inhibit NF-κB signaling even while it antagonizes the entrapment of virus-like particles. GP from *Reston* Ebola virus, a non-pathogenic species in humans, showed a similar phenotype to GP from *Zaire* Ebola, a highly pathogenic species, in terms of both the activation of NF-κB and the antagonism of virion-entrapment. Although Ebola VP40 and GP both activate NF-κB independently of BST2, VP40 is the more potent activator. Activation of NF-κB by the Ebola proteins either alone or together with BST2 requires the canonical NF-κB signaling pathway. Mechanistically, the maximal NF-κB activation by GP, VP40, and BST2 together requires the ectodomain cysteines needed for BST2-dimerization, the putative BST2 tetramerization residue L70, and Y6 of a potential hemi-ITAM motif in BST2's cytoplasmic domain. BST2 with a GPI anchor signal-deletion, which is not expressed at the plasma membrane and is unable to entrap virions, activated NF-κB in concert with the Ebola proteins at least as effectively as wild type BST2. Signaling by the GPI-anchor mutant also depended on Y6 of BST2. Overall, our data show that activation of NF-κB by BST2 is independent of virion-entrapment in

the case of Ebola virus. Nonetheless, BST2 may induce or amplify proinflammatory signaling during Ebola virus infection, potentially contributing to the dysregulated cytokine response that is a hallmark of Ebola virus disease.

Importance

Understanding how the host responds to viral infections informs the development of therapeutics and vaccines. We asked how proinflammatory signaling by the host protein BST2/tetherin, which is mediated by the transcription factor NF-κB, responds to Ebola proteins. Although the Ebola virus envelope glycoprotein ($GP_{1,2}$) antagonizes the trapping of newly formed virions at the plasma membrane by BST2, we found that it does not inhibit BST2's ability to induce NF-κB activity. This distinguishes $GP_{1,2}$ from the HIV-1 protein Vpu, the prototype BST2-antagonist, which inhibits both virion-entrapment and the induction of NF-κB activity. Ebola $GP_{1,2}$, the Ebola matrix protein VP40, and BST2 are at least additive with respect to the induction of NF-κB activity. The effects of these proteins converge on an intracellular signaling pathway that depends on a protein-modification termed neddylation. Better mechanistic understanding of these phenomena could provide targets for therapies that modulate the inflammatory response during Ebola virus disease.

Introduction

BST2 (bone marrow stromal cell antigen 2), also known as tetherin, is an interferon-inducible anti-viral protein (1-3). Two functions of BST2 have been associated with viral infections: BST2 traps newly assembled enveloped virions at the plasma membrane of infected cells, and it induces the activation of the proinflammatory transcription factor NF-κB (2-5). The exact mechanism of how BST2 initiates NF-κB

activity in response to viral infections is unknown. One model suggests that upon trapping of virions at the plasma membrane, aggregation of BST2 initiates a kinase cascade culminating in the activation of NF-κB and the release of proinflammatory cytokines (4). This model is based on signaling studies that used retroviruses, namely the murine leukemia virus (MLV) and the human immunodeficiency virus type 1 (HIV-1) lacking the accessory protein Vpu, which enhances virion-release by antagonizing BST2 (4). Another model suggests that BST2-mediated activation of NF-κB is independent of virion-entrapment; this model is based on the identification of a BST2 mutant that is unable to entrap virions but retains signaling activity as discussed below (5). Since BST2's restrictive function is not unique to retroviruses, studies using other families of enveloped viruses have the potential to extend or challenge the above models of the BST2 signaling mechanism and characterize how BST2 responds to the expression of viral genes.

BST2 is a dimeric type II transmembrane protein that physically tethers nascent virions of enveloped viruses to the plasma membrane of infected cells (6). BST2 contains an N-terminal cytoplasmic tail, a transmembrane domain, a rigid coiled-coil ectodomain, and a glycosylphosphatidylinositol (GPI) anchor at its C-terminus (7). This unusual, if not unique, structure enables BST2 to trap newly formed virions on the cell surface by physically cross-linking the lipid bilayers of the plasma membrane and the enveloped virion (8). BST2 requires a tyrosine residue (Y6) within its cytoplasmic tail to activate NF-κB but not to entrap virions (4, 5, 9). The GPI anchor of BST2 is required for virion-entrapment, while it is dispensable for NF-κB activation in some studies but required in others (4, 5, 9). These findings suggest that virion-entrapment, while

apparently contributory to BST2-mediated activation of NF-κB by retroviruses, might be generally unnecessary for BST2 to induce NF-κB activity. Consensus in the field exists regarding the notion that BST2 signals through a TGF-β activated kinase-1 (TAK1)-dependent cascade leading to the activation of the canonical NF-κB pathway (4, 5). This pathway requires the degradation of Iκβ by a cullin-1-based ubiquitin ligase complex, which requires modification of cullin-1 with the ubiquitin-like molecule nedd8 (5, 10, 11).

Various viral proteins have evolved to counteract the BST2-function of virion-entrapment (12-15). As mentioned earlier, HIV-1 Vpu is the prototype antagonist of BST2 (2, 3); Vpu mistrafficks BST2 away from the plasma membrane, removes it from virion assembly sites, and targets it for degradation (13, 16-21). On the other hand, the Ebola virus envelope glycoprotein ($GP_{1,2}$) antagonizes BST2 to enhance virion-release through an unclear mechanism that requires neither the removal of BST2 from the cell surface nor its degradation but might instead involve dissociation of BST2 from the Ebola matrix protein VP40; this activity requires proper N-linked glycosylation of the GP1 subunit and the interaction of BST2 with the GP2 subunit (12, 22-28).

In this study, we used Ebola $GP_{1,2}$ as a tool to determine whether, within the context of a filovirus, the antagonism of virion-entrapment impairs the ability of BST2 to induce NF-κB activity. To do this, we used an Ebola virus-like particle (VLP) model using the matrix protein, VP40. VP40-expression is sufficient to produce particles that resemble actual virions of Ebola virus and incorporate $GP_{1,2}$ (29). $GP_{1,2}$ is a glycoprotein that forms trimeric surface spikes on the Ebola virions and VLPs (29, 30). $GP_{1,2}$ is a heterodimer that consists of GP1 and GP2, which are linked by disulfide bonds; GP2 contains the transmembrane domain of $GP_{1,2}$ (31). We found that, unlike Vpu, $GP_{1,2}$ did

not inhibit NF-κB signaling despite antagonizing BST2-mediated VLP-entrapment. Rather, $GP_{1,2}$ cooperated with BST2 and VP40 to produce maximal NF-κB activity as compared to BST2 signaling in response to VP40-expression alone. To further support the independence of virion-entrapment and NF-κB activation by BST2, we found that BST2 lacking its GPI-anchor signal (ΔGPI BST2), which is not expressed at the cell surface and is defective for virion-entrapment (5), was fully functional for NF-κB activation, both alone and in the context of expression of Ebola $GP_{1,2}$ and VP40. Thus, our data indicate that virion-entrapment is not required for BST2 to induce NF-κB activity in the case of Ebola virus, and that relief of virion-entrapment by Ebola $GP_{1,2}$ does not inhibit NF-κB activity. The data nonetheless leave open the possibility that BST2 acts as an amplifier of the signal generated by the Ebola proteins.

Materials and Methods

Tissue Culture and Plasmids.

HEK293T cells (obtained from Nathaniel Landau at New York University) were maintained in Dulbeco's Minimum Essential Media (DMEM) containing high glucose and L-glutamine (Gibco Thermofisher, Waltham, MA, USA) supplemented with 10% Fetal Bovine Serum (FBS) (Gimini Bio Products, West Sacramento, CA, USA), 1% Pen/Strep (Gibco), 1X non-essential amino acids (NEAA) (Gibco), and 1X sodium pyruvate (Gibco). pcDNA3.1-BST2 expression plasmid was described previously (5). Hu6-BST2 stable cells were created from parental HEK293T cells by co-transfection with linearized plasmids encoding BST2 (pcDNA3.1-BST2 WT) and Zeocin-resistance in a 10:1 ratio. Single cell clones were selected using Zeocin. BST2-expression was screened using surface staining of BST2 by a fluorescent antibody followed by flow cytometry. The

Quikchange mutagensis kit (Stratagene) was used to create the pcDNA3.1-BST2-Y6A, -Y8A, -Y6,8A mutants as described previously (5, 32). The pcDNA-BST2-C3A (C53, 63, 91A) has been described previously (6). The L70D putative tetramerization-defective mutants, N2Q (N65Q/N92Q) glycosylation-free, and ΔGPI (Δ156-163) mutant of BST2 were described previously (5). pCAGGS-zaire$GP_{1,2}$-His/V5 and pCAGGS-FLAG-zaireVP40 were a kind gift from Paul Bates at the University of Pennsylvania. Glycoprotein (GP) open reading frames that produce proteins corresponding to the 2014 *Zaire ebolavirus* strain Ebola virus/H. sapiens-wt/SLE/2014/Makona-EM095B (accession AIE11800.1) and *Reston ebolavirus* strain Philippine 1992 (accession U23416.1) were cloned into expression plasmid pCAGGS by standard methods. The pcDNA3.1-VpHu plasmid expressing human codon-optimized HIV-1 Vpu was a kind gift from Klaus Strebel at the National Institute of Allergy and Infectious Diseases. and described previously (33). pRC-HA-Iκβ WT and pRC-HA-Iκβ S32/36A (dominant negative, DN) were a kind gift from Michael Karin at the University of California San Diego and described previously (34). pGL4.74 [hRluc/TK] plasmid expressed the reporter *Renilla* luciferase (Promega) under the transcriptional control of a herpes sarcoma virus thymidine kinase promoter. pGL4.32 [luc2P/NF-κB-RE/Hygro] NF-κB firefly luciferase (Promega) plasmid expressed firefly luciferase under the transcriptional control of five copies of an NF-kβ response element. The pCG-GFP plasmid was a kind gift from Jacek Skowronski at Case Western Reserve University.

Antibodies and reagents.

Rabbit antisera for BST2 and HIV-1 Vpu were obtained from the NIH AIDS Reference Repository and contributed by Klaus Strebel. Alexa-Fluor-647-conjugated

anti-BST2 (RS38E) and unconjugated anti-Iκβ mouse monoclonal antibodies were purchased from Biolegend, Inc (San Diego, CA, USA). Anti-tubulin and anti-FLAG monoclonal mouse antibodies were purchased from Sigma-Aldrich (St. Louis, MO, USA). Rabbit serum (R12) raised against the Ebola secreted glycoprotein (GP), which shares a common N-terminal domain with full-length, membrane-bound GP, recognizes $GP_{1,2}$ and was a generous gift from Paul Bates and described previously (12). Recombinant TNFα was purchased from Biolegend, Inc (San Diego, CA, USA).

SDS-PAGE/Western blotting.

Cells were lysed in Western blot sample buffer (100mM Tris, 0.79% sodium dodecyl sulfate (SDS), 19.8% glycerol, 9.9% β-mercaptoethanol, and 0.002% bromophenol blue in de-ionized water). Samples were run on SDS-polyacrylamide (PAGE) gels. Proteins were then transferred into polyvinylidene difluoride (PVDF) membranes (Bio-Rad) using the Trans-blot turbo transfer apparatus (Bio-Rad). Goat anti-mouse IgG or goat anti-rabbit IgG secondary antibodies conjugated to horse-radish peroxidase (HRP) (Bio-Rad) were used for detection of protein signal by chemi-luminescence. Blot images were captured using the ChemiDoc MP system (Bio-Rad). Raw images were converted to the TIF format using ImageLab software (Bio-Rad) and edited usig Adobe Photoshop.

Measuring NF-κB activity using a luciferase reporter system.

Cells were seeded in quadruplicate wells of 12-well tissue culture plates (Corning) in DMEM without antibiotics. The next day, cells were transfected using 5ul of Lipofetamine2000 (Invitrogen) following the manufacturer's protocol. The amounts of DNA used for each transfection are indicated in the figure legends. For the Iκβ

experiment in FIG 4A, one experimental replicate used 20ng of the Iκβ plasmids and the other used 40ng Iκβ plasmid. For the MLN4924 experiment in FIG 4C, one experimental replicate used 100nM MLN4924 and the other used 500nM MLN4924. Cells were harvested 24-hours after transfection. Two thirds of the cells from each well were used for the Dual-Glo Luciferase Assay (Promega) according to the manufacturer's protocol. A SpectraMax M3 plate reader (Molecular Devices, Sunnyvale, CA, USA) was used to measure luminescence for signaling experiments done in Figure III.2 through III.8. The Enspire Multimode Plate Reader (Perkin Elmer, Waltham, MA, USA) was used to measure luminescence for the signaling experiments of Figure III.1. Using both devices, firefly luciferase activity was measured first, quenched, and the *Renilla* luciferase was measured subsequently. The remaining one third of cells from each of the wells was used for the detection of protein expression by Western blotting (WB).

VLP collection and detection.

One day after transfection, media from two wells of a 12-well plate were combined and cleared from cellular debris by centrifugation at 300xg for 6-min at 4°C. The media were stored at -80°C or immediately added to a monolayer of 200ul of 20% sucrose (prepared in 1X PBS) (Invitrogen, Thermofisher, Waltham, MA, USA). VLPs were pelleted at 23,500xg for 1-hour at 4°C. The supernates were aspirated and the pellets resuspended in Western blot sample buffer. The pelleted VLPs were subjected to SDS-PAGE/WB.

MLN4924 treatment.

The nedd8 activation inhibitor MLN4924 was purchased from Active Biochem (Maplewood, NJ, USA) and described previously (35). The lyophilized drug was

dissolved in dimethyl sulfoxide (DMSO) and aliquots were stored at -80°C. HEK293T cells were seeds in quadruplicate wells and transfected as described above. Four to six hours after transfection, fresh DMEM containing DMSO alone or MLN4924 at 100nM (or 500nM) final concentration was added to the wells. The cells were harvested the next day and luciferase activity was measured as described above.

Flow cytometry.

Cells were plated in single wells of a 12-well plate. Twenty-four hours later, the cells were transfected using 200ng pcg-GFP together with either pcDNA3.1 control plasmid, pcDNA3.1-BST2 WT, or pcDNA3.1-ΔGPI plasmid as described above. The next day, the cells were assayed for surface BST2 expression by flow cytometry using a AF647-conjugated anti-BST2 antibody. Cells were fixed in 3% paraformaldhyde (Affymetrix, Santa Clara, CA, USA) and assayed using an Accuri C6 flow cytometer (BD Biosciences, San Jose, CA, USA). The data were analyzed using FlowJo software.

Statistical analysis.

In GraphPad Prism 5, we used the Wilcoxon rank sum statistical test, assuming a 95% confidence interval, for non-parametric data to determine statistical significance of changes in NF-κB activity when comparing two groups. We used the Kruskall-Wallis test, followed by the Dunn's multiple comparisons test assuming a 95% confidence interval, to compare multiple groups of normalized NF-κB fold changes. Box and whiskers graphs represent median values and the range between the 25^{th} and 75^{th} percentile of the data of independent experiments, where the whiskers represent the maximum and minimum values of the data.

Results

Ebola $GP_{1,2}$ does not inhibit BST2-mediated activation of NF-κB.

Since Ebola $GP_{1,2}$ is an antagonist of virion-entrapment like HIV-1 Vpu, we hypothesized that it could decrease BST2 signaling as a result of decreased virion-entrapment. To test this hypothesis, we used Ebola VP40 as a model for VLP formation and release, and an NF-κB-responsive luciferase reporter assay. We analyzed three independent experiments, each containing four replicates for the groups compared (Figure III.1, Tables III.1 and III.2). In these experiments, we used HEK293T cells engineered to express BST-2 stably and compared them to parental cells. Stable expression of BST2 in HEK293T cells (designated Hu6) induced a significant although quantitatively small increase of NF-κB activity compared to the background activity in parental HEK293T cells, which express undetectable levels of BST2 as measured by western blot and flow cytometry (Figure III.1B and III.7B); (Figure III.1A and Tables III.1 and III.2). We found that $GP_{1,2}$ expressed in BST2-stable cells (Hu6) significantly increased NF-κB activity when compared to Hu6 cells alone or to $GP_{1,2}$ expressed in parental 293T cells (Tables III.1 and III.2). In contrast, Vpu expressed in Hu6 cells significantly decreased NF-κB activity when compared to Hu6 cells alone, but not when compared to Vpu-expression in parental 293T cells. Expression of $GP_{1,2}$ significantly increased the NF-κB activity of Hu6 (BST2-expressing) cells expressing VP40, while Vpu significantly decreased this activity (Figure III.1A and Tables III.1 and III.2); these data indicate that unlike Vpu, Ebola $GP_{1,2}$ is not an antagonist of signaling. Interestingly, we found that VP40 and $GP_{1,2}$ induced NF-κB activity regardless of BST2 expression, although a trend of increased NF-κB activity in Hu6 cells as compared to parental 293T

cells was apparent for either protein expressed alone or both expressed together (Figure III.1A and Table III.2).. The western blot of Figure III.1B confirmed the expression of the various proteins in a representative experiment.

We next determined whether the trends observed for NF-κB activation by BST2 and the Ebola proteins were recapitulated in cells transiently expressing BST2, because we wanted to test various mutants of BST2 for mechanistic studies as shown below. To do this, we transfected parental HEK293T cells to transiently express BST2 either alone or with the viral proteins and the reporter plasmids and measured NF-κB activity (Figure III.2A and Table III.4). When we analyzed two sets of experiments, each containing four replicates, we found that transient expression of BST2 induced a significant increase in NF-κB activity compared to the background empty vector (pcDNA) control. We found that $GP_{1,2}$ co-expressed with BST2 did not decrease NF-κB activity when compared to BST2 alone, whereas Vpu did (Tables III.3 and III.4). Expression of $GP_{1,2}$ significantly increased NF-κB activity in concert with BST2 and VP40, while Vpu significantly decreased this activity (Tables III.3 and III.4). Thus, the overall effects of $GP_{1,2}$ and Vpu on BST2-mediated NF-κB signaling were similar in BST2-stable cells and cells transiently expressing BST2. However, we observed differences in protein expression between the two systems using western blot (Figure III.1B and Figure III.2B). Levels of transiently expressed BST2 were increased due to the expression of the Ebola viral proteins (Figure III.2B, lane 4 vs. 6, 10, and 12); this effect was not observed in the stable Hu6 cells, where the expression of Ebola viral proteins did not increase BST2-expression (Figure III.1B, lane 7 vs. 8, 10, and 12). Finally, we wanted to confirm the ability of $GP_{1,2}$ and Vpu to antagonize the virion-trapping function of BST2. As expected,

we found that both $GP_{1,2}$ and Vpu antagonized BST2-mediated entrapment and restored VLP release (Figure III.2B, lanes 7-12 for VLPs). Overall, these data indicated that Ebola $GP_{1,2}$ does not inhibit BST2 signaling despite enhancing virion-release; this result does not support our initial hypothesis and suggests instead a disconnection between virion-entrapment and NF-κB activation.

$GP_{1,2}$ from the *Zaire* and *Reston* species cooperate similarly with VP40 and BST2 to activate NF-κB.

We wanted to determine whether $GP_{1,2}$ from *Zaire* and *Reston* species differed in their abilities to activate NF-κB in concert with BST2 or to counteract BST2-mediated VLP-entrapment, because *Reston* is not pathogenic in humans while *Zaire* is highly pathogenic . To address this question, we tested two clones of *Zaire* $GP_{1,2}$ (1976 Zaire $GP_{1,2}$, the 2014 Zaire $GP_{1,2}$), and Reston $GP_{1,2}$ in an experiment similar in set-up to that presented in Figure III.2. The 1976 Zaire $GP_{1,2}$ was used in the two previous experiments and the remainder of this paper. We observed no inhibition of NF-κB activation as a result of the expression of any of the different GPs; instead, these proteins increased NF-κB activity. We found that Reston $GP_{1,2}$ ($rGP_{1,2}$) produced a significant increase in NF-κB activity when compared to either of the Zaire GPs, whether expressed alone or in combination with BST2 and VP40 (Figure III.3A and Table III.5). All of the GPs tested antagonized BST2 and enhanced VLP release (Figure III.3B, lane 10 vs. 14-16). We observed increases in BST2 expression levels due to the co-expression of VP40 with the various GPs, consistent with our findings in Figure III.2B, in which BST2 was also expressed transiently. Overall, $GP_{1,2}$ from the two Ebola species

cooperated with BST2 and VP40 to induce NF-κB activity, and GPs from both species effectively antagonized VLP-entrapment by BST2.

BST2 and the Ebola proteins activate the canonical NF-κB pathway in a manner dependent on neddylation.

Since we observed cooperation in the activation of NF-κB by BST2, VP40, and $GP_{1,2}$, we asked whether all these proteins use the same intracellular signaling pathway. To answer this question, we inhibited the canonical NF-κB pathway by expressing a dominant negative (DN), degradation-resistant, Iκβ and by pharmacological treatment using the Nedd8-activating enzyme (NAE) inhibitor MLN4924, which prevents activation of the cullin1-RING E3 ligase complex that degrades Iκβ (10, 35, 36). Next, we asked whether overexpression of the NF-κB inhibitor protein Iκβ would reduce activity induced by BST2 and the Ebola proteins, VP40 and $GP_{1,2}$. We expected that the dominant negative form of Iκβ would inhibit signaling, and used the Iκβ-WT as a plasmid control, where Iκβ-WT would inhibit NF-κB activity less than the Iκβ-DN. We found that DN and wild type Iκβ over-expression significantly inhibited the NF-κB activity that was induced by BST2 and the Ebola proteins, whether they were expressed in combinations or alone (Figure III.4A and Table III.6). Although Iκβ-WT inhibited NF-κB activity as compared to samples without any Iκβ expression plasmid, Iκβ-DN more robustly inhibited activity indicating that this pathway in particular is being targeted and that there were no observable side-effects of the plasmid expression. Using western blot, we confirmed the expression of all the transfected proteins and again observed an increase in BST2 when transiently co-expressed with either $GP_{1,2}$, VP40, or both (Figure III.4B). We found that MLN4924

significantly and substantially inhibited NF-κB activity in a similar manner to the over-expression of Iκβ (Figure III.4C and Table III.7). As a control for MLN4924 activity in HEK293T cells, we found that signaling by TNF-α, which utilizes the canonical pathway of NF-κB activation, was suppressed by MLN4924-treatment. Thus, the data suggest a cooperative signaling activity between the Ebola proteins VP40 and $GP_{1,2}$, and BST2 that merges at the canonical NF-κB activation-pathway and requires neddylation.

Determinants of BST2-mediated activation of NF-κB in the context of Ebola protein-expression.

We next wanted to determine whether the maximal activation of NF-κB that we observed when BST2 was co-expressed with VP40 and $GP_{1,2}$ depended on the motifs and residues previously described as important for BST2 signaling, either when BST2 was expressed in isolation or in the context of retroviral assembly. First, we tested the cytoplasmic tyrosine-6 and -8 alanine substitution mutants of BST2, expressed either alone or in combination with the Ebola proteins. As expected, we observed that BST2-Y6A and BST2-Y6,8A, but not BST2-Y8A, were significantly impaired for signaling when expressed alone. The same trend was observed when these mutants were co-expressed with the Ebola proteins; BST2-Y6A and -Y6,8A did not cooperate with the Ebola proteins to induce the high level of NF-κB activity observed with wild type BST2 (Figure III.5A and Table III.8). We confirmed by western blot that all proteins were expressed (Figure III.5B). These data suggested that the cooperative activation of NF-κB by BST2 and the Ebola viral proteins occurs by the same or a similar mechanism as has been proposed for BST2 signaling in other settings, that is, via the cytoplasmic tyrosine 6 residue.

Next, we wanted to extend this apparent mechanistic similarity through the use of additional examples. To do this, we tested ectodomain mutants of BST2: a putative tetramerization mutant L70D, a glycosylation mutant in which the two ectodomain asparagines that are subject to N-linked glycosylation were mutated to glutamines (N2Q), a mutant impaired for cysteine-dependent dimerization (C3A), and a mutant lacking the GPI-anchor signal sequence (specifically an in-frame deletion of that sequence from residues 156 to 162). These mutants were expressed in HEK293T cells either alone or in combination with the Ebola proteins. We tested their ability to activate NF-κB, entrap VLPs, and respond to $GP_{1,2}$-mediated counteraction of VLP-entrapment (Figure III.6). Compared to wild type BST2, we found that BST2-L70D and the -C3A mutants were statistically significantly impaired in their ability to active NF-κB, whether expressed alone or in concert with the Ebola proteins (Figure III.6A and Table III.9). In contrast, we did not observe a significant difference in NF-κB activation between BST2-N2Q and wild type BST2, whether alone or with the Ebola proteins. Interestingly, we found a significant increase in NF-κB activation by the BST2-ΔGPI mutant compared to wild type BST2, whether alone or with the Ebola proteins (Figure III.6A and Table III.9). This ability of BST2-ΔGPI to activate NF-κB is consistent with our previous data regarding the phenotype of this mutant when expressed in the absence of viral proteins, but it is at odds with another study of a "ΔGPI" mutant in which a stop codon occurs before the anchor sequence; that mutant was reportedly defective for signaling (2, 4, 9). We confirmed the expression of the viral proteins and all the BST2 mutants by western blot, which showed the expected mobility shift of the N2Q mutant (Figure III.6B). We also measured VLP release (Figure III.6B) and found that, as expected, the C3A and

ΔGPI mutants were defective for VLP-entrapment. Also, we found that $GP_{1,2}$ antagonized the ability of L70D and N2Q to trap virions, since the release of VLPs was restored in cells expressing those BST2 mutants in response to $GP_{1,2}$ expression (Figure III.6B, lanes 10, 12, 14, and 16 vs. 2). Overall, we found that the determinants in BST2 for maximal signaling when combined with the Ebola proteins were the same as the previously reported determinants of BST2 signaling when expressed alone or in the context of retroviral expression, with the possible exception of the above-noted controversy regarding mutants of the GPI-anchor sequence.

Activation of NF-κB by BST2 in concert with the Ebola proteins is independent of VLP-entrapment.

Thus far, we observed a disconnect between BST2-mediated activation of NF-κB and VLP-entrapment: VLP entrapment was antagonized by $GP_{1,2}$ yet NF-κB activity was enhanced (Figures III.1 and III.2). We also found that the BST2 ΔGPI mutant, which is defective for VLP-entrapment, was more effective than wild type BST2 at inducing NF-κB activity (Figure III.6A and III.6B). Here, we asked whether the ΔGPI mutant signals using the same mechanism as wild type BST2 with respect to the requirement of tyrosine 6 (Figure III.5A). We wanted to ensure that the ΔGPI mutant was not signaling through an aberrant mechanism, perhaps associated with its mis-localization within the cell, since it does not reach the plasma membrane (5) (Figure III.7B). Consistent with a mechanistic similarity, the Y6A mutation impaired the induction of NF-κB activity by the ΔGPI mutant (Figure III.7A and Table III.10), just as it impairs the activity of wild type BST2. Using western blot, we confirmed the expression of all the tested proteins (Figure III.7C). We also compared the BST2-ΔGPI/Y6A mutant to wild type BST2, BST2-ΔGPI

and BST2-Y6A for its ability to entrap VLPs. We found that the BST2-ΔGPI/Y6A mutant was defective for VLP-entrapment, similar to the ΔGPI single-mutant (Figure III.7C, lanes 10 and 18). These data on BST2-ΔGPI suggest that the entrapment of VLPs was not required for the induction of maximal NF-κB activity, and they support the hypothesis that BST2-ΔGPI is not signaling aberrantly, at least with respect to its dependence on tyrosine 6.

Statistical analysis confirms that BST2 cooperates with Ebola VP40 and $GP_{1,2}$ to induce maximal NF-κB activity.

The experiments presented thus far contain eight core samples that were used repeatedly as controls during the transient expression of BST2: BST2 alone, Zaire $GP_{1,2}$ alone, Zaire VP40 alone, and all the combinations of these proteins. Since substantial variations in the fold-changes occurred between these experiments, we wanted to test whether statistically significant differences between the groups held true when these conditions were compared from all of the experiments together (Figure III.8, Tables III.11 and III.12). To test this, we performed statistical analysis on the fourteen experiments using transient expression of BST2, each representing two independent replicates and each replicate containing two to four technical replicates, for a total of twenty-eight independent replicates of the same groups. We used the Wilcoxon Rank Sum test for groups of single variables compared to background NF-κB activity; i.e., two-group comparisons pre-normalization to the background control. We found that BST2, VP40, and $GP_{1,2}$ all induced a significant increase in NF-κB activity (Table III.11). We used the Kruskall-Wallis test followed by a Dunn's multiple comparisons test; i.e., multiple-group comparisons post-normalization to the background control. The NF-κB

activity induced by BST2 with $GP_{1,2}$ was significantly more than the activity induced by either protein alone (Tables III.11 and III.12). The NF-κB activity produced by BST2 in concert with both Ebola proteins (i.e., when BST2, $GP_{1,2}$, and VP40 were co-expressed) was significantly more than the activity produced by any of the three combinations of two proteins together (BST2 + VP40, BST2 + $GP_{1,2}$, or $GP_{1,2}$ + VP40) (Table III.11 and III.12). By pooling our data sets and using rigorous statistical analyses, we supported the notion that the induction of NF-κB activity by BST2, Ebola $GP_{1,2}$, and Ebola VP40 is at least additive, and that despite its ability to antagonize restricted VLP release, $GP_{1,2}$ is not an antagonist of BST2-mediated signaling.

Discussion

In this study, we sought to confirm that BST2 induced NF-κB activity in response to the Ebola VLP-forming protein, VP40, and asked whether this signaling was reduced when BST2-mediated VLP-entrapment was antagonized by Ebola $GP_{1,2}$. BST2 restricts the release of several families of enveloped viruses (2, 3). It also induces NF-κB activity when expressed alone or, to a greater extent, when co-expressed with the virion-forming proteins of retroviruses (4, 5).

We found that the co-expression of BST2-WT with the Ebola VLP-forming VP40 protein produced more NF-κB activity than either protein alone. This was observed in cells that expressed BST2 stably or transiently (Tables III.1-4), although this effect did not reach statistical significance in the stable-expression model when analyzed by Dunn's test for multiple comparisons (Figure III.1A and Table III.2). These results regarding the co-expression of BST2 with VP40 are consistent with the reported ability of BST2 to induce an increase in NF-κB activity in response to the expression of HIV-

1ΔVpu and murine leukemia virus(4, 5). Consequently, the induction of NF-κB activity by BST2 in concert with VP40 could fit a model in which signaling is induced (or enhanced) by BST2-aggregation, which is presumably associated with VLP-entrapment at the plasma membrane.

When we introduced the virus-encoded BST2-restriction antagonists, we found that while HIV-1 Vpu inhibited NF-κB signaling, $GP_{1,2}$ did not. Although Vpu inhibits virion-restriction by BST2 and thus reduces VLP-entrapment at the plasma membrane, it also degrades BST2, downregulates its expression at the plasma membrane, and targets it away from virion assembly sites (13, 17, 21, 37). Any of these effects could potentially affect the activation of NF-κB. Perhaps most importantly, HIV-1 Vpu directly and generally inhibits the canonical NF-κB pathway independently of BST2 signaling; Vpu usurps the β-TrCP/cullin-1 ubiquitin ligase complex and consequently inhibits the ubiquitination and degradation of Iκβ (38). Thus, a primary cause of the inhibition of BST2-mediated NF-κB activation by Vpu could be its general effect on NF-κB signaling, an activity that, to our knowledge, is unique among virally-encoded BST2-antagonists. This model is supported by the observation that a Vpu mutant unable to interact with BST2 nonetheless inhibits the activation of NF-κB (5). Previous reports have shown that $GP_{1,2}$ neither removes BST2 from the plasma membrane nor targets BST2 for degradation (25, 26); however, it does prevent the immunoprecipitation and microscopic co-localization of VP40 with BST2 (27). While these activities might be key to GP's ability to antagonize virion-entrapment, they appear to have no negative influence on signaling by BST2. Instead, and paradoxically, we observed using both stable and

transient BST2-expression systems that $GP_{1,2}$ increases NF-κB signaling when expressed together with VP40 and BST2.

Based on the preceding results, we propose that, unlike the model proposed for retroviruses, VP40 VLP-entrapment is not the main driving force behind the activation of NF-κB by BST2 in the setting of Ebola protein expression. We further supported this hypothesis by showing that a defect in BST2's VLP-restriction function, as demonstrated by the BST2-ΔGPI mutant, did not hinder the activation of NF-κB in response to VP40 expression. Moreover, this mutant was not expressed at the cell surface, which suggests that the cooperative enhancement of NF-κB activity resulting from VP40 and BST2 co-expression did not depend on their interaction at the plasma membrane. Rather, the two proteins could be interacting within intracellular membranes.

We propose two potential explanations for how BST2, VP40, and $GP_{1,2}$ might work together to activate NF-κB. The first is simply the merging of the signaling pathways of BST2 alone and of the Ebola proteins alone at or before the Iκβ degradation step of the canonical NF-κB activation-pathway. Consistent with this model, we observed that the determinants of BST2 activity in isolation were the same as the determinants of its activity in concert with the Ebola proteins, as demonstrated by the BST2-Y6A, BST2-Y6,8A, and C3A mutants. Expression of these BST2 mutants along with both Ebola proteins reduced the observed NF-κB activity when compared to the Ebola proteins alone, although this reduction did not reach significance using rigorous statistical analysis. Nonetheless, these BST2 mutants might act as dominant negative inhibitors of signaling by the Ebola proteins, possibly due to sequestration of shared co-factors along the signaling pathways. In this model, how VP40 and $GP_{1,2}$ induce NF-κB

activity independently of BST2 requires further investigation. One mechanism that cannot be excluded by our data is that VLPs containing $GP_{1,2}$, or shed forms of GP (39, 40), signal from the extracellular space through an unknown surface receptor on HEK293T cells. Ebola VLPs containing $GP_{1,2}$ or extracellular shed forms of GP trigger NF-κB activation through signal transduction from the surface of certain cell types (40, 41). Specifically, Toll-like receptor 4 and the myeloid-specific C-type lectin receptor (LSECtin) act as surface pattern recognition receptors for GP-containing VLPs and shed GP (42, 43). Extracellular signaling by VLPs formed by VP40 alone in the absence of GP seems less likely, favoring the possibility that signaling by VP40, alone or in concert with BST2, occurs by an intracellular mechanism. The second, alternative explanation is that direct intracellular interactions occur between BST2, VP40, and $GP_{1,2}$, which result in structural or conformational modifications in the proteins that enhance their ability to induce NF-κB activity. This hypothesis could be tested by defining and characterizing the signaling activity of mutants of BST2, VP40, and $GP_{1,2}$ that do not interact with each other.

How the BST2 ectodomain structure and topology contributes to the induction of NF-κB activity is not fully understood. We have previously shown and confirmed here that the putative tetramerization residue L70 is important for BST2 signaling, yet it is largely dispensable for virion-entrapment (5). Given that the BST2 ectodomain tetramer forms *in vitro* under reducing conditions, whereas the extracellular environment is oxidizing, whether tetramerization *per se* is required for signaling is unclear. We confirmed that cysteines required for the dimerization of BST2 are required for signaling as well as virion-entrapment (5). Dimerization has been proposed to provide signaling

activity by juxtaposing two hemi-ITAM motifs in each of the BST2 cytoplasmic domains (the YxYxxV sequence). Each of these features of BST2 are required both for BST2 to signal on its own and for its concerted signaling with the Ebola proteins.

While the role of the GPI anchor in BST2 signaling remains elusive, our data support its dispensability. During GPI-anchor addition in the endoplasmic reticulum (ER), a C-terminal, hydrophobic membrane-insertion signal-sequence is cleaved, and the GPI-anchor is attached to a serine residue just N-terminal of the cleavage site (44, 45). The ΔGPI mutant used here encodes an in-frame deletion; the C-terminal region of the precursor protein remains encoded, potentially providing a second membrane anchor despite the lack of a GPI anchor (46). This mutant is active for signaling but defective for restriction. In contrast, the "BST2-ΔGPI mutant" previously reported as defective both for signaling and virion-restriction (4, 9) encodes a stop codon rather than an in-frame deletion at the site of GPI anchor-addition (2); it therefore lacks a hydrophobic region that could attach the C-terminus to the membrane by acting as a second TM domain. We suspect that lack of the second TM domain in the stop-codon mutant, rather than its inability to trap virions at the PM, explains its inability to induce NF-κB activity. In contrast, our in-frame GPI signal deletion mutant, by virtue of its alternative mode of C-terminal membrane-attachment, might maintain an ectodomain-topology required for signaling. Our mutant nonetheless fails to restrict virion-release, which we suspect is due to its failure to reach the plasma membrane. Based on these observations and comparisons, we propose that signaling by BST2 requires a C-terminal attachment to the plasma membrane in addition to its N-terminal TM domain. Moreover, BST2 can signal whether expressed on the plasma membrane or on

intracellular membranes and whether or not it is able to entrap virions. The notion that BST2 requires a membrane-anchored C-terminus to signal suggests that the topology of protein's ectodomain is important for this function. This raises the possibility that an interaction with another membrane protein(s), or BST2-multimerization, is important.

What are the caveats to our study, in particular in comparison to previous ones that focused on retroviruses? One difference is that the Ebola VLP system utilizes the expression of just two viral proteins rather than the whole viral genomes used in the case of HIV-1 and MLV. As a result, we report only the isolated effects of VP40 and $GP_{1,2}$ on BST2-mediated NF-κB signaling. Non-structural proteins of Ebola virus, which are missing in our experiment, could in principle antagonize BST2-signaling. Moreover, the absolute and relative amounts of VP40 and $GP_{1,2}$ expressed here might not be the same as those that are expressed from the intact virus. These caveats could be addressed using a full Ebola infection system, which requires a BSL-4 facility.

Our findings regarding the activation of NF-κB were largely reproducible in two separate HEK293T cell-based settings, one in which parental cells were engineered to express BST2 constitutively and the other in which BST2 was expressed by transient transfection from a plasmid. Differences in the molecular weight patterns observed for BST2 in these two systems were nonetheless striking (compare Figure III.1B for BST2 to the WB of all other figures). In the stable expression system, as expected, higher molecular weights species, which are likely the more highly glycosylated and mature forms of BST2, were much more evident than in the transient expression systems, in which lower molecular weight, immature forms predominate. The intensities of the BST2-specific bands were essentially unchanged by the expression of Ebola viral

proteins in the stable expression system, whereas in the transient expression system, the intensities of low molecular weight BST2-specific bands were increased by the expression of the Ebola proteins. The basis for this phenomenon is unclear, but it might explain why, although consistently observed in replicate experiments, the increase in signaling caused by BST2 when VP40 and GP were co-expressed did not reach statistical significance in the stable expression system, whereas it did in the transient expression system (compare Tables 1 and 11). Given the low molecular weight of the BST2 species that accumulated after transient expression, we speculate that they might be trapped in the ER. This speculation leads to the hypothesis that signaling by BST2 can occur from ER membranes, a hypothesis consistent with the ability of the ΔGPI mutant to signal despite its lack of residence at the plasma membrane. A limitation of our use of HEK293T cells is that they are not representative of early cellular targets during Ebola infections, although kidney cells are late targets during infection (47, 48). Studies using macrophages or dendritic cells will be required to extend our results to cells that are targeted early during Ebola virus infection.

To summarize, our data support a model of BST2-mediated NF-κB-activation that does not require the entrapment of virions at the plasma membrane. Instead of acting as an antagonist of signaling, Ebola $GP_{1,2}$ stimulates maximal NF-κB activity when co-expressed with VP40 and BST2. GP protein from the Reston species, which is not pathogenic in humans, is just as effective as an antagonist of virion-entrapment and as a stimulator of signaling as are GP proteins from Zaire species, which is pathogenic. Despite the lack of specific pattern recognition receptors in our cell model, Ebola VP40 and $GP_{1,2}$ induce NF-κB activity even in the absence of BST2. Additional studies are

needed to understand the interplay between these two viral proteins and BST2 in Ebola infection models and through the use of cells that are specific early targets of Ebola virus infection. Determining whether other viral antagonists of virion-entrapment by BST2 are, like Ebola GP, inactive as signaling antagonists will enable conclusions about the generalizability of models derived from the study of HIV-1 and other retroviruses regarding BST2 as a virus-sensor.

Acknowledgements

We thank Ned Landau for providing the HEK293T cells. We thank Paul Bates, Klaus Strebel, Jacek Skowronski, and the NIH AIDS Reagent Program for providing antibodies and plasmids as indicated in the Materials and Methods. We thank Sonia Jain and Feng He from the University of California San Diego Center for AIDS Research (UCSD CFAR) Biostatistics Core for their help with statistical analysis. We thank David Lau for the creation of the stable BST2 cell line. We thank members of the Guatelli lab for their assistance with the editing of this manuscript.

The work was supported in part by The James B. Pendleton Charitable Trust, the UCSD CFAR, and the San Diego Fellowship.

Chapter III, in full, is a reprint of the material as it appears in Rizk MG, Basler CF, Guatelli J. 2017. Cooperation of the Ebola proteins VP40 and GP1,2 with BST2 to activate NF-κB independently of virus-like particle trapping. *Journal of Virology* doi:10.1128/JVI.01308-17. The dissertation author was the primary investigator and author of this paper.

Figures and Tables

Figure III.1 Ebola $GP_{1,2}$ and VP40 cooperate with BST2 to induce NF-κB activity in Hu6 cells. (A) Hu6 cells (HEK293T cells stably engineered to express BST2-WT) or parental 293T cells were transfected with 75ng of a plasmid expressing *Renilla* luciferase (to measure transfection efficiency) and 150ng of a plasmid expressing firefly luciferase downstream of NF-κB response-sequences (to measure NF-κB activity). Wherever indicated on the graph, cells were transfected with the following quantities of plasmids: 900ng VP40, 900ng $GP_{1,2}$, and/or 900ng Vpu. An empty vector, pcDNA3.1, was used to equalize the total amount of plasmids transfected in each sample. After 24 hrs, firefly luciferase and *Renilla* luciferase activities were measured by luminometry. The ratio of firefly to *Renilla* luciferase-luminescence for each condition is graphed relative to parental HEK293T cells transfected only with the pcDNA plasmid, which was set at 1.0; this value represents the fold-enhancement of NF-κB activity by the tested proteins. The bars represent medians within the 25^{th} to 75^{th} percentile range of data and the whiskers represent maximum and minimums. Statistical analyses are values are presented in Tables III.1 and III.2. (B) Western blots of total cell lysates from one representative experiment out of three. Ebola GP, HIV-1 Vpu, and BST2 were detected using their respective rabbit anti-sera. VP40 was detected using mouse anti-FLAG antibody. Tubulin was used a loading control and detected using mouse anti-Tubulin antibody.

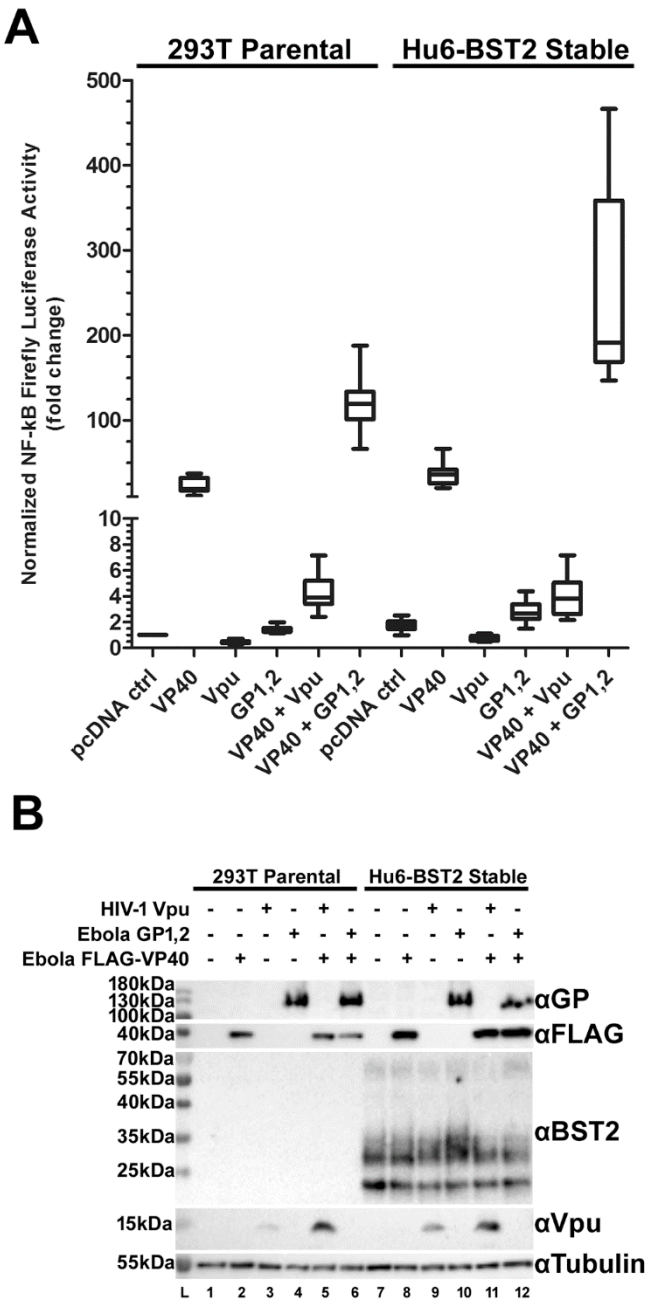
A
293T Parental
Hu6-BST2 Stable
Normalized NF-kB Firefly Luciferase Activity (fold change)
500
400
300
200
100
10
8
6
4
2
0
pcDNA ctrl
VP40
Vpu
GP1,2
VP40 + Vpu
VP40 + GP1,2
pcDNA ctrl
VP40
Vpu
GP1,2
VP40 + Vpu
VP40 + GP1,2
B
293T Parental
Hu6-BST2 Stable
HIV-1 Vpu - - + - + - - - + - + -
Ebola GP1,2 - - - + - + - - - + - +
Ebola FLAG-VP40 - + - - + + - + - - + +
180kDa
130kDa
100kDa
40kDa
70kDa
55kDa
40kDa
35kDa
25kDa
15kDa
55kDa
αGP
αFLAG
αBST2
αVpu
αTubulin
L 1 2 3 4 5 6 7 8 9 10 11 12

Table III.1 Statistical analysis of NF-κB luciferase activities presented in Figure III.1A[a]

Group 1	Group 2			
		Wilcoxon Rank Sum		**Significant?**
pcDNA[b]	VP40	< 0.0001; ****		Yes
	Vpu	< 0.0001; ****		Yes
	$GP_{1,2}$	0.0002; ***		Yes
	Hu6+pcDNA	< 0.0001;****		Yes
		Kruskall-Wallis; ctrl =1	**Dunn's**	**Significant?**
VP40 + Vpu	VP40	<0.0001; ****	*	Yes
	Vpu		*	Yes
VP40 + $GP_{1,2}$	VP40	<0.0001; ****	*	Yes
	$GP_{1,2}$		***	Yes
Hu6 + VP40	VP40	<0.0001; ****	n.s.	No
	Hu6+pcDNA		***	Yes
Hu6 + Vpu	Vpu	<0.0001; ****	n.s.	No
	Hu6		**	Yes
Hu6 + $GP_{1,2}$	$GP_{1,2}$	<0.0001; ****	***	Yes
	Hu6+pcDNA		*	Yes
Hu6 + VP40 + Vpu	Hu6 + Vpu	<0.0001; ****	**	Yes
	Hu6 + VP40		**	Yes
	VP40 + Vpu		n.s.	No
Hu6 + VP40 + $GP_{1,2}$	Hu6 + $GP_{1,2}$	<0.0001; ****	***	Yes
	Hu6 + VP40		***	Yes
	VP40 + $GP_{1,2}$		n.s.	No

*: p-value ≤0.05, **: p-value ≤0.005, ***: p-value ≤0.0005, ****: p-value <0.0001, n.s.: not significant

[a] The indicated viral proteins were expressed in parental HEK293T cells except where indicated by “Hu6,” which indicates the use of HEK293T cells constitutively expressing BST2.

[b] A plasmid control expressing no viral protein.

Table III.2 Normalized NF-κB luciferase values presented in Figure III.1A[a]

Group	Median*	Min**	Max***	25th %	75th %
VP40	18.92	10.99	37.27	17.30	32.35
Vpu	0.46	0.30	0.72	0.37	0.52
$GP_{1,2}$	1.42	1.13	1.98	1.24	1.54
Hu6-pcDNA[b]	1.81	0.98	2.53	1.46	2.05
VP40 + Vpu	3.88	2.41	7.14	3.43	5.19
VP40 + $GP_{1,2}$	119.30	66.22	187.70	101.10	133.50
Hu6 + VP40	36.50	20.27	66.63	25.72	42.13
Hu6 + Vpu	0.6977	0.4908	1.107	0.5449	0.9299
Hu6 + $GP_{1,2}$	2.68	1.49	4.37	2.25	3.37
Hu6 + VP40 + Vpu	3.80	2.17	7.16	2.63	5.05
Hu6 + VP40 + $GP_{1,2}$	191.50	146.70	466.20	168.70	358.40

*control=1; **Min: Minimum value; ***Max: Maximum value

[a] The indicated viral proteins were expressed in parental HEK293T cells except where indicated by "Hu6," which indicates the use of HEK293T cells constitutively expressing BST2.

[b] A plasmid control expressing no viral protein. The value for pcDNA in parental HEK293T cells was arbitrarily set to 1.0

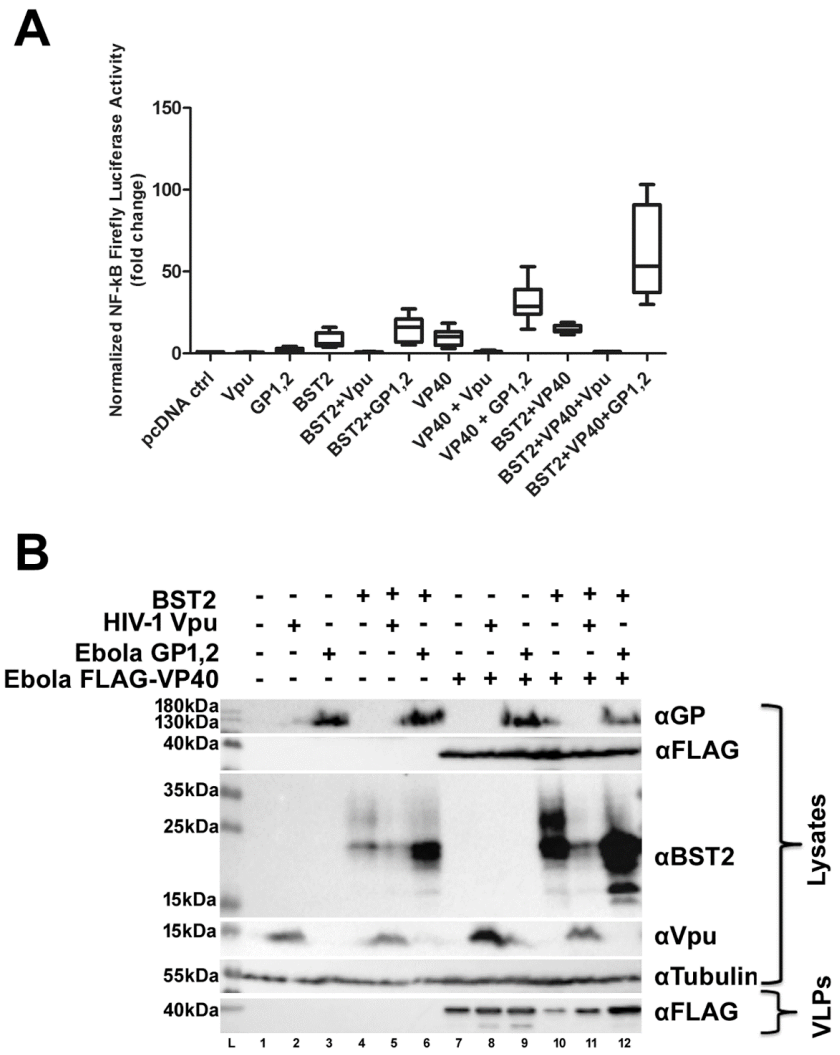

Figure III.2 Ebola $GP_{1,2}$ and VP40 cooperate with BST2 to induce NF-κB activity in HEK293T cells that transiently express BST2. (A) Parental 293T cells were transfected with 63ng *Renilla* luciferase plasmid and 125ng NF-κB firefly luciferase plasmid. Wherever indicated on the graph, cells were transfected with following plasmid quantities: 85ng BST2, 300ng VP40, 900ng $GP_{1,2}$, and 900ng Vpu. An empty vector, pcDNA3.1, was used to equalize the total amount of plasmids transfected in each sample. After 24 hrs, NF-κB luciferase activity was measured by luminometry. The data are presented as in Figure III.1A, with the pcDNA control set to 1.0. The boxes represent medians within the 25^{th} to 75^{th} percentile range and the whiskers represent maximum and minimums from two independent experiments, each containing four technical replicates. Statistical analyses are presented in Tables III.3 and III.4. (B) Western blots of total cell lysates and isolated VLPs from one representative experiment out of two. The antibodies used for detection of the proteins are the same as those used in Figure III.1B.

Table III.3 Statistical analysis of NF-κB luciferase activities presented in Figure III.2A.

Group 1	Group 2			
		Wilcoxon Rank Sum		**Significant?**
pcDNA	VP40	< 0.0001; ****		Yes
	Vpu	0.0122; *		Yes
	$GP_{1,2}$	0.0051; **		Yes
	BST2	< 0.0001;****		Yes
		Kruskall-Wallis; ctrl =1	**Dunn's**	**Significant?**
VP40 + Vpu	VP40	<0.0001; ****	**	Yes
	Vpu		n.s.	No
VP40 + $GP_{1,2}$	VP40	<0.0001; ****	**	Yes
	$GP_{1,2}$		***	Yes
BST2 + VP40	VP40	0.0020; **	*	Yes
	BST2		**	Yes
BST2 + Vpu	Vpu	<0.0001; ****	n.s.	No
	BST2		**	Yes
BST2 + $GP_{1,2}$	$GP_{1,2}$	<0.0001; ****	***	Yes
	BST2		n.s.	No
BST2 + VP40 + Vpu	BST2 + Vpu	<0.0001; ****	n.s.	No
	BST2 + VP40		**	Yes
	VP40 + Vpu		n.s.	No
BST2 + VP40 + $GP_{1,2}$	BST2 + $GP_{1,2}$	<0.0001; ****	***	Yes
	BST2 + VP40		***	Yes
	VP40 + $GP_{1,2}$		n.s.	No

*: p-value ≤0.05, **: p-value ≤0.005, ***: p-value ≤0.0005, ****: p-value <0.0001, n.s.: not significant

Table III.4 Normalized NF-κB luciferase values presented in Figure III.2A.

Group	Median*	Min**	Max***	25th %	75th %
VP40	10.21	3.00	18.49	4.94	13.36
Vpu	0.6056	0.4146	0.97	0.51	0.81
$GP_{1,2}$	1.97	0.83	4.36	1.09	3.07
BST2	6.10	3.86	16.00	4.73	12.53
VP40 + Vpu	1.11	0.56	2.08	0.92	1.33
VP40 + $GP_{1,2}$	28.67	14.78	53.09	24.03	39.03
BST2 + VP40	14.35	11.50	18.94	13.30	17.01
BST2 + Vpu	0.781	0.5789	1.208	0.6665	1.025
BST2 + $GP_{1,2}$	15.96	5.22	27.16	6.88	20.90
BST2 + VP40 + Vpu	1.11	0.64	1.27	0.93	1.19
BST2 + VP40 + $GP_{1,2}$	53.35	29.96	103.20	37.22	90.83

*control=1; **Min: Minimum value; ***Max: Maximum value

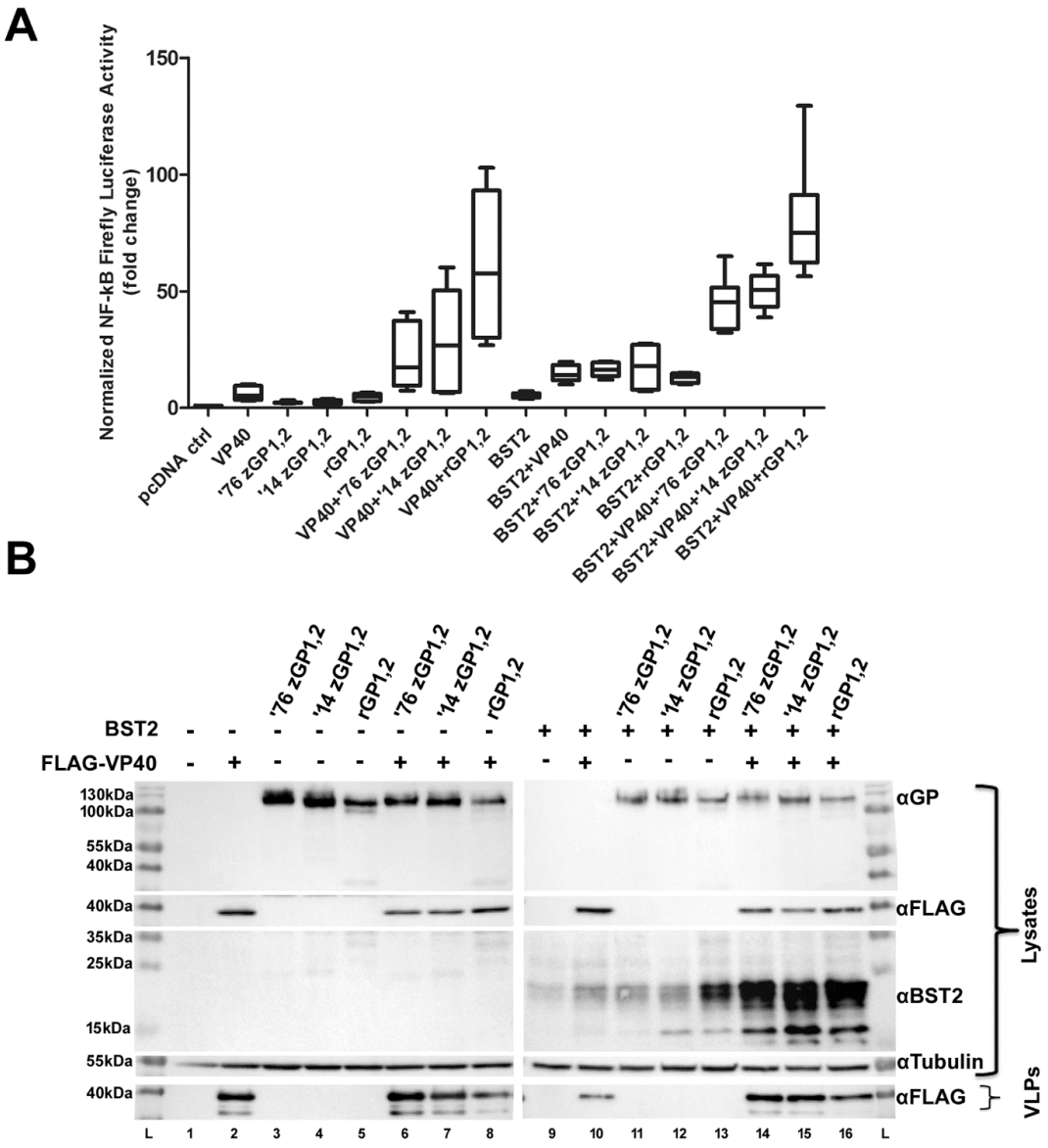

Figure III.3 Ebola $GP_{1,2}$ from both Zaire and Reston species cooperate with VP40 and BST2 for maximal NF-κB activity. (A) Parental 293T cells were transfected with the same amounts of plasmids as those used in Figure III.2A. After 24 hrs, NF-κB luciferase activity was measured by luminometry. The bars represent medians within the 25th to 75th percentile range of data and the whiskers represent maximum and minimums. Statistics corresponding to this figure are in Table 5. (B) Western blots of total cell lysates and isolated VLPs from one representative experiment out of two. The antibodies used for detection of the proteins are the same as those used in Figure III.1. '76 $zGP_{1,2}$ (1976 Zaire Ebola $GP_{1,2}$), '14 $zGP_{1,2}$ (2014 Zaire Ebola $GP_{1,2}$ from Sierra Leone), $rGP_{1,2}$ (Reston Ebola $GP_{1,2}$).

Table III.5 Statistical analyses of differences in NF-κB activities presented in Figure III.3A.

Group 1	Group 2	Wilcoxon Rank Sum ctrl = 1	Significant?
'76 $zGP_{1,2}$[a]	'14 $zGP_{1,2}$[b]	0.7984; n.s.	No
	$rGP_{1,2}$[c]	0.0011; **	Yes
VP40 + '76 $zGP_{1,2}$	VP40 + '14 $zGP_{1,2}$	0.9591; n.s.	No
	VP40 + $rGP_{1,2}$	0.0379; *	Yes
BST2 + '76 $zGP_{1,2}$	BST2 + '14 $zGP_{1,2}$	0.9591; n.s.	No
	BST2 + $rGP_{1,2}$	0.0379; *	Yes
BST2 + VP40 + '76 $zGP_{1,2}$	BST2 + VP40 + '14 $zGP_{1,2}$	0.2786; n.s.	No
	BST2 + VP40 + $rGP_{1,2}$	0.0011; **	Yes

*: p-value ≤0.05, **: p-value ≤0.005, ***: p-value ≤0.0005, ****: p-value <0.0001, n.s.: not significant; [a]: 1976 *Zaire* GP1,2; [b]: 2014 *Zaire* GP1,2; [c]: *Reston* GP1,2

Figure III.4 Ebola proteins signal in concert with BST2 using the canonical NF-κB pathway and neddylation. (A) HEK293T cells were transfected similarly to those in Figure III.2A, with the addition of Iκβ WT and DN (dominant negative) plasmids as indicated. The box and whiskers graph represents two independent experiments. Statistics corresponding to this figure are shown in Table III.6. (B) Western blots of total cell lysates from one experiment. Proteins were detected using the same antibodies used in Figure III.1B in addition to a mouse anti-Iκβ. (C) MLN4924-treated HEK293T cells compared to DMSO treated control samples transfected similarly to those in Figure III.2A. 40ng/ml recombinant TNFα diluted in 2% bovine serum albumin and 1X PBS was added for 2-hrs prior to harvest to the samples labeled “TNFα” and “MLN4924 + TNFα”. The box and whiskers graph represents two independent experiments. Statistics for this figure are presented in Table III.7. See Materials and Methods section for additional details.

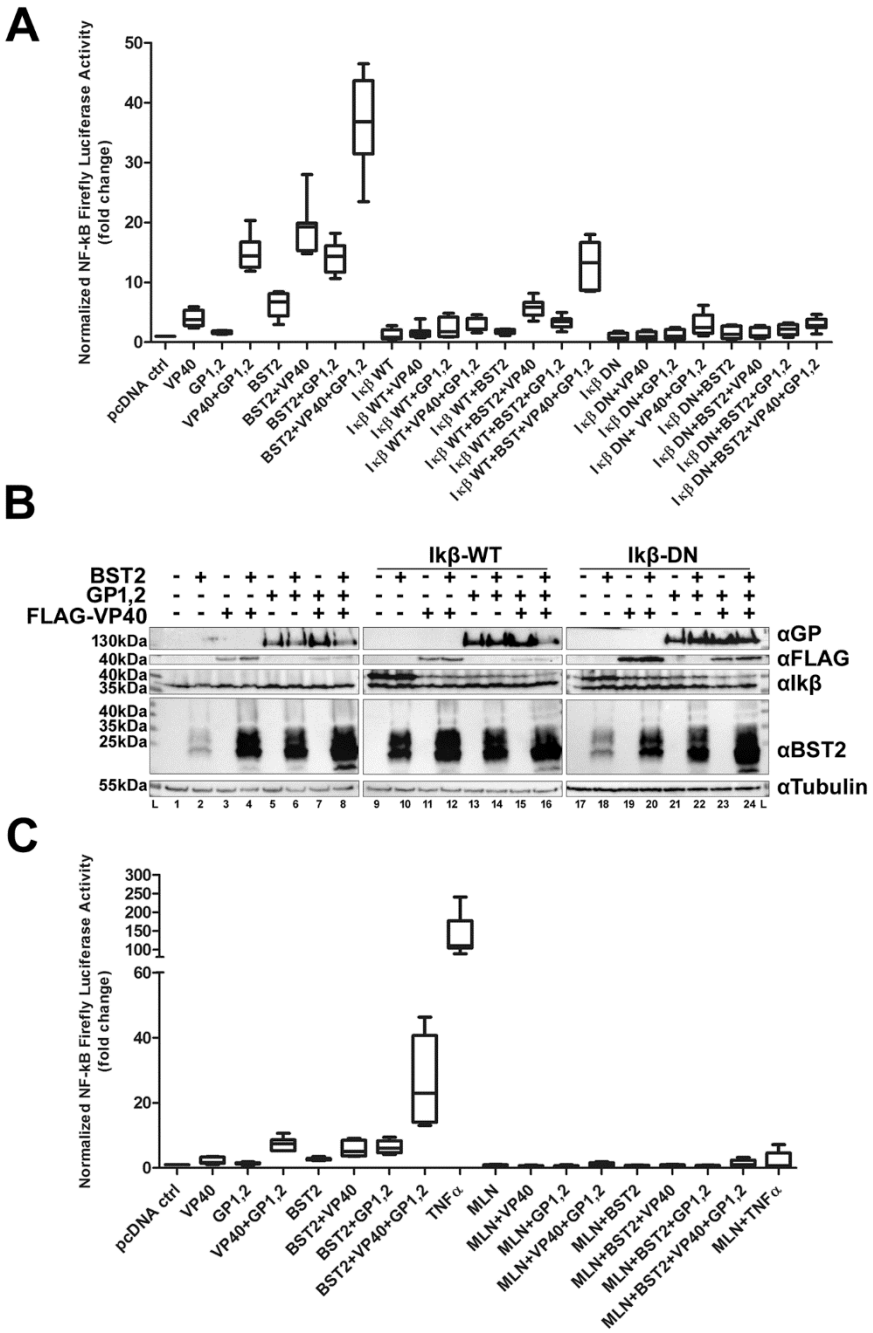
A
Normalized NF-kB Firefly Luciferase Activity (fold change)
pcDNA ctrl
VP40
GP1,2
VP40+GP1,2
BST2
BST2+VP40
BST2+GP1,2
BST2+VP40+GP1,2
IκβWT
IκβWT+VP40
IκβWT+GP1,2
IκβWT+VP40+GP1,2
IκβWT+BST2
IκβWT+BST2+VP40
IκβWT+BST2+GP1,2
IκβWT+BST+VP40+GP1,2
IκβDN
IκβDN+VP40
IκβDN+GP1,2
IκβDN+ VP40+GP1,2
IκβDN+BST2
IκβDN+BST2+VP40
IκβDN+BST2+GP1,2
IκβDN+BST2+VP40+GP1,2
B
Ikβ-WT
Ikβ-DN
BST2
GP1,2
FLAG-VP40
130kDa
40kDa
40kDa
35kDa
40kDa
35kDa
25kDa
55kDa
αGP
αFLAG
αIkβ
αBST2
αTubulin
C
Normalized NF-kB Firefly Luciferase Activity (fold change)
pcDNA ctrl
VP40
GP1,2
VP40+GP1,2
BST2
BST2+VP40
BST2+GP1,2
BST2+VP40+GP1,2
TNFα
MLN
MLN+VP40
MLN+GP1,2
MLN+VP40+GP1,2
MLN+BST2
MLN+BST2+VP40
MLN+BST2+GP1,2
MLN+BST2+VP40+GP1,2
MLN+TNFα

Table III.6 Statistical analyses of differences in NF-κB activities presented in Figure III.4A.

Group 1	Group 2	Wilcoxon Rank Sum	Significant?
pcDNA	Iκβ-WT	0.7209; n.s.	No
	Iκβ-DN	0.2786; n.s.	No
		ctrl = 1	
VP40	VP40 + Iκβ-WT	0.0019; **	Yes
	VP40 + Iκβ-DN	0.0002; ***	Yes
$GP_{1,2}$	$GP_{1,2}$ + Iκβ-WT	1.0000; n.s	No
	$GP_{1,2}$ + Iκβ-DN	0.5054; n.s.	No
VP40 + $GP_{1,2}$	VP40 + $GP_{1,2}$ + Iκβ-WT	0.0002; ***	Yes
	VP40 + $GP_{1,2}$ + Iκβ-DN	0.0002; ***	
BST2	BST2 + Iκβ-WT	0.0002; ***	Yes
	BST2 + Iκβ-DN	0.0002; ***	
BST2 + VP40	BST2 + VP40 + Iκβ-WT	0.0002; ***	Yes
	BST2 + VP40 + Iκβ-DN	0.0002; ***	
BST2 + $GP_{1,2}$	BST2 + $GP_{1,2}$ + Iκβ-WT	0.0002; ***	Yes
	BST2 + $GP_{1,2}$ + Iκβ-DN	0.0002; ***	
BST2 + VP40 + $GP_{1,2}$	BST2 + VP40 + $GP_{1,2}$ + Iκβ-WT	0.0002; ***	Yes
	BST2 + VP40 + $GP_{1,2}$ + Iκβ-DN	0.0002; ***	

*: p-value ≤0.05, **: p-value ≤0.005, ***: p-value ≤0.0005, ****: p-value <0.0001, n.s.: not significant

Table III.7 Statistical analyses of differences in NF-κB activities presented in Figure III.4C.

Group 1	Group 2	Wilcoxon Rank Sum **ctrl = 1**	Significant?
pcDNA	pcDNA + MLN	0.0530; n.s.	No
TNFα	TNFα + MLN	0.0006; ***	Yes
VP40	VP40 + MLN	0.0006; ***	Yes
$GP_{1,2}$	$GP_{1,2}$ + MLN	0.0012; **	Yes
VP40 + $GP_{1,2}$	VP40 + $GP_{1,2}$ + MLN	0.0006; ***	Yes
BST2	BST2 + MLN	0.0006; ***	Yes
BST2 + VP40	BST2 + VP40 + MLN	0.0006; ***	Yes
BST2 + $GP_{1,2}$	BST2 + $GP_{1,2}$ + MLN	0.0006; ***	Yes
BST2 + VP40 + $GP_{1,2}$	BST2 + VP40 + $GP_{1,2}$ + MLN	0.0006; ***	Yes

*: p-value ≤0.05, **: p-value ≤0.005, ***: p-value ≤0.0005, ****: p-value <0.0001, n.s.: not significant

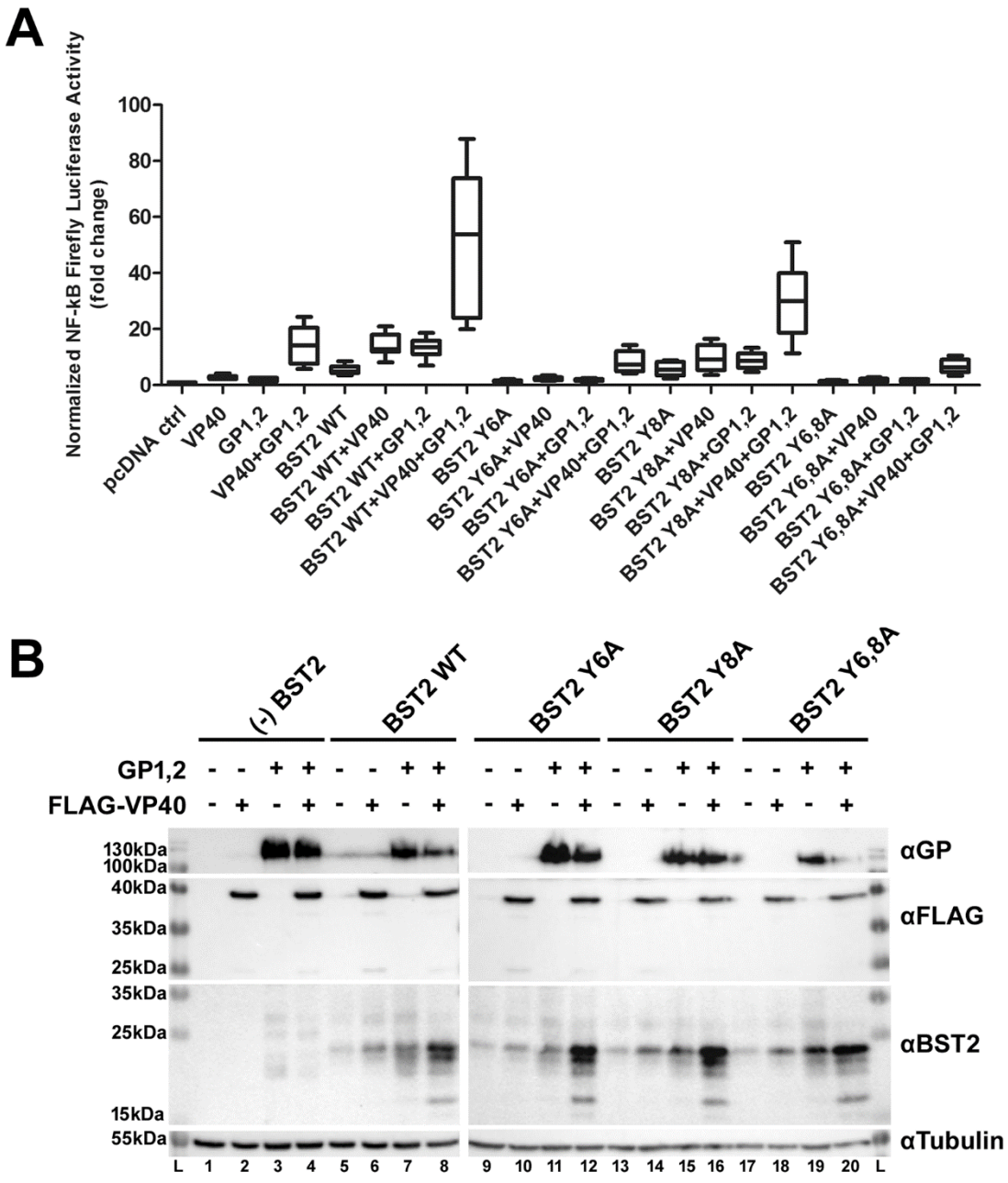

Figure III.5 BST2 signaling in concert with Ebola proteins requires the cytoplasmic tyrosine 6 residue. (A) Parental 293T cells were transfected similarly to those in Figure III.2A. After 24 hrs, NF-κB luciferase activity was measured by luminometry. The box and whiskers graph represents two independent experiments. Statistics for this figure are presented in Table III.8. (B) Western blots of total cell lysates from one representative experiment out of two. The antibodies used for detection of the proteins are the same as those used in Figure III.1B.

Table III.8 Statistical analyses of differences in NF-κB activities presented in Figure III.5A.

Group 1	Group 2	Wilcoxon Rank Sum	Significant?
pcDNA	BST2-WT	0.0002; ***	Yes
	BST2-Y6A	0.1949; n.s.	No
	BST2-Y8A	0.0002; ***	Yes
	BST2-Y6,8A	0.5737; n.s.	No
		ctrl = 1	
BST2-WT	BST2-Y6A	0.0002; ***	Yes
	BST2-Y8A	0.8785; n.s.	No
	BST2-Y6,8A	0.0002; ***	Yes
BST2-WT + VP40	BST2-Y6A + VP40	0.0002; ***	Yes
	BST2-Y8A + VP40	0.1049; n.s.	No
	BST2-Y6,8A + VP40	0.0002; ***	Yes
BST2-WT + $GP_{1,2}$	BST2-Y6A + $GP_{1,2}$	0.0002; ***	Yes
	BST2-Y8A + $GP_{1,2}$	0.0207; *	Yes
	BST2-Y6,8A + $GP_{1,2}$	0.0002; ***	Yes
BST2-WT + VP40 + $GP_{1,2}$	BST2-Y6A + VP40 + $GP_{1,2}$	0.0002; ***	Yes
	BST2-Y8A + VP40 + $GP_{1,2}$	0.2345; n.s.	No
	BST2-Y6,8A + VP40 + $GP_{1,2}$	0.0002; ***	Yes

*: p-value ≤0.05, **: p-value ≤0.005, ***: p-value ≤0.0005, ****: p-value <0.0001, n.s.: not significant

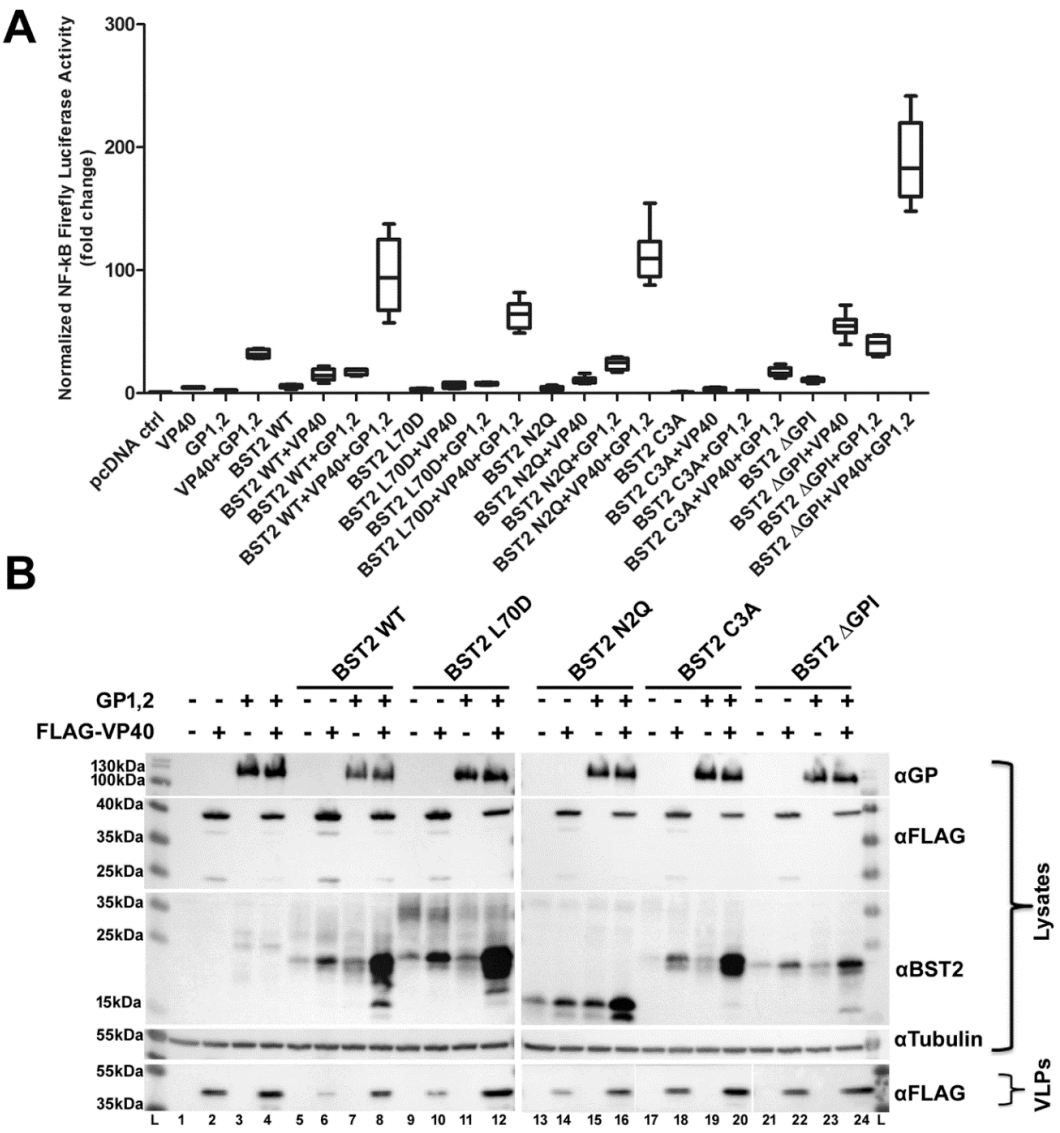

Figure III.6 BST2 signaling in concert with Ebola proteins requires the putative L70 tetramerization residue and cysteine-dependent dimerization but not glycosylation or the GPI-anchor signal sequence. (A) Parental 293T cells were transfected similarly to those in Figure III.2A with the indicated BST2 mutants at 85ng. After 24 hrs, NF-κB luciferase activity was measured by luminometry. The box and whiskers graph represents two independent experiments. Statistics for this figure are presented in Table III.9. (B) Western blots of total cell lysates and VLPs from one representative experiment out of two. The antibodies used for detection of the proteins are the same as those used in Figure III.1B. The VLP blots for lanes 13 through 24 are from the same gel, which was run in a different order from the lysates; therefore, the image was cut and reordered to match the order of the lanes for the lysates.

Table III.9 Statistical analyses of differences in NF-κB activities presented in Figure III.6A.

Group 1	Group 2	Wilcoxon Rank Sum	Significant?
pcDNA	BST2-WT	0.0002; ***	Yes
	BST2-L70D	0.0002; ***	Yes
	BST2-N2Q	0.0002; ***	Yes
	BST2-C3A	0.3282; n.s.	No
	BST2-ΔGPI	0.0002; ***	Yes
		ctrl = 1	
BST2-WT	BST2-L70D	0.0011; **	Yes
	BST2-N2Q	0.1304; n.s.	No
	BST2-C3A	0.0002; ***	Yes
	BST2-ΔGPI	0.0002; ***	Yes
BST2-WT + VP40	BST2-L70D + VP40	0.0006; ***	Yes
	BST2-N2Q + VP40	0.0830; n.s.	No
	BST2-C3A + VP40	0.0002; ***	Yes
	BST2-ΔGPI + VP40	0.0002; ***	Yes
BST2-WT + $GP_{1,2}$	BST2-L70D + $GP_{1,2}$	0.0286; *	Yes
	BST2-N2Q + $GP_{1,2}$	0.2000; n.s.	No
	BST2-C3A + $GP_{1,2}$	0.0286; *	Yes
	BST2-ΔGPI + $GP_{1,2}$	0.0286; *	Yes
BST2-WT + VP40 + $GP_{1,2}$	BST2-L70D + VP40 + $GP_{1,2}$	0.0148; *	Yes
	BST2-N2Q + VP40 + $GP_{1,2}$	0.3282; n.s.	No
	BST2-C3A + VP40 + $GP_{1,2}$	0.0002; ***	Yes
	BST2-ΔGPI + VP40 + $GP_{1,2}$	0.0002; ***	Yes

*: p-value ≤0.05, **: p-value ≤0.005, ***: p-value ≤0.0005, ****: p-value <0.0001, n.s.: not significant

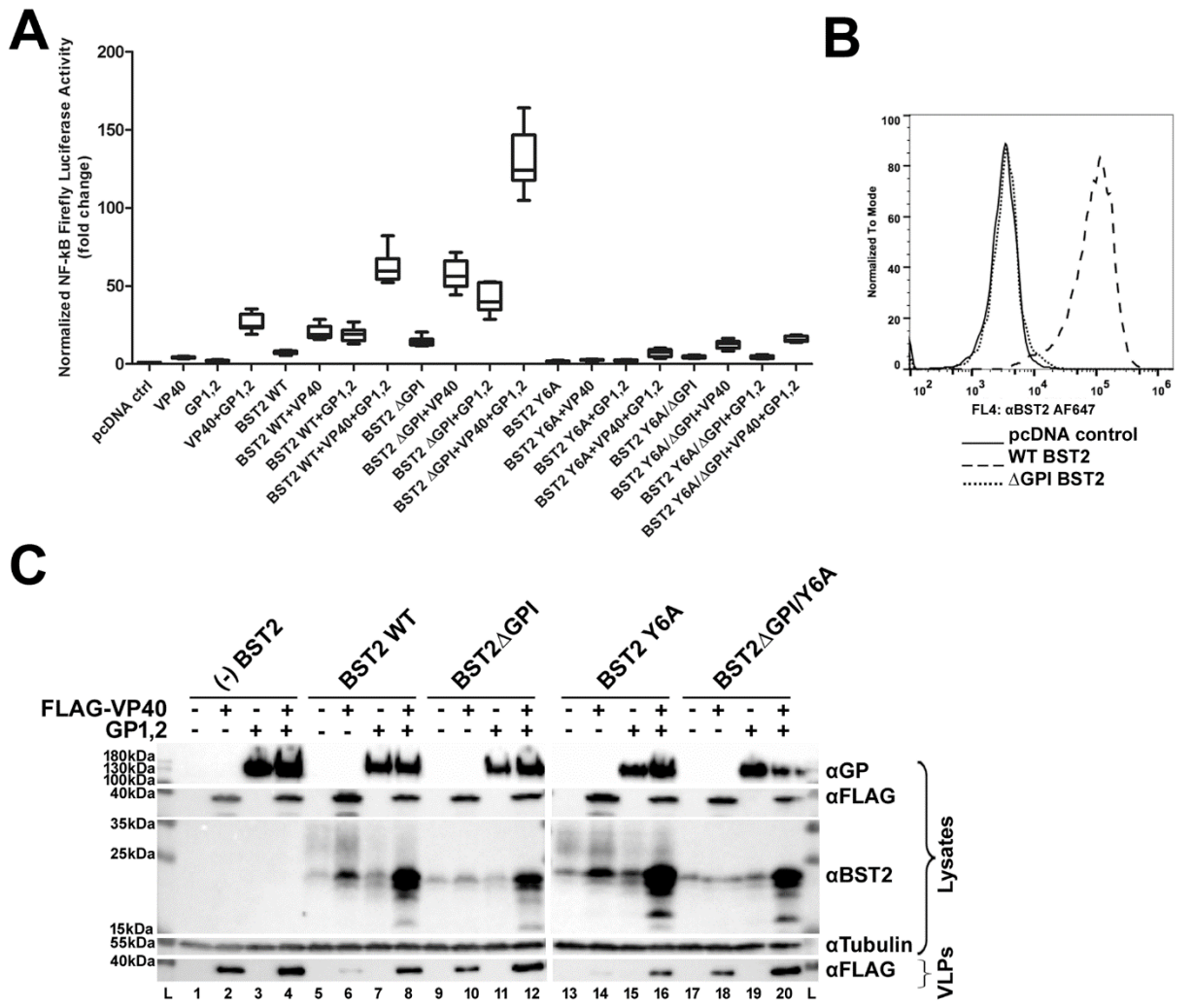

Figure III.7 BST2 signaling in concert with Ebola proteins is independent of VLP entrapment yet dependent on the cytoplasmic tyrosine 6 of BST2. (A) HEK293T cells were transfected similarly to those in Figure III.2A with plasmids expressing the indicated BST2 mutants (85ng). After 24 hrs, NF-κB luciferase activity was measured by luminometry. The box and whiskers graph represents two independent experiments. Statistics for this figure are in Table III.10. (B) Surface BST2-WT and BST2-ΔGPI detected by flow cytometry. GFP was used as a transfection control, and GFP-positive (transfected) cells are shown. (C) Western blots of total cell lysates from one representative experiment out of two. The antibodies used for detection of the proteins are the same as those used in Figure III.1B.

Table III.10 Statistical analyses of differences in NF-κB activities presented in Figure III.7A.

Group 1	Group 2	Wilcoxon Rank Sum	Significant?
pcDNA	BST2-WT	0.0002; ***	Yes
	BST2-ΔGPI	0.0002; ***	Yes
	BST2-Y6A	0.0047; **	Yes
	BST2-Y6A/ΔGPI	0.0002; ***	Yes
		ctrl = 1	
BST2-WT	BST2-ΔGPI	0.0002; ***	Yes
	BST2-Y6A	0.0002; ***	Yes
	BST2-Y6A/ΔGPI	0.0003; ***	Yes
BST2-WT + VP40	BST2-ΔGPI + VP40	0.0002; ***	Yes
	BST2-Y6A + VP40	0.0002; ***	Yes
	BST2-Y6A/ΔGPI + VP40	0.0006; ***	Yes
BST2-WT + $GP_{1,2}$	BST2-ΔGPI + $GP_{1,2}$	0.0002; ***	Yes
	BST2-Y6A + $GP_{1,2}$	0.0002; ***	Yes
	BST2-Y6A/ΔGPI + $GP_{1,2}$	0.0002; ***	Yes
BST2-WT + VP40 + $GP_{1,2}$	BST2-ΔGPI + VP40 + $GP_{1,2}$	0.0002; ***	Yes
	BST2-Y6A + VP40 + $GP_{1,2}$	0.0002; ***	Yes
	BST2-Y6A/ΔGPI + VP40 + $GP_{1,2}$	0.0002; ***	Yes
BST2-ΔGPI	BST2-Y6A/ΔGPI	0.0002; ***	Yes
BST2-ΔGPI + VP40	BST2-Y6A/ΔGPI + VP40	0.0002; ***	Yes
BST2-ΔGPI + $GP_{1,2}$	BST2-Y6A/ΔGPI + $GP_{1,2}$	0.0002; ***	Yes
BST2-ΔGPI + VP40 + $GP_{1,2}$	BST2-Y6A/ΔGPI + VP40 + $GP_{1,2}$	0.0002; ***	Yes

*: p-value ≤0.05, **: p-value ≤0.005, ***: p-value ≤0.0005, ****: p-value <0.0001, n.s.: not significant

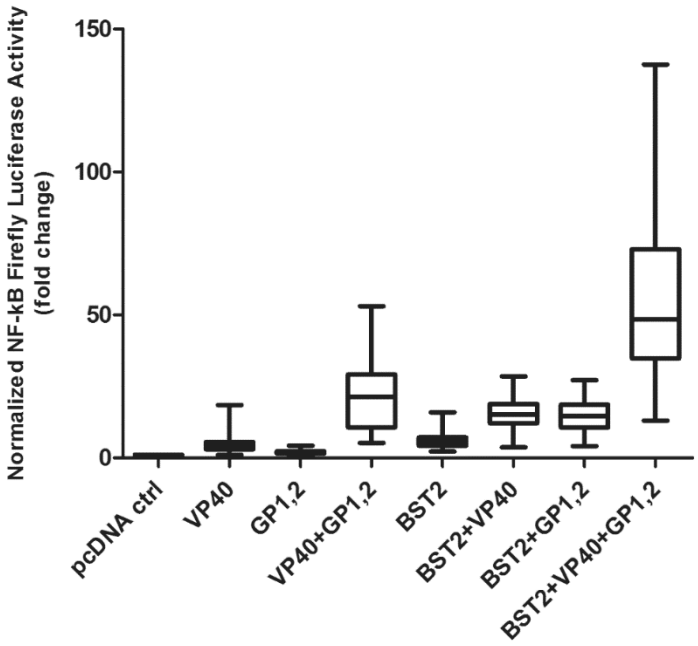

Figure III.8 BST2 signaling in concert with Ebola VP40 and $GP_{1,2}$ as a reproducible phenotype. Here, we combined the normalized NF-κB firefly luciferase values from the fourteen independent experiments of Figure III.2 through FIG 7 for the groups indicated on the box and whiskers graph. We used the samples expressing the 1976 Zaire $GP_{1,2}$ for this figure. Statistical analyses are presented in Tables III.11 and III.12.

Table III.11 Statistical analysis of differences in NF-κB activities presented in Figure III.8.

Group 1	**Group2**			
		Wilcoxon Rank Sum		Significant?
pcDNA	BST2	<0.0001; ****		Yes
	VP40	<0.0001; ****		Yes
	$GP_{1,2}$	<0.0001; ****		Yes
		Kruskall-Wallis	Dunn's	Significant?
VP40 + GP	GP		***	Yes
	VP40	< 0.0001; ****	***	Yes
BST2 + VP40	VP40		***	Yes
	BST2	< 0.0001; ****	***	Yes
BST2 + GP	BST2		***	Yes
	GP	< 0.0001; ****	***	Yes
BST2 + VP40 + GP	BST2 + VP40		***	Yes
	VP40 + GP		***	Yes
	GP + BST2	< 0.0001; ****	***	Yes

*: p-value ≤0.05, **: p-value ≤0.005, ***: p-value ≤0.0005, ****: p-value <0.0001, n.s.: not significant

Table III.12 Normalized NF-κB luciferase values presented in Figure III.8.

Group	**Median***	**Min****	**Max*****	**25th %**	**75th %**
VP40	4.129	1.052	18.49	3.035	5.62
$GP_{1,2}$	1.93	0.8319	4.363	1.483	2.316
VP40 + $GP_{1,2}$	21.43	5.248	53.09	10.66	29.15
BST2	5.651	2.208	16	4.315	7.116
BST2 + VP40	15.23	3.641	28.54	12.11	18.87
BST2 + $GP_{1,2}$	14.57	4.164	27.16	10.66	18.59
BST2 + VP40 + GP	48.48	13.09	137.6	34.87	72.91

*control=1; **Min: Minimum value; ***Max: Maximum value

References

1. **Blasius AL, Giurisato E, Cella M, Schreiber RD, Shaw AS, Colonna M.** 2006. Bone marrow stromal cell antigen 2 is a specific marker of type I IFN-producing cells in the naive mouse, but a promiscuous cell surface antigen following IFN stimulation. J Immunol **177:**3260-3265.

2. **Neil SJ, Zang T, Bieniasz PD.** 2008. Tetherin inhibits retrovirus release and is antagonized by HIV-1 Vpu. Nature **451:**425-430.

3. **Van Damme N, Goff D, Katsura C, Jorgenson RL, Mitchell R, Johnson MC, Stephens EB, Guatelli J.** 2008. The interferon-induced protein BST-2 restricts HIV-1 release and is downregulated from the cell surface by the viral Vpu protein. Cell Host Microbe **3:**245-252.

4. **Galao RP, Le Tortorec A, Pickering S, Kueck T, Neil SJ.** 2012. Innate sensing of HIV-1 assembly by Tetherin induces NFkappaB-dependent proinflammatory responses. Cell Host Microbe **12:**633-644.

5. **Tokarev A, Suarez M, Kwan W, Fitzpatrick K, Singh R, Guatelli J.** 2013. Stimulation of NF-kappaB activity by the HIV restriction factor BST2. J Virol **87:**2046-2057.

6. **Andrew AJ, Miyagi E, Kao S, Strebel K.** 2009. The formation of cysteine-linked dimers of BST-2/tetherin is important for inhibition of HIV-1 virus release but not for sensitivity to Vpu. Retrovirology **6:**80.

7. **Kupzig S, Korolchuk V, Rollason R, Sugden A, Wilde A, Banting G.** 2003. Bst-2/HM1.24 is a raft-associated apical membrane protein with an unusual topology. Traffic **4:**694-709.

8. **Hammonds J, Wang JJ, Yi H, Spearman P.** 2010. Immunoelectron microscopic evidence for Tetherin/BST2 as the physical bridge between HIV-1 virions and the plasma membrane. PLoS Pathog **6:**e1000749.

9. **Galao RP, Pickering S, Curnock R, Neil SJ.** 2014. Retroviral retention activates a Syk-dependent HemITAM in human tetherin. Cell Host Microbe **16:**291-303.

10. **Tan P, Fuchs SY, Chen A, Wu K, Gomez C, Ronai Z, Pan ZQ.** 1999. Recruitment of a ROC1-CUL1 ubiquitin ligase by Skp1 and HOS to catalyze the ubiquitination of I kappa B alpha. Mol Cell **3:**527-533.

11. **Winston JT, Strack P, Beer-Romero P, Chu CY, Elledge SJ, Harper JW.** 1999. The SCFbeta-TRCP-ubiquitin ligase complex associates specifically with phosphorylated destruction motifs in IkappaBalpha and beta-catenin and stimulates IkappaBalpha ubiquitination in vitro. Genes Dev **13:**270-283.

12. **Kaletsky RL, Francica JR, Agrawal-Gamse C, Bates P.** 2009. Tetherin-mediated restriction of filovirus budding is antagonized by the Ebola glycoprotein. Proc Natl Acad Sci U S A **106:**2886-2891.

13. **Hauser H, Lopez LA, Yang SJ, Oldenburg JE, Exline CM, Guatelli JC, Cannon PM.** 2010. HIV-1 Vpu and HIV-2 Env counteract BST-2/tetherin by sequestration in a perinuclear compartment. Retrovirology **7:**51.

14. **Mansouri M, Viswanathan K, Douglas JL, Hines J, Gustin J, Moses AV, Fruh K.** 2009. Molecular mechanism of BST2/tetherin downregulation by K5/MIR2 of Kaposi's sarcoma-associated herpesvirus. J Virol **83:**9672-9681.

15. **Zhang F, Wilson SJ, Landford WC, Virgen B, Gregory D, Johnson MC, Munch J, Kirchhoff F, Bieniasz PD, Hatziioannou T.** 2009. Nef proteins from simian immunodeficiency viruses are tetherin antagonists. Cell Host Microbe **6:**54-67.

16. **Goffinet C, Allespach I, Homann S, Tervo HM, Habermann A, Rupp D, Oberbremer L, Kern C, Tibroni N, Welsch S, Krijnse-Locker J, Banting G, Krausslich HG, Fackler OT, Keppler OT.** 2009. HIV-1 antagonism of CD317 is species specific and involves Vpu-mediated proteasomal degradation of the restriction factor. Cell Host Microbe **5:**285-297.

17. **Iwabu Y, Fujita H, Kinomoto M, Kaneko K, Ishizaka Y, Tanaka Y, Sata T, Tokunaga K.** 2009. HIV-1 accessory protein Vpu internalizes cell-surface BST-2/tetherin through transmembrane interactions leading to lysosomes. J Biol Chem **284:**35060-35072.

18. **Mangeat B, Gers-Huber G, Lehmann M, Zufferey M, Luban J, Piguet V.** 2009. HIV-1 Vpu neutralizes the antiviral factor Tetherin/BST-2 by binding it and directing its beta-TrCP2-dependent degradation. PLoS Pathog **5:**e1000574.

19. **Andrew A, Strebel K.** 2010. HIV-1 Vpu targets cell surface markers CD4 and BST-2 through distinct mechanisms. Mol Aspects Med **31:**407-417.

20. **Dube M, Paquay C, Roy BB, Bego MG, Mercier J, Cohen EA.** 2011. HIV-1 Vpu antagonizes BST-2 by interfering mainly with the trafficking of newly synthesized BST-2 to the cell surface. Traffic **12:**1714-1729.

21. **Lewinski MK, Jafari M, Zhang H, Opella SJ, Guatelli J.** 2015. Membrane Anchoring by a C-terminal Tryptophan Enables HIV-1 Vpu to Displace Bone Marrow Stromal Antigen 2 (BST2) from Sites of Viral Assembly. J Biol Chem **290:**10919-10933.

22. **Kuhl A, Banning C, Marzi A, Votteler J, Steffen I, Bertram S, Glowacka I, Konrad A, Sturzl M, Guo JT, Schubert U, Feldmann H, Behrens G, Schindler**

M, Pohlmann S. 2011. The Ebola virus glycoprotein and HIV-1 Vpu employ different strategies to counteract the antiviral factor tetherin. J Infect Dis **204 Suppl 3:**S850-860.

23. **Gnirss K, Fiedler M, Kramer-Kuhl A, Bolduan S, Mittler E, Becker S, Schindler M, Pohlmann S.** 2014. Analysis of determinants in filovirus glycoproteins required for tetherin antagonism. Viruses **6:**1654-1671.

24. **Vande Burgt NH, Kaletsky RL, Bates P.** 2015. Requirements within the Ebola Viral Glycoprotein for Tetherin Antagonism. Viruses **7:**5587-5602.

25. **Lopez LA, Yang SJ, Hauser H, Exline CM, Haworth KG, Oldenburg J, Cannon PM.** 2010. Ebola virus glycoprotein counteracts BST-2/Tetherin restriction in a sequence-independent manner that does not require tetherin surface removal. J Virol **84:**7243-7255.

26. **Lopez LA, Yang SJ, Exline CM, Rengarajan S, Haworth KG, Cannon PM.** 2012. Anti-tetherin activities of HIV-1 Vpu and Ebola virus glycoprotein do not involve removal of tetherin from lipid rafts. J Virol **86:**5467-5480.

27. **Gustin JK, Bai Y, Moses AV, Douglas JL.** 2015. Ebola Virus Glycoprotein Promotes Enhanced Viral Egress by Preventing Ebola VP40 From Associating With the Host Restriction Factor BST2/Tetherin. J Infect Dis doi:10.1093/infdis/jiv125.

28. **Brinkmann C, Nehlmeier I, Walendy-Gnirss K, Nehls J, Gonzalez Hernandez M, Hoffmann M, Qiu X, Takada A, Schindler M, Pohlmann S.** 2016. The Tetherin Antagonism of the Ebola Virus Glycoprotein Requires an Intact Receptor-Binding Domain and Can Be Blocked by GP1-Specific Antibodies. J Virol **90:**11075-11086.

29. **Noda T, Sagara H, Suzuki E, Takada A, Kida H, Kawaoka Y.** 2002. Ebola virus VP40 drives the formation of virus-like filamentous particles along with GP. J Virol **76:**4855-4865.

30. **Licata JM, Johnson RF, Han Z, Harty RN.** 2004. Contribution of ebola virus glycoprotein, nucleoprotein, and VP24 to budding of VP40 virus-like particles. J Virol **78:**7344-7351.

31. **Volchkov VE, Feldmann H, Volchkova VA, Klenk HD.** 1998. Processing of the Ebola virus glycoprotein by the proprotein convertase furin. Proc Natl Acad Sci U S A **95:**5762-5767.

32. **Jia X, Weber E, Tokarev A, Lewinski M, Rizk M, Suarez M, Guatelli J, Xiong Y.** 2014. Structural basis of HIV-1 Vpu-mediated BST2 antagonism via hijacking of the clathrin adaptor protein complex 1. Elife **3:**e02362.

33. **Nguyen KL, llano M, Akari H, Miyagi E, Poeschla EM, Strebel K, Bour S.** 2004. Codon optimization of the HIV-1 vpu and vif genes stabilizes their mRNA and allows for highly efficient Rev-independent expression. Virology **319:**163-175.

34. **DiDonato J, Mercurio F, Rosette C, Wu-Li J, Suyang H, Ghosh S, Karin M.** 1996. Mapping of the inducible IkappaB phosphorylation sites that signal its ubiquitination and degradation. Mol Cell Biol **16:**1295-1304.

35. **Soucy TA, Smith PG, Milhollen MA, Berger AJ, Gavin JM, Adhikari S, Brownell JE, Burke KE, Cardin DP, Critchley S, Cullis CA, Doucette A, Garnsey JJ, Gaulin JL, Gershman RE, Lublinsky AR, McDonald A, Mizutani H, Narayanan U, Olhava EJ, Peluso S, Rezaei M, Sintchak MD, Talreja T, Thomas MP, Traore T, Vyskocil S, Weatherhead GS, Yu J, Zhang J, Dick LR, Claiborne CF, Rolfe M, Bolen JB, Langston SP.** 2009. An inhibitor of NEDD8-activating enzyme as a new approach to treat cancer. Nature **458:**732-736.

36. **Kroll M, Margottin F, Kohl A, Renard P, Durand H, Concordet JP, Bachelerie F, Arenzana-Seisdedos F, Benarous R.** 1999. Inducible degradation of IkappaBalpha by the proteasome requires interaction with the F-box protein h-betaTrCP. J Biol Chem **274:**7941-7945.

37. **McNatt MW, Zang T, Bieniasz PD.** 2013. Vpu binds directly to tetherin and displaces it from nascent virions. PLoS Pathog **9:**e1003299.

38. **Bour S, Perrin C, Akari H, Strebel K.** 2001. The human immunodeficiency virus type 1 Vpu protein inhibits NF-kappa B activation by interfering with beta TrCP-mediated degradation of Ikappa B. J Biol Chem **276:**15920-15928.

39. **Dolnik O, Volchkova V, Garten W, Carbonnelle C, Becker S, Kahnt J, Stroher U, Klenk HD, Volchkov V.** 2004. Ectodomain shedding of the glycoprotein GP of Ebola virus. EMBO J **23:**2175-2184.

40. **Escudero-Perez B, Volchkova VA, Dolnik O, Lawrence P, Volchkov VE.** 2014. Shed GP of Ebola virus triggers immune activation and increased vascular permeability. PLoS Pathog **10:**e1004509.

41. **Martinez O, Valmas C, Basler CF.** 2007. Ebola virus-like particle-induced activation of NF-kappaB and Erk signaling in human dendritic cells requires the glycoprotein mucin domain. Virology **364:**342-354.

42. **Wahl-Jensen V, Kurz S, Feldmann F, Buehler LK, Kindrachuk J, DeFilippis V, da Silva Correia J, Fruh K, Kuhn JH, Burton DR, Feldmann H.** 2011. Ebola virion attachment and entry into human macrophages profoundly effects early cellular gene expression. PLoS Negl Trop Dis **5:**e1359.

43. **Zhao D, Han X, Zheng X, Wang H, Yang Z, Liu D, Han K, Liu J, Wang X, Yang W, Dong Q, Yang S, Xia X, Tang L, He F.** 2016. The Myeloid LSECtin Is a DAP12-Coupled Receptor That Is Crucial for Inflammatory Response Induced by Ebola Virus Glycoprotein. PLoS Pathog **12:**e1005487.

44. **Caras IW, Weddell GN, Williams SR.** 1989. Analysis of the signal for attachment of a glycophospholipid membrane anchor. J Cell Biol **108:**1387-1396.

45. **Rosenbaum EE, Brehm KS, Vasiljevic E, Gajeski A, Colley NJ.** 2012. Drosophila GPI-mannosyltransferase 2 is required for GPI anchor attachment and surface expression of chaoptin. Vis Neurosci **29:**143-156.

46. **Andrew AJ, Kao S, Strebel K.** 2011. C-terminal hydrophobic region in human bone marrow stromal cell antigen 2 (BST-2)/tetherin protein functions as second transmembrane motif. J Biol Chem **286:**39967-39981.

47. **Falasca L, Agrati C, Petrosillo N, Di Caro A, Capobianchi MR, Ippolito G, Piacentini M.** 2015. Molecular mechanisms of Ebola virus pathogenesis: focus on cell death. Cell Death Differ **22:**1250-1259.

48. **Martines RB, Ng DL, Greer PW, Rollin PE, Zaki SR.** 2015. Tissue and cellular tropism, pathology and pathogenesis of Ebola and Marburg viruses. J Pathol **235:**153-174.

Chapter IV

Conclusion and Future Directions

Summary

The objectives of this dissertation were to study the role of the cytoplasmic tail of BST2 towards the trafficking of the protein and the activation of NF-κB and to advance the understanding of the BST2 signaling mechanism. By studying direct protein-protein interactions between the BST2 CD with the clathrin AP1 complex, investigating changes in NF-κB activity by BST2 in presence of Ebola virus proteins GP1,2 and VP40, and studying various mutants of BST2, the objectives of the dissertation were met.

The BST2 cytoplasmic tail domain plays a major role in the trafficking and signaling functions of the protein.

Tyrosines 6 and 8 and valine 11 of BST2 are required for direct protein-protein interaction between BST2 and μ1 of the AP1 complex in the presence of the HIV-1 Vpu. Mutations of these residues to alanines abolished the interaction of BST2 with μ1 as demonstrated by yeast 2-hybrid assays. Since this interaction appears to require the close proximity of HIV-1 Vpu, whether BST2 interacts with AP-1 for its natural trafficking within the cells remains unclear (1). In this sense, having tyrosines at positions 6 and 8 and a valine (or a hydrophobic residue) at position 11 present a disadvantage to the host since they sensitize BST2 to the antagonistic effects of Vpu, which lead to the increase in viral release. From a therapeutic perspective, would creating small molecules, inserted into the interface for the interaction between BST2 with Vpu, Vpu with AP1, or BST2 with AP1, confer resistance towards the negative effects of the Vpu viral protein on the host? This remains as an open question that requires further investigation. On the other hand, the two tyrosine residues studies here could provide the basis for understanding BST2 trafficking within the cell that contributes to its function in ways that remain undetermined. Moreover, we found that these two tyrosine residues

were important for the signaling activity of BST2 in our study system, where it was expressed alone or with viral proteins. Overall, we observed that a distinction between the role of these tyrosines in trafficking and signaling exists, where only tyrosine 6 was essential for signaling while tyrosine 8 was dispensable or only secondarily contributory to signaling activity.

Further studies are needed to dissect the exact significance of the tyrosine residues within the cytoplasmic tail of BST2 for the trafficking of BST2 and its signaling activity. For instance, immunoprecipitation of BST2 WT and the varoius tyrosine mutants used here followed by mass spectrometry assays could reveal the BST2 interactome and identify new possible pathways where BST2 participates within the cell. Also, sequencing BST2 genes from patients who have differential responses to viral infections could help identify important polymorphisms within the cytoplasmic tail domain residues of BST2. Identification of polymorphisms that confer resistance to disease can aid in our understanding of the host response to viral infections and provide additional tools to study viral-host interactions through BST2 using tissue culture and *in vitro* studies.

The Ebola virus glycoprotein does not act as an antagonist of BST2-mediated activation of NF-κB, but rather cooperates with BST2 to increase NF-κB activity.

The Ebola virus proteins, VP40 and GP1,2, both cooperate with BST2 in order to activate NF-κB (2). This finding was unexpected because instead of acting as an antagonist of the BST2 signaling function, Ebola GP1,2 seems to enhance the activity of NF-κB. Our findings show that GP1,2 enhances NF-κB activity that is induced by VP40 as well; thus, we concluded that all three proteins act cooperatively to induce NF-κB

activity. Currently, there is not clear understanding of which protein increases the activity of the other protein. We attempted to decipher this question by studying mutants of BST2 and found that the forms of BST2, which are normally defective for signaling such as the Y6A or C3A mutants (See Figures III.5 and 6), were also defective for this cooperative activity with the Ebola proteins. This suggests that NF-κB activity depends, in a large part, on whether BST2 is functional for signaling within the system, although the individual contribution of GP1,2 and VP40 towards the induction of NF-κB activity remains to be investigated.

We wanted to begin to investigate this phenomenon by mutating GP1,2 and asking whether the mutants of the Ebola glycoprotein had limiting effects on signaling. Identifying the limiting role of GP1,2 would provide an understanding of how GP1,2 specifically contributes to the activity of NF-κB in cooperation with BST2 and VP40. We used the same transient HEK293T expression system to over-express BST2, VP40, and various mutants of GP. We found that the full-length furin-resistant form of GP (ΔCI-GP in Figure IV.1) was defective for cooperating with BST2, VP40, or BST2 with VP40 to activate NF-κB. ΔCI-GP was the only form of GP that was defective for increasing signaling under all conditions tested (Table IV.2). Neither soluble forms of GP (sGP and secGP) nor having a deletion of the mucin-like domain of GP had a pattern of being defective for the cooperative activity under all conditions tested (Table IV.2). Full-length GP accumulates in the endoplasmic reticulum (ER) and is defective for the antagonism of BST2-mediated virion entrapment (3, 4). Early studies have also shown that full length GP can be present in the Golgi apparatus as an Endo H-resistent glycoprotein (5). Thus, there are two possible explanations for the inhibition of NF-κB activity as a

result of full-length GP expression: 1) the accumulation of GP within the ER-Golgi interface negatively affects signaling or 2) structural modifications within GP1,2 after furin cleavage are required for signaling.

To attempt to understand the first possibility, we tested for the effect of Brefeldin A on NF-κB activity by the three proteins (BST2, VP40, and GP1,2) alone and in the various combinations shown in Figure IV.2A. Brefeldin A causes the retention of transmembrane proteins within the ER (6) and can cause the activation of NF-κB due to ER stress (7). As shown in Figure VI.2A, HEK293T cells that were transfected only with pcDNA3.1 control plasmid and treated with BFA at 2μg/ml for 20 hours showed greater activity for NF-κB than cells that were treated with DMSO control. We also observed that for cells expressing BST2-WT or BST2-ΔGPI alone or with GP1,2, NF-κB activity was unaffected (Figure IV.2A). We confirmed that BST2 was not expressed at the surface of these cells, as shown in Figure IV.2C. Although we do not show experimentally that GP1,2 is also not expressed at the plasma membrane, we reason that it is unlikely to have escaped the ER-Golgi interface due to the BFA treatment. The data suggest that the accumulation of both BST2 and GP1,2 within the ER-Golgi interface does not negatively affect the activity of NF-κB. This indirectly supports the notion that the cleavage of full-length GP by furin is an important feature of GP1,2 that is required for its cooperative activity with VP40 and BST2 for the activation of NF-κB. Further experiments using knockouts of furin protease with GP1,2-WT could confirm this phenomenon. Also, additional experiments using BFA and fluorescent microscopy could provide more detailed information regarding the localization of BST2 and GP1,2 within the cellular membrane system.

Another interesting observation from our BFA-treated cells was the reduced NF-κB activity of VP40-expressing cells (Figure IV.2A). We observed that for cells that co-expressed BST2-WT or BST2-ΔGPI with VP40 or with VP40 and GP1,2, NF-κB activity was significantly inhibited. As shown earlier in Chapter III, BST2-ΔGPI did not localize to the plasma membrane of cells although it was fully functional for the activation of NF-κB in cooperation with the Ebola virus proteins (2). This suggests that the reduction of NF-κB activity that resulted from the Brefeldin A did not occur due to the inability of BST2 to tether VP40 VLPs at the plasma membrane, since the effects of BFA on BST2-WT and BST2-ΔGPI coexpressed with VP40 were similar. Thus, we propose that BST2 and VP40 are interacting (either directly or indirectly) to affect NF-κB activity within the endoplasmic membrane system within the cell and not at the plasma membrane, or at least not exclusively at the plasma membrane. The direct role of BFA towards the trafficking and assembly of VP40 is not fully understood although studies have shown that GBF1 (Golgi-specific BFA resistant factor 1) and Arf1 (ADP ribosylation factor 1) are involved in the membrane trafficking and assembly of VP40 through the COPII and COPI pathways (8). Further studies looking at the NF-κB signaling by BST2 and VP40 in response to the expression of dominant negative forms of GBF1 and Arf1 will be required to better understand the cooperatively between VP40 and BST2 signaling. Also, immunofluorescence microscopy experiments of BST2 and VP40 in the presence of BFA could shed further light on the co-localization dynamics between the two proteins and how localization correlates to signaling.

The HIV-2 Envelope protein does not inhibit BST2-mediated activation of NF-κB.

The HIV-2 envelope protein antagonizes BST2 with respect to its function of the entrapment of virions by downregulating the levels of BST2 at the plasma membrane (9, 10). We asked whether the expression of HIV-2 Env would downregulate the levels of NF-κB activity in cells that were engineered to stably express BST2 (Hu6 in Figure IV.3A). Considering the different effects that HIV-1 Vpu and Ebola GP1,2 had on BST2-mediated NF-κB activity (Chapter III and Figures IV.1 and 2), we hypothesized that HIV-2 Env would either inhibit or have not effect on BST2-mediated NF-κB activity. When tested with HIV-1ΔVpu provirus, we found that, indeed, HIV-2 Env did not inhibit BST2 signaling (Figure IV.3A). To confirm that the expression of Env enhanced virion release, we performed an ELISA assay on released particles of the HIV-1 gag p24 protein of the viral capsid (Figure VI.3B). Based on the median values of pg/ml of p24, we confirmed that the HIV-2 Env-WT (Rod10) efficiently enhanced virion release when compared to Hu6 cells expressing HIV-1ΔVpu provirus only, as expected (10). On the other hand, the mutant of HIV-2 Env (Rod10 Y/A) and the variant (Rod14), which were previously shown to be defective for the antagonism of BST2, did not increase virion release as demonstrated by the median levels of p24 in Figure VI.3B. Thus, we conclude that HIV-2 Env does not inhibit BST2-mediated activation of NF-κB, despite counteracting BST2-mediate restriction of virion release, and that this supports our general conclusion regarding the disconnection between the virion-entrapment and signaling functions of BST2.

Conclusion

The work presented here was focused on understanding how the host anti-viral protein BST2 responds to viral proteins of HIV-1, Ebola virus, and HIV-2 for its

trafficking and signaling activities. Specifically, the work focused on how BST2 interacts with intracellular trafficking machinery of the AP1 clathrin coat complex, which is hijacked by HIV-1 Vpu for the enhanced release of virions. Additionally, we suggested that BST2-mediated activation of NF-κB does not sense entrapped virions in the case of Ebola virus, but it might still provide an anti-viral sensing mechanism by activating NF-κB in response to viral proteins VP40 and $GP_{1,2}$. We further supported this by the disconnection between BST2-mediated signaling and the restriction of virion release by the HIV-2 envelope. Future studies of BST2 function and localization are needed in order to understand the dynamics of BST2 trafficking and signaling in response to viral proteins and how such response affect the release of virions and proinflammatory cytokines during infection. *In vivo* studies of primate animal models would be ideal for a full understanding of how the BST2 protein contributes to the anti-viral and proinflammatory responses at the level of an organism.

Continuing research on host-viral interactions is of utmost importance as many viruses continue to evolve within the host as more individuals and populations become infected, as in the case of HIV-1. Also, understanding the cellular mechanisms that govern highly pathogenic viruses such as the Ebola virus will continue to be essential in order to develop effective vaccines and appropriate treatment therapies.

Acknowledgements

We thank Dr. Paula Cannon (USC Keck School of Medicine, Los Angeles, CA) for providing the pSA91-HIV2-ROD10, pSA91-HIV2-ROD10Y/A and the pSA91-HIV2-ROD14 envelope plasmids. We thank Dr. Paul Bates (University of Pennsylvania, Phildelphia, PA) for the pCAGGS-zaireVP40, -zaireGP1,2, -sGP, -secGP, -Δmuc-GP, and -ΔCI-GP and the anti-GP polyclonal rabbit serum.

Figures and Tables

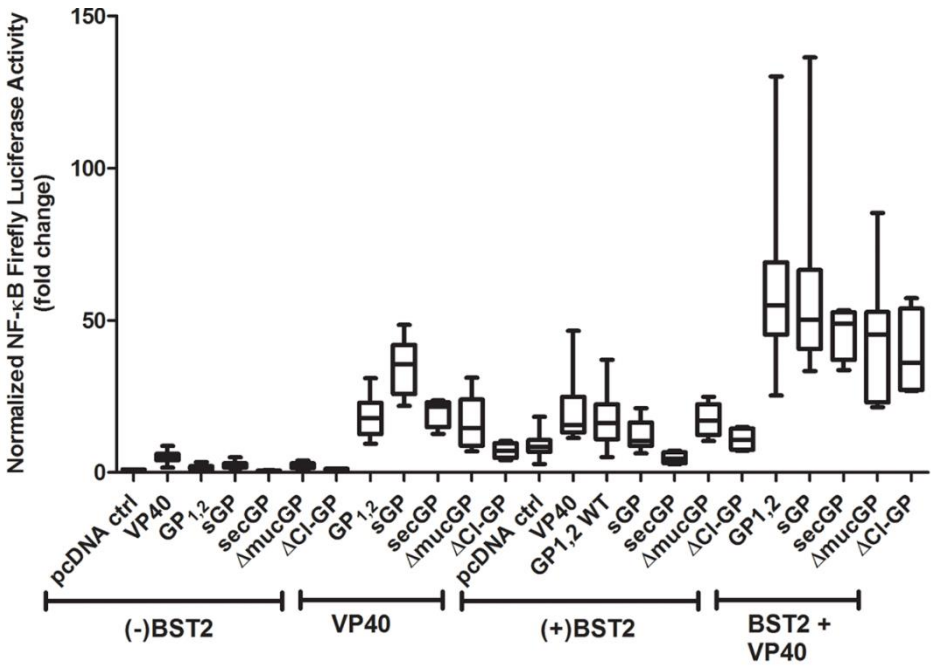

Figure IV.1. NF-κB activity in response to the expression of mutants of Ebola virus glycoprotein. HEK293T cells expressing the indicated proteins, where pcDNA ctrl indicates that only a pcDNA3.1 empty plasmid was transfected into the cells. Cells were plated in 12-well plates, transfected, and harvested in a similar manner to those shown in Figure III.3A. VP40 (300ng), BST2 (85ng), and each of the GPs (900ng) were expressed alone and in the combinations indicated. GP1,2 is the trimer of dimers that forms the spike on the surface of VLPs. The non-structural sGP is a soluble dimeric form of GP that expresses the first 320 amino acids of GP (11). A deletion of the transmembrane domain produces a secreted form of GP (labeled secGP). ΔmucGP stands for GP1,2 lacking the mucin-like domain. ΔCl-GP stands for full-length GP, where the furin-cleavage site is mutated to be resistant for cleavage. The data presented here is a combination of three independent experiments.

Table IV.1 Wilcoxon rank sum test statistics of NF-κB activity of groups compared to the pcDNA control group presented in Figure IV.1.

Group 1	Group 2	Wilcoxon Rank Sum	Significant?
pcDNA ctrl	VP40	<0.0001; ****	Yes
	GP1,2	**0.0601; ns**	**No**
	sGP	<0.0001; ****	Yes
	secGP (ΔTM)	**0.0672; ns**	**No**
	ΔmucGP	0.005; **	Yes
	ΔCl-GP	0.012; *	Yes
	BST2	<0.0001; ****	Yes

Table IV.2 Kruskall-Wallis test statistics for group comparisons of NF-κB activity presented in Figure IV.1

Group 1	Group 2	Kruskall-Wallis	Dunn's	Significant?
	VP40		***	Yes
VP40 + GP1,2	GP1,2	<0.0001; ****	***	Yes
	VP40		***	Yes
VP40 + sGP	sGP	<0.0001; ****	***	Yes
	VP40		*	Yes
VP40 + secGP (ΔTM)	secGP (ΔTM)	0.003; ***	***	Yes
	VP40		**	Yes
VP40 + ΔmucGP	ΔmucGP	<0.0001; ****	***	Yes
	VP40		**ns**	**No**
VP40 + ΔCl-GP	ΔCl-GP	0.0035; **	**	Yes
	VP40		***	Yes
VP40 + BST2	BST2	<0.0001; ****	**	Yes
	BST2		**ns**	**No**
BST2 + GP1,2	GP1,2	<0.0001; ****	***	Yes
	BST2		**ns**	**No**
BST2 + sGP	sGP	<0.0001; ****	***	Yes
	BST2		**ns**	**No**
BST2 + secGP (ΔTM)	secGP (ΔTM)	0.0013; **	**ns**	**No**
	BST2		*	Yes
BST2 + ΔmucGP	ΔmucGP	<0.0001; ****	***	Yes
	BST2		**ns**	**No**
BST2 + ΔCl-GP	ΔCl-GP	0.0058; **	**	Yes
	VP40 + BST2		***	Yes
	VP40 + GP1,2		***	Yes
VP40 + BST2 + GP1,2	BST2 + GP1,2	<0.0001; ****	***	Yes
	VP40 + BST2		***	Yes
	VP40 + sGP		**ns**	**No**
VP40 + BST2 + sGP	BST2 + sGP	<0.0001; ****	***	Yes
	VP40 + BST2		*	Yes
	VP40 + secGP (ΔTM)		**ns**	**No**
VP40 + BST2 + secGP (ΔTM)	BST2 + secGP (ΔTM)	0.0009; ***	***	Yes
	VP40 + BST2		**	Yes
VP40 + BST2 + ΔmucGP	VP40 + ΔmucGP		***	Yes
	BST2 + ΔmucGP	0.0012; **	**	Yes
	VP40 + BST2		**ns**	**No**
	VP40 + ΔCl-GP		***	Yes
VP40 + BST2 + ΔCl-GP	BST2 + ΔCl-GP	0.0008; ***	*	Yes

Table IV.3 Normalized NF-κB activity values presented in Figure IV.1.

Group	Median	Min	Max	25th %	75th %
pcDNA ctrl	1.00	1.00	1.00	1.00	1.00
VP40	4.79	1.60	8.75	4.10	6.12
GP1,2	1.30	0.60	3.46	0.98	2.08
sGP	2.22	1.35	4.96	1.66	3.03
secGP (ΔTM)	0.48	0.36	0.81	0.39	0.73
ΔmucGP	2.09	0.77	3.91	1.49	3.07
ΔCl-GP	1.01	0.61	1.30	0.70	1.23
BST2	8.51	2.76	18.28	6.77	10.68
VP40 + GP1,2	17.88	9.46	30.95	12.61	22.92
VP40 + sGP	35.57	21.87	48.46	25.75	41.95
VP40 + secGP (ΔTM)	21.52	12.74	23.62	14.90	23.13
VP40 + ΔmucGP	14.56	6.95	31.13	8.81	23.95
VP40 + ΔCl-GP	7.21	4.12	10.37	4.83	9.64
VP40 + BST2	15.54	11.29	46.55	13.18	24.89
BST2 + GP1,2	16.24	5.10	37.07	10.91	22.40
BST2 + sGP	10.45	6.26	21.13	8.78	16.42
BST2 + secGP (ΔTM)	4.58	2.73	7.19	3.02	6.71
BST2 + ΔmucGP	17.03	10.34	24.84	12.36	22.47
BST2 + ΔCl-GP	10.67	7.14	15.00	7.47	14.46
VP40 + BST2 + GP1,2	54.90	25.28	130.10	45.30	69.05
VP40 + BST2 + sGP	50.12	33.35	136.30	40.51	66.49
VP40 + BST2 + secGP (ΔTM)	48.83	33.64	53.28	36.97	52.64
VP40 + BST2 + ΔmucGP	45.36	21.48	85.23	22.98	52.70
VP40 + BST2 + ΔCl-GP	36.11	26.71	57.25	27.13	53.89

Figure IV.2 Effects of Brefeldin A treatment on BST2 signaling activity in cooperation with the Ebola virus VP40 and GP1,2 proteins. A) HEK293T cells were plated at $2.3x10^5$ cells per well of a 12-well plate. The next day, the cells were transfected with plasmids encoding the indicated proteins as follows: 85ng pcDNA3.1-BST2, 85ng pcDNA3.1-BST2Δ156-162, 900ng pCAGGS-Zaire $GP_{1,2}$–His/V5, and/or 300ng pCAGGS-FLAG-Zaire VP40. All samples were co-transfected with 63ng *Renilla* luciferase plasmid and 125ng NF-κB firefly luciferase plasmid. Total plasmid quantity was normalized using an empty pcDNA3.1 vector. Four hours after transfection, the media was removed and fresh media that contained either DMSO alone or 2ug/ml Brefeldin A was added for an additional 20hrs. The media was then removed from cells, clarified, and loaded onto a 20% sucrose layer to pellet VLP's using high-speed centrifugation (see Materials and Methods of Chapter III). The cells were harvested for luciferase assays, and the fold-changes in NF-κB activity were calculated and ploted in the box and whiskers graph. P-values indicated are the result of a Wilcoxon Rank Sum statistical test of three independent experiments, each with four technical replicates. (B) Cells were lysed and analyzed by SDS/PAGE and Western blot. The collected VLP's were resuspended in Western sample buffer and analyzed by SDS/PAGE and Western blot as a measure of VLP release. BST2 was detected using polyclonal rabbit anti-BST2. Tubulin-α was used as a loading control and detected using a monoclonal anti-tubulin antibody. Ebola $GP_{1,2}$ was detected using a rabbit anti-sera to $sGP_{1,2}$. FLAG-tagged Ebola VP40 was detected using mouse monoclonal anti-FLAG. Data are representative of three independent experiments. (C) Flow cytometric analysis of HEK293T cells that were plated, transfected, and treated with BFA similarly to those in panel A, but without the luciferase indicator plasmids. Instead, a GFP-expression plasmid was included at 100ng/well to enable gating on the transfected cells. The GFP-positive population is shown in the plots of relative cell number (normalized to mode) vs. BST2 fluorescence. Surface BST2 was detected using Alexa-fluor647 (A647)-conjugated anti-BST2 antibody (clone RS38E). The flow cytometry experiment was repeated three times with similar results.

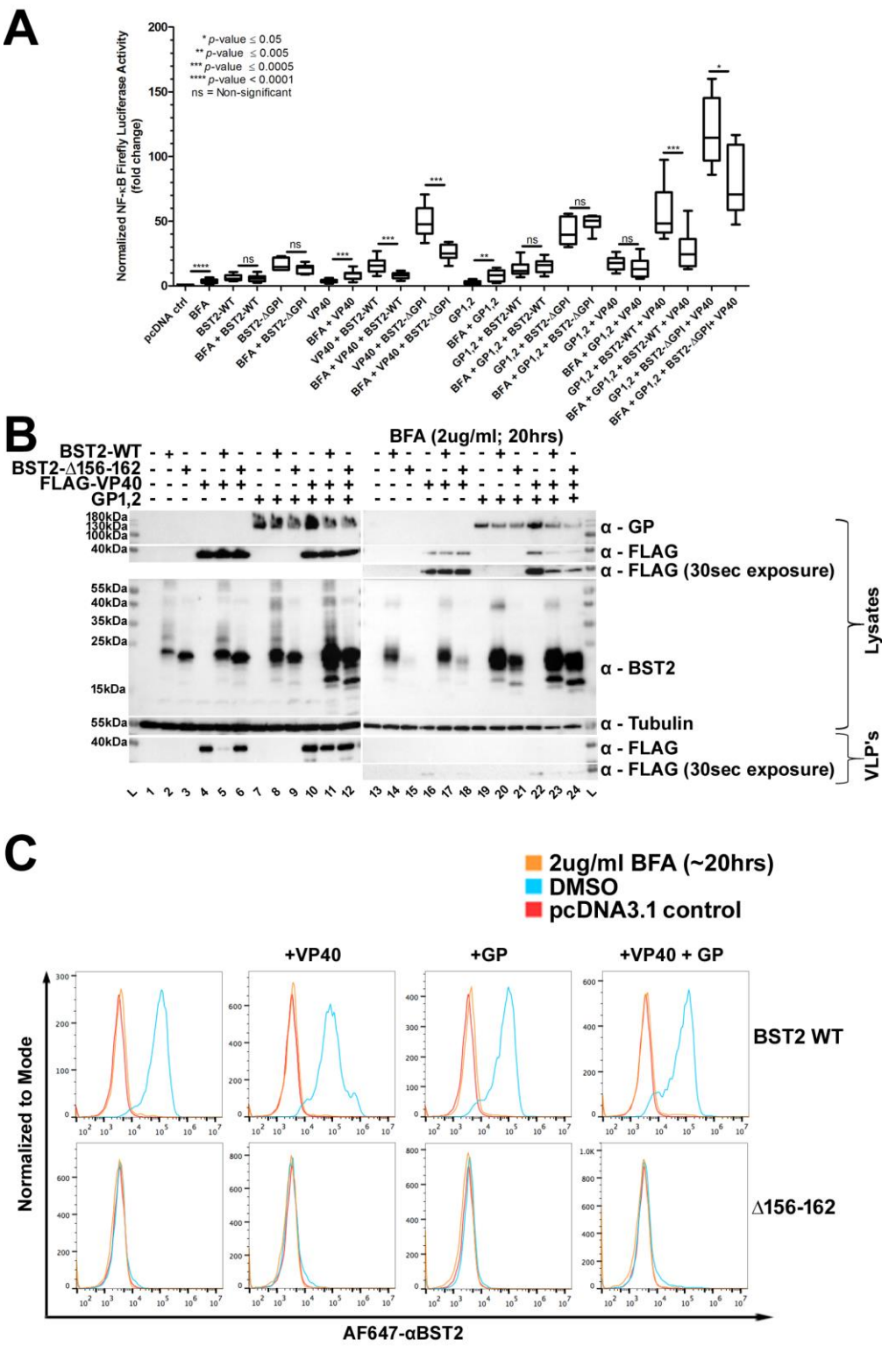
A
Normalized NF-κB Firefly Luciferase Activity (fold change)
* p-value ≤ 0.05
** p-value ≤ 0.005
*** p-value ≤ 0.0005
**** p-value < 0.0001
ns = Non-significant
pcDNA ctrl
BFA
BST2-WT
BFA + BST2-WT
BST2-ΔGPI
BFA + BST2-ΔGPI
VP40
BFA + VP40
VP40 + BST2-WT
BFA + VP40 + BST2-WT
VP40 + BST2-ΔGPI
BFA + VP40 + BST2-ΔGPI
GP1,2
BFA + GP1,2
GP1,2 + BST2-WT
BFA + GP1,2 + BST2-WT
GP1,2 + BST2-ΔGPI
BFA + GP1,2 + BST2-ΔGPI
GP1,2 + VP40
BFA + GP1,2 + VP40
GP1,2 + BST2-WT + VP40
BFA + GP1,2 + BST2-WT + VP40
GP1,2 + BST2-ΔGPI + VP40
BFA + GP1,2 + BST2-ΔGPI+ VP40
B
BFA (2ug/ml; 20hrs)
BST2-WT
BST2-Δ156-162
FLAG-VP40
GP1,2
180kDa
130kDa
100kDa
40kDa
α - GP
α - FLAG
α - FLAG (30sec exposure)
55kDa
40kDa
35kDa
25kDa
15kDa
α - BST2
55kDa
α - Tubulin
Lysates
40kDa
α - FLAG
α - FLAG (30sec exposure)
VLP's
L 1 2 3 4 5 6 7 8 9 10 11 12 13 14 15 16 17 18 19 20 21 22 23 24 L
C
2ug/ml BFA (~20hrs)
DMSO
pcDNA3.1 control
+VP40
+GP
+VP40 + GP
BST2 WT
Δ156-162
Normalized to Mode
AF647-αBST2

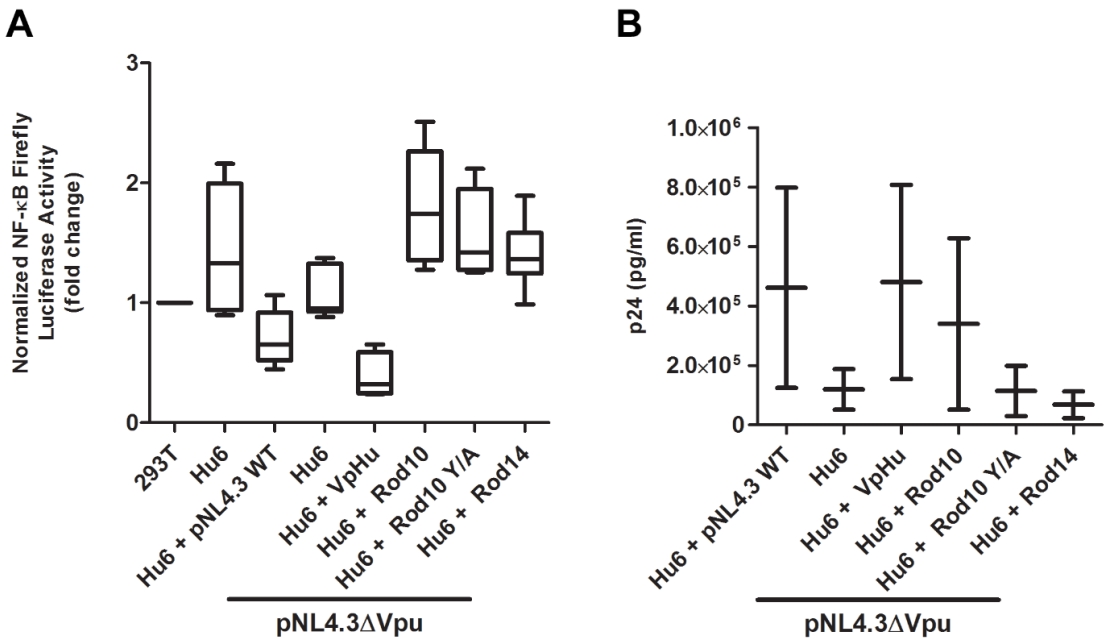

Figure IV.3 Effects of the HIV2 Env on BST2-mediated NF-κB activity and virion release. HEK293T cells that were engineered to stably express human-BST2 (designated as Hu6) were transfected with pcDNA3.1 alone or with 1.75μg of human codon optimized Vpu (VpHu) of HIV1 or HIV2 Env (Rod10 or Rod14) (12). Rod10$_{Y707A}$ (Rod10Y/A) is a mutant of HIV2 Env that is defective the antagonism of BST2-mediated virion-entrapment. Cells were transfected with excess pcDNA empty plasmid or 1.78μg of HIV-1ΔVpu expression plasmid (pNL4.3ΔVpu). A) NF-κB normalized fold changes over HEK293T cells that did not express BST2 (where 293T received only pcDNA3.1 as a control plasmid). Box and whiskers represent median, maximum, and minimum values from one experiment that consisted of five technical replicates. Statistical analysis for the data is presented in Table IV.4. B) p24-ELISA assay results of HIV-1 p24 protein as pg/ml of media as a representation of virion release of virions purified over a 20% sucrose cushion. Data are from two data points within one experiment.

Table IV.4. Statistical analysis of NF-κB activities presented in Figure IV.3A.

Group 1	Group 2	Wilcoxon Rank Sum	Significant?
		ctrl = 1	
Hu6	Hu6 + pNL4.3 WT	0.0152	Yes
	Hu6 + pNL4.3ΔVpu	0.2403	No
Hu6 + pNL4.3ΔVpu	Hu6 + pNL4.3 WT	0.026	Yes
	Hu6 + pNL4.3ΔVpu + Vpu	0.0022	Yes
	Hu6 + pNL4.3ΔVpu + ROD10	0.0087	Yes
	Hu6 + pNL4.3ΔVpu + ROD10Y/A	0.0411	Yes
	Hu6 + pNL4.3ΔVpu + ROD14	0.026	Yes

Table IV.5. Normalized NF-κB activity values presented in Figure IV.3A.

Group Name	Median	Minimum	Maximum	25th %	75th %
HEK293T (pcDNA ctrl)	1	1	1	1	1
Hu6	1.33	0.8972	2.161	0.9391	1.995
Hu6 + pNL4.3 WT	0.6513	0.4459	1.064	0.5209	1.064
Hu6 + pNL4.3ΔVpu	0.9552	0.8818	1.375	0.9269	1.326
Hu6 + pNL4.3ΔVpu + Vpu	0.3216	0.2387	0.6545	0.244	0.5907
Hu6 + pNL4.3ΔVpu + ROD10	1.74	1.276	2.509	1.355	2.264
Hu6 + pNL4.3ΔVpu + ROD10Y/A	1.41	1.255	2.118	1.275	1.95
Hu6 + pNL4.3ΔVpu + ROD14	1.365	0.9876	1.894	1.244	1.894

References

1. **Jia X, Weber E, Tokarev A, Lewinski M, Rizk M, Suarez M, Guatelli J, Xiong Y.** 2014. Structural basis of HIV-1 Vpu-mediated BST2 antagonism via hijacking of the clathrin adaptor protein complex 1. Elife **3:**e02362.

2. **Rizk MG, Basler CF, Guatelli J.** 2017. Cooperation of the Ebola proteins VP40 and GP1,2 with BST2 to activate NF-kappabeta independently of virus-like particle trapping. J Virol doi:10.1128/JVI.01308-17.

3. **Bhattacharyya S, Hope TJ.** 2011. Full-length Ebola glycoprotein accumulates in the endoplasmic reticulum. Virol J **8:**11.

4. **Kaletsky RL, Francica JR, Agrawal-Gamse C, Bates P.** 2009. Tetherin-mediated restriction of filovirus budding is antagonized by the Ebola glycoprotein. Proc Natl Acad Sci U S A **106:**2886-2891.

5. **Volchkov VE, Feldmann H, Volchkova VA, Klenk HD.** 1998. Processing of the Ebola virus glycoprotein by the proprotein convertase furin. Proc Natl Acad Sci U S A **95:**5762-5767.

6. **Fujiwara T, Oda K, Yokota S, Takatsuki A, Ikehara Y.** 1988. Brefeldin A causes disassembly of the Golgi complex and accumulation of secretory proteins in the endoplasmic reticulum. J Biol Chem **263:**18545-18552.

7. **Lin WC, Chuang YC, Chang YS, Lai MD, Teng YN, Su IJ, Wang CC, Lee KH, Hung JH.** 2012. Endoplasmic reticulum stress stimulates p53 expression through NF-kappaB activation. PLoS One **7:**e39120.

8. **Yamayoshi S, Noda T, Ebihara H, Goto H, Morikawa Y, Lukashevich IS, Neumann G, Feldmann H, Kawaoka Y.** 2008. Ebola virus matrix protein VP40 uses the COPII transport system for its intracellular transport. Cell Host Microbe **3:**168-177.

9. **Le Tortorec A, Neil SJ.** 2009. Antagonism to and intracellular sequestration of human tetherin by the human immunodeficiency virus type 2 envelope glycoprotein. J Virol **83:**11966-11978.

10. **Hauser H, Lopez LA, Yang S, Oldenburg JE, Exline CM, Guatelli JC, Cannon PM.** 2011. HIV-1 Vpu and HIV-2 Env counteract BST-2/tetherin by sequestration in a perinuclear compartment. Retrovirology **8:**85.

11. **Volchkova VA, Feldmann H, Klenk HD, Volchkov VE.** 1998. The nonstructural small glycoprotein sGP of Ebola virus is secreted as an antiparallel-orientated homodimer. Virology **250:**408-414.

12. **Jia B, Serra-Moreno R, Neidermyer W, Rahmberg A, Mackey J, Fofana IB, Johnson WE, Westmoreland S, Evans DT.** 2009. Species-specific activity of SIV Nef and HIV-1 Vpu in overcoming restriction by tetherin/BST2. PLoS Pathog **5:**e1000429.